1-1-1999

The use of continuum models for conducting both linear and nonlinear analyses of lattice structures

Simon Yi Luk
University of Nevada, Las Vegas

INFORMATION TO USERS

This manuscript has been reproduced from the microfilm master. UMI films the text directly from the original or copy submitted. Thus, some thesis and dissertation copies are in typewriter face, while others may be from any type of computer printer.

The quality of this reproduction is dependent upon the quality of the copy submitted. Broken or indistinct print, colored or poor quality illustrations and photographs, print bleedthrough, substandard margins, and improper alignment can adversely affect reproduction.

In the unlikely event that the author did not send UMI a complete manuscript and there are missing pages, these will be noted. Also, if unauthorized copyright material had to be removed, a note will indicate the deletion.

Oversize materials (e.g., maps, drawings, charts) are reproduced by sectioning the original, beginning at the upper left-hand corner and continuing from left to right in equal sections with small overlaps. Each original is also photographed in one exposure and is included in reduced form at the back of the book.

Photographs included in the original manuscript have been reproduced xerographically in this copy. Higher quality 6" x 9" black and white photographic prints are available for any photographs or illustrations appearing in this copy for an additional charge. Contact UMI directly to order.

UMI

A Bell & Howell Information Company
300 North Zeeb Road, Ann Arbor MI 48106-1346 USA
313/761-4700 800/521-0600

NOTE TO USERS

The original manuscript received by UMI contains broken or light print. All efforts were made to acquire the highest quality manuscript from the author or school. Microfilmed as received.

This reproduction is the best copy available

UMI

THE USE OF CONTINUUM MODELS FOR CONDUCTING BOTH LINEAR AND NONLINEAR ANALYSES OF LATTICE STRUCTURES

by

Simon Luk

Bachelor of Science
University of Nevada, Las Vegas
1997

A thesis submitted in partial fulfillment
of the requirements for the degree of

Master of Science
in
Engineering

Department of Civil and Environmental Engineering
University of Nevada, Las Vegas
December 1998

UNLV
UNIVERSITY OF NEVADA LAS VEGAS

Thesis Approval

The Graduate College
University of Nevada, Las Vegas

Nov. 18, 1998

The Thesis prepared by

Simon Luk

Entitled

The Use of Continuum Models for Conducting Both Linear and Nonlinear Analyses of Lattice Structures

is approved in partial fulfillment of the requirements for the degree of

Master of Science in Engineering - Civil

Gerald R. Frederick
Examination Committee Chair

Penny Cuny
Dean of the Graduate College

Samaan G. Ladkany
Examination Committee Member

Barbara A. Luke
Examination Committee Member

Henry Tovia
Graduate College Faculty Representative

ABSTRACT

The use of continuum models for conducting both linear and nonlinear analyses for lattice structures

by

Simon Graduate Student

Dr. Gerald Frederick, Examining Committee Chair
Professor of Engineering
University of Nevada, Las Vegas

Large structural projects, such as lattices for framing tall buildings or space purpose can result in huge finite element models. The use of continuum methodology for conducting both linear and nonlinear analyses of lattice structures in finite-element models results in significantly fewer degrees of freedom than discrete finite-element models, which individually model each structural element. Hence, the use of continuum models can result in a considerable reduction in computational effort with a corresponding savings in cost, at least during early 1990s when Pentium computer was not available. Now, it can still be a good design method especially for tall buildings in the preliminary stages of structural design because through the displacements under the axial, shear and moments stresses on the continuum model, the sizes and shapes of members can be determined for the structural system. Besides, it is also useful to check the results obtained from a commercially available computer structural program.

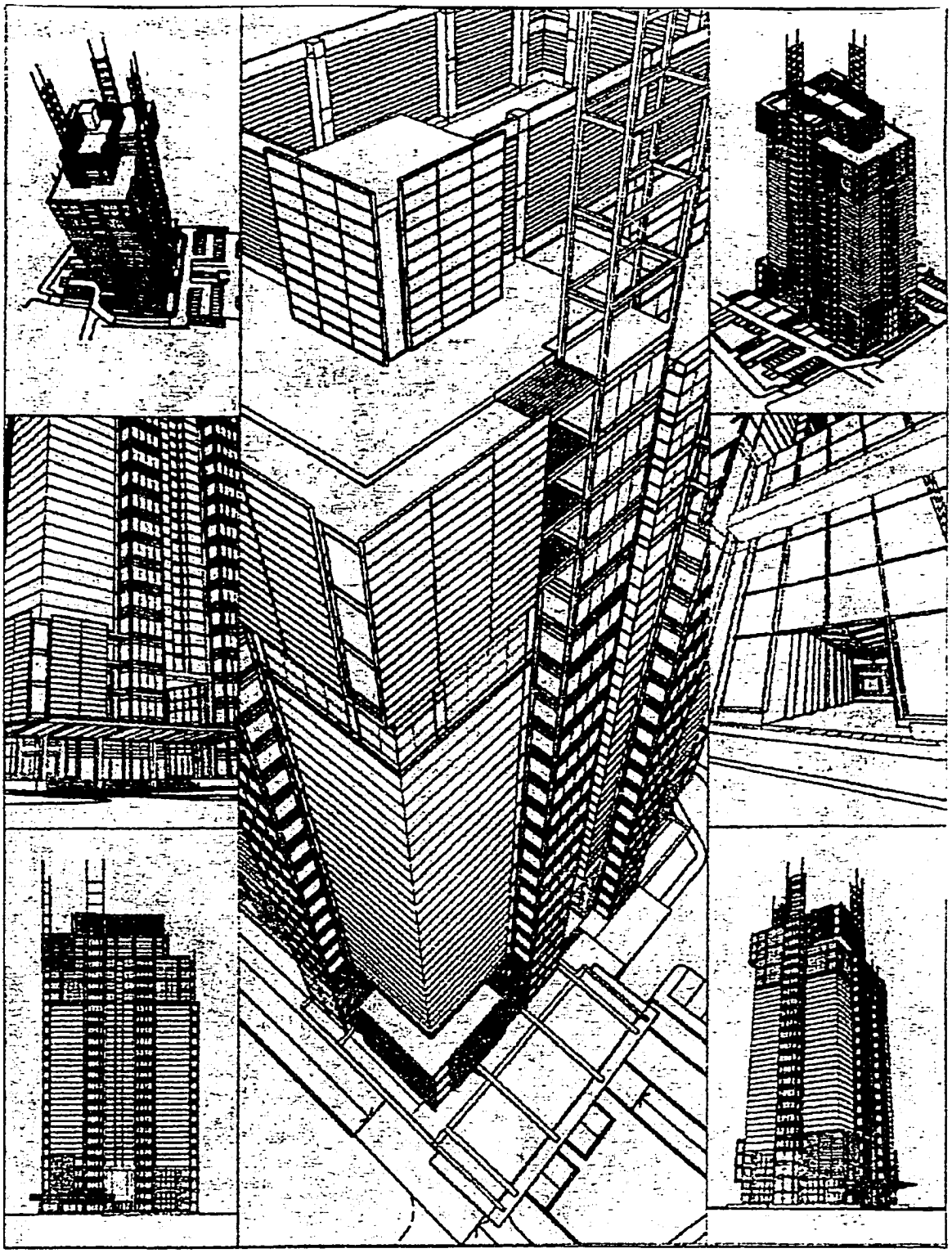

ACKNOWLEDGMENTS

I would like to express my appreciation to my graduate advisor, Prof. Gerald R. Frederick, for his guidance and support throughout this project. I would also like to thank the members of my Examining Committee for their valuable time and suggestions to make this thesis more perfect. I also wish to thank my friend David Liu for his assistance. Finally, I would like to thank my family for their patience and especially my wife, Cheryl, for her help, endurance and taking care of our two lovely kids, Leslie and Ivan, during this project and my entire master program.

TABLE OF CONTENTS

LIST OF FIGURES

LIST OF MATRICES

LIST OF NOMENCLATURE

A_i = discrete element cross-sectional area;
A_C = column cross-sectional area;
A_s = effective shear area of cell;
E = modulus of elasticity;
F = applied load vector;
F_{Ci} = column axial force;
F_I = inertia force vector;
F_i = continuum element generalized forces;
F_S = spring force vector;
G = shear modulus;
I_C = column moments of inertia;
I_i = discrete element moment of inertia;
K = system stiffness matrix;
L = length;
M = system mass matrix;
M_C = column bending moment;
NC = number of columns in lattice cross section;
θ = cross-sectional rotation;
k = curvature of the reference axis;
ξ_i = modal damping;
ϕ = slope of reference axis due to shear deformation;
ϕi = mode shape vector; and
ωi = modal circular frequency.

CHAPTER 1

INTRODUCTION

Continuum models to approximate the response of a discrete structures existed before computers were invented. Engesser (1907), one of the pioneers in this area, developed an equivalent, continuous beam to estimate buckling loads of built-up lattice columns. Timoshenko (1943) showed how simple continuum models could be used to describe the behavior of complex structures. Other early works in the area included Chitty's (1947) analysis of frames and Fl *ü* gge's (1962) study of frame stability.[1]

With the advent of modern high-speed computers, many of the problems solved by the early researchers using continuum models are now solved using discrete finite-element models. However, large lattice structures of increasing size and complexity are being used in a variety of applications from aerospace to super high-rise building system. To make lattice structures economical in terms of materials and overall costs, the ability to span large areas, high strength-to-weight ratios, novel prefabrication and erection schemes have to be exploited. The advent of the use of lattice structures in large complex structures, such as those proposed for space, has necessarily paralleled the introduction of computers and matrix analysis techniques. But the computational effort required under

discrete finite element analysis for these enormous projects can result in enormous finite-element models and may be prohibitive for large lattices. This is especially true for structures in which non-linear behavior is prevalent.

The use of continuum models in structural analysis, studied by some scholars in the 80s and early 90s, concentrated on large lattice structures which were proposed for space or used in the framing of tall buildings that resulted in very large finite-element models. There models were represented by repetitive patterns of these lattice structures. Such continuum representations of the finite-element models can yield significantly fewer degrees of freedom than those generated by using classical discrete finite-element methods. This leads to a considerable reduction in the computational effort associated with analysis. As a result, continuum models offer an attractive, inexpensive, approximate or controlling method for analyzing large structures. It can also provide a supplemental tool for preliminary design and parametric studies. Even some large problems can be solved efficiently using discrete methods by using super-speed personal computer now, such as those computers with a 300 MHz Pentium processor, calculated results from continuum models are still a good way to compare with the results obtained by using a discrete model so as to assure the correct behavior of a structural lattice framework.

In this paper, Continuum Theory is introduced in chapter 2. A continuum model is demonstrated in chapter 3. In chapter 4, results from continuum finite element models are compared with those obtained from discrete finite element models. Finally, continuum models are used to explore seismic dynamic analysis in chapter 5.

PURPOSE

The purpose of this thesis is to demonstrate the use of a small number of continuum elements to accurately predict the response of large lattice system in order to determine the behavior of a building framework under lateral wind load and seismic dynamic conditions. The results obtained using the continuum element are compared with the results obtained using commercially available finite element programs.

CHAPTER 2

THEORY

2-1. FOUNDATION OF ELASTICITY

If an object of any material resumes its initial form completely from a deformed shape after removal of the external forces, which produced the deformation of the object, the material such as steel, is considered as perfectly elastic.

It is assumed that the matter of an elastic engineering material is homogeneous and continuously distributed over its volume so that the smallest element cut from the body possesses the same elastic properties as the body. It is also assumed here that engineering materials are isotropic, i.e., the elastic properties are the same in all directions.

In analyzing the behavior of framework made of steel, it is necessary to know whether this material satisfies the above assumptions so as to affirm the elastic behavior of steel. A material, such as steel, when studied with a microscope, is seen to consist of crystals of various kinds and various orientations. The material is very far from being homogeneous, but experience shows that solutions of theory of elasticity based on the assumptions of homogeneity and isotropy can be applied to steel structures with very

millions of them in one cubic inch of steel. While the elastic properties of a single crystal may be very different in different directions, the crystals are ordinarily distributed at random and the elastic properties of larger pieces of metal represent averages of properties of the crystals. So long as the geometrical dimensions defining the form of an object are very large in comparison with the dimensions of a single crystal, the assumption of homogeneity can be used with great accuracy, and if the crystals are orientated at random, the material can be treated as isotropic.[2] Therefore, experimentally accepted linear elastic properties of the modulus of elasticity, E, and modulus of rigidity, G, can be applied to steel in the matrix technique in chapter 4. Otherwise, if the kind of steel has a plastic deformation instead of linear elastic deformation, it will be under the topic of plastic design other than the topic it is going to be discussed.

The foundation of the classical three-dimensional theory of elasticity utilizes the assumption of very small deformations and the stress-strain or constitutive relation in the mathematical representation of an isotropic, homogeneous, linearly elastic[1] solid. In the analysis of local deformation, the field equations that apply to all continuous media, such as steel column, must be supplemented by constitutive equations that describe the particular nature of a given material. As discussed above, the nature of steel generally satisfies these conditions. Then, the theory concludes with a brief introduction to solid mechanics where the assumption of very small deformations, such as infinitesimal

[1] In the straight line region of the strain and stress curve for tension of steel, loading and unloading results in no permanent deformation. It is referred as linear elastic.

displacements of the second order are dropped from the consideration of energy and virtual work.

2-2. COMPATIBILITY EQUATION AND STRAIN ENERGY IN CONTINUUM THEORY

Now, consider the strain-displacement relation

$$\varepsilon_{ij} = \frac{1}{2}\left(u_{i,j} + u_{j,i}\right), \tag{1}$$

which is an alternate form of the common *engineering shear strain-displacement relation*

$$\varepsilon_{xy} = \frac{1}{2}\left(\frac{\partial u_x}{\partial y} + \frac{\partial u_y}{\partial x}\right) = \frac{1}{2}\gamma_{xy}. \tag{2}$$

If the displacement field is given, the strain tensor[2] field can readily be computed by substituting u_i into the above equations. Here the displacement field, composed of three functions u_i, must be determined by integration of six partial differential equations given by Eq. (1). In order to ensure single-valued, continuous solutions u_i, certain restrictions are imposed on ε_{ij}. That is, any strain field ε_{ij} cannot be used and expected to automatically be associated with a single-valued, continuous displacement field. But actual deformations must have single-valued displacement fields. Furthermore, the deformations of interest are those having continuous displacement fields. Hence, the

---

[2] A tensor, τ_{ij}, is a magnitude by which components of a system may be transformed linearly and of which the notion of a vector is a special case. The first subscript gives the coordinate direction of the normal of the area element, and the second subscript gives the direction of the force intensity itself.

restrictions used in rendering u_i single-valued and continuous are called the **Compatibility Equations.**[3]

In elasticity, some problems can be posed entirely in terms of the stresses in which

the stresses are given on the boundary of an object and are to be determined in its interior. Once the stresses are known, the strains can be determined. Knowing the strains, the displacements can be calculated. Again, The integrability conditions, known as compatibility conditions, require that a given strain tensor be compatible with a single-valued displacement. Compatible displacements are those that satisfy the boundary conditions and ensure that no discontinuities, such as voids or overlaps, occur within the body.

For the displacement field in the Continuum theory, a particle located at a point P_0 at the coordinates **A** with the initial time t_0. Later, at time t, the particle is located at P, which has the coordinates **x**(**B**,t). The continuous medium, of which this is a generic particle, is said to be strained and deformed when the relative position of two particles is altered.

For a continuous media, the rate of work is given by the scalar product of force and velocity (Appendix E). Then, in the time interval $0 \le t \le T$, the **rate of work of the external forces,** W_E, of an elastic body with interior R and bounding surface ∂R will be given by

$$W_E = \int_0^T \oiint_{\partial R} t_i \dot{u}_i dA dt + \int_0^T \iiint_R f_i \dot{u}_i d\tau dt. \qquad (3)$$

where t_i is the stress over the surface of the ith component, $\dot{u}_i$ is the derivative of the displacement u, i.e., the velocity of the ith component (remember that $t_i dA = df$,i.e., stress times area = force), and f_i is the body force per unit volume of the ith component.

To compute the work of the internal forces for $0 \le t \le T$, an arbitrary portion of the interior R is considered, which will be designated by **D**, and the corresponding boundary ∂**D**. The ith component of the total force acting on **D** is given by

$$\iiint_D f_i d\tau + \oiint_{\partial D} t_i d\sigma = \iiint_D f_i d\tau + \oiint_{\partial D} T_{ji} n_j d\sigma = \iiint_D (f_i + T_{ji,j}) d\tau .^{3} \qquad (4)$$

where $t_i = T_{ji} n_j$[4]. Since **D** is arbitrary, it can concluded that

the internal force per unit volume equals $f_i + T_{ji,j}$. Thus, the **rate of work of the internal forces**, W_I, is given by

$$W_I = \int_0^T \iiint_R (f_i + T_{ji,j}) \dot{u}_i d\tau dt . \qquad (5)$$

Since

---

[3] Here, the Divergence Theorem for a third order tensor is employed as follows

$$\oiint_{\partial R} n_j T_{ij} d\sigma = \iiint_R \partial_j T_{ij} d\tau = \iiint_R T_{ij,j} d\tau$$

The divergence theorem states that the volume integral of the divergence of any continuously differentiable vector is the closed surface integral of the outward normal component of the vector [7]. The vector could be a stress vector and here is a stress tensor with the relation of vector and tensor mentioned before.

[4] A fundamental result in continuum mechanics is that the stress vector t(x,t,n) is a special function of the unit normal vector n given (using summation notation) by

$$t_i(x,t,n) = n_j T_{ji}(x,t)$$

Here the stress tensor T_{ji} is, by definition, the jth component of the stress vector acting on the surface element whose exterior normal points in the direction of the ith Cartesian base vector $e^{(i)}$.

$$\iiint_R T_{ji,j}\dot{u}_i d\tau = \oiint_{\partial R} t_i \dot{u}_i d\sigma - \iiint_R T_{ji}\dot{u}_{i,j} d\tau, \tag{6}$$

and that

$$T_{ji}\dot{u}_{i,j} = T_{ji}\dot{\varepsilon}_{ij}. \tag{7}$$

Using the stress-strain relation[5],

$$T_{ji}\dot{\varepsilon}_{ij} = \frac{1}{2}\frac{\partial}{\partial t}(2\mu\varepsilon_{ij}\varepsilon_{ij} + \lambda\varepsilon_{kk}\varepsilon_{jj}) \tag{8}$$

Thus,

$$\begin{aligned} W_I = \int_0^T \Big(\iiint_R f_i \dot{u}_i d\tau + \oiint_{\partial R} t_i \dot{u}_i d\sigma \Big) dt \\ - \iiint_R \frac{1}{2}(2\mu\varepsilon_{ij}\varepsilon_{ij} + \lambda\varepsilon_{kk}\varepsilon_{jj}) \Big|_0^T d\tau \end{aligned} \tag{9}$$

It is anticipated that the work by external forces will be transformed into work by internal forces plus a stored potential energy of strain. Accordingly, we define the change in strain energy as the difference between the work of the external forces and that of the internal forces. From Eq. (3) and (9), we see that

$$\text{Change in Strain Energy} = \frac{1}{2}\iiint_R (2\mu\varepsilon_{ij}\varepsilon_{ij} + \lambda\varepsilon_{kk}\varepsilon_{jj}) d\tau \Big|_0^T. \tag{10}$$

Consequently, the **strain energy**, E_ε, satisfies

$$E_\varepsilon(T) = \frac{1}{2}\iiint_R (2\mu\varepsilon_{ij}\varepsilon_{ij} + \lambda\varepsilon_{kk}\varepsilon_{jj}) \Big|_0^T d\tau + constant. \tag{11}$$

---

[5] The generalized Hooke's law or the stress and strain relation takes the form

$$T_{ij} = 2\mu\varepsilon_{ij} + \lambda\varepsilon_{kk}\delta_{ij}$$

where λ and μ are known as the *Lame*.

Setting the arbitrary constant equal to zero, thereby identifying the arbitrary zero of strain energy with the strain-free state ($\varepsilon_{ij} = 0$),

$$E_\varepsilon = \frac{1}{2}\iiint_R (2\mu\varepsilon_{ij}\varepsilon_{ij} + \lambda\varepsilon_{kk}\varepsilon_{jj})d\tau. \tag{12}$$

In terms of the engineering constants,

$$E_\varepsilon = \frac{E}{2(1+\upsilon)}\iiint_R (\varepsilon_{ij}\varepsilon_{ij} + \frac{\upsilon}{1-2\upsilon}\varepsilon_{kk}\varepsilon_{jj})d\tau. \tag{13}$$

where $0 \le \upsilon \le \frac{1}{2}$, so that E_ε is non-negative which implies that any deviation from the unstrained state leads to positive strain energy.[4]

To obtain a useful "mixed" expression for E_ε, the stress-strain relations are introduced into Eq. (13) as

$$2\mu\varepsilon_{ij}\varepsilon_{ij} + \lambda\varepsilon_{kk}\varepsilon_{jj} = (2\mu\varepsilon_{ij} + \lambda\varepsilon_{kk}\delta_{ij})\varepsilon_{ij} = T_{ij}\varepsilon_{ij} \tag{14}$$

This gives

$$E_\varepsilon = \frac{1}{2}\iiint_R T_{ij}\varepsilon_{ij}d\tau.^{6} \tag{15}$$

---

[6] To interpret eq. (15 recall the elementary physics problem of determining the potential energy stored in a spring. Let the spring possess a Hooke's constant k, so that the force F exerted by a spring stretched a distance x is given by F(x) = kx. The work required to stretch the spring a total of s units is

$$W(s) = \int_0^s F dx = \int_0^s kx dx = \frac{1}{2}ks^2 = \frac{1}{2}sF(s).$$

The correct result may be obtained by multiplying the total extension s by the average of the initial and final forces 0 and F(s). This is the most convincing way to obtain the factor $\frac{1}{2}$.

Then, the local potential energy stored in a strained elastic body, E_ε, can be regarded as being due to the stretching of three Hookean linear springs aligned along the mutually perpendicular principal axes.

For principal axes, with principal stresses, T_i, and strains, ε_i,

$$E_\varepsilon = \frac{1}{2}\iiint T_i \varepsilon_i d\tau = \frac{1}{2}\int_0^x \sigma A x dx = \frac{1}{2}\int_0^x F x dx . \qquad (16)$$

which is the formula for strain energy used for the continuum strain energy, U_C, or the approximate lattice strain energy, $\hat{U}_L$, in the coming sections.

2-3. LATTICE DEFORMATION MODES & LATTICE STRAIN ENERGY EXPRESSION

Large lattice structures are made of discrete structural members that are framed together. Often these members are connected in ways that form repeated geometric patterns or "cells." In a building, each cell may contain many beams and columns as shown in Fig. 1.

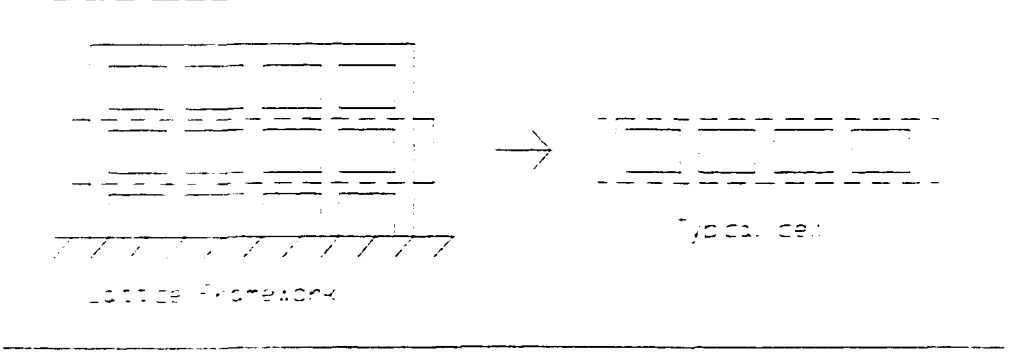

FIGURE 1
Typical Cell

The entire framework is often a combination of just a few different types of cells. The objective of the continuum model is to replace these repetitive cells with an "equivalent" continuum, thereby greatly reducing the number of elements used to model the lattice. This results in a significant reduction in the number of global degrees of freedom needed to describe the structure, such as the one shown in Fig. 2.

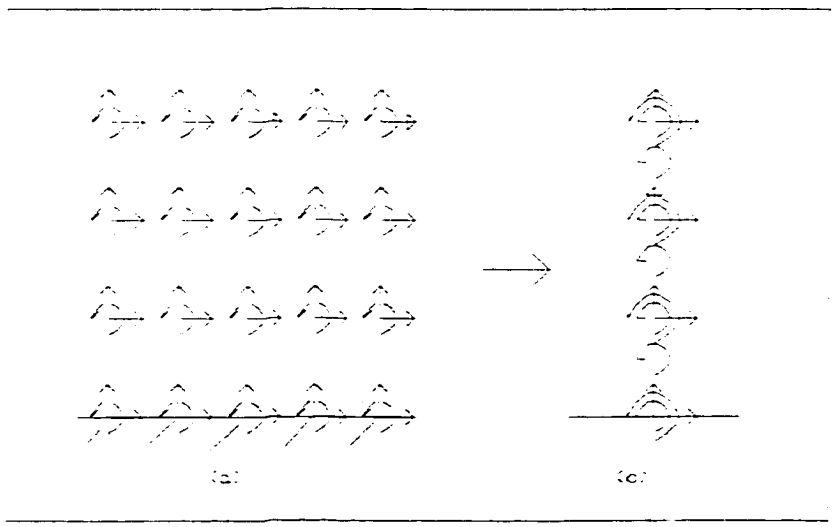

FIGURE 2
Global Degrees of Freedom for (a) Discrete and
(b) Continuum Models

In developing an appropriate model, there are three assumed deformation modes, i.e., bending, axial, and shear modes of deformation as shown in Fig. 3. They are used to represent the possible lattice deformation patterns (modes).

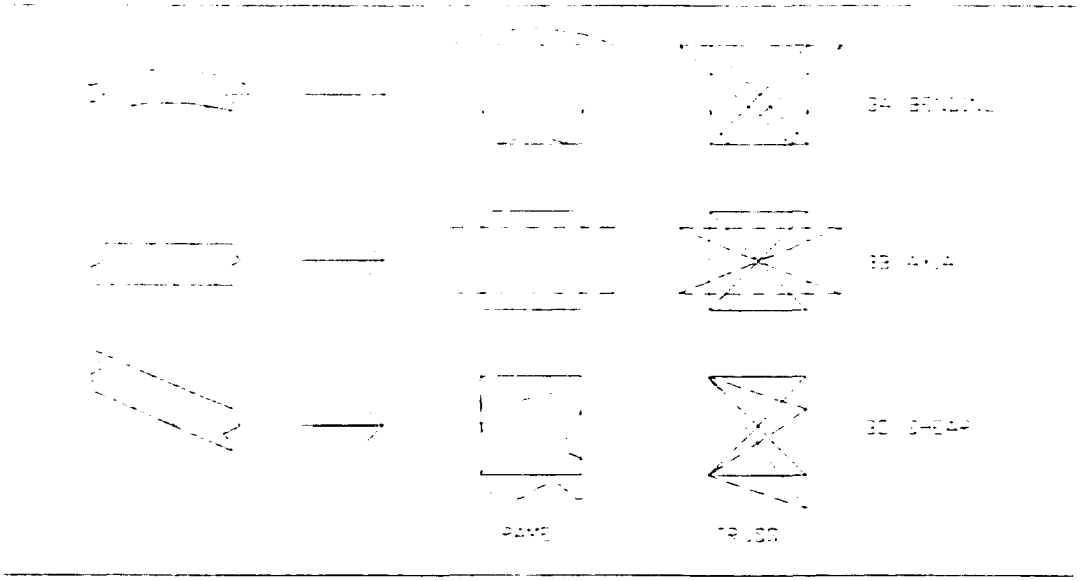

FIGURE 3
Lattice Deformation Modes

The kinematic assumptions which will be invoked here are most accurate when the lattice is symmetrical with respect to the longitudinal reference (middle) axis. In

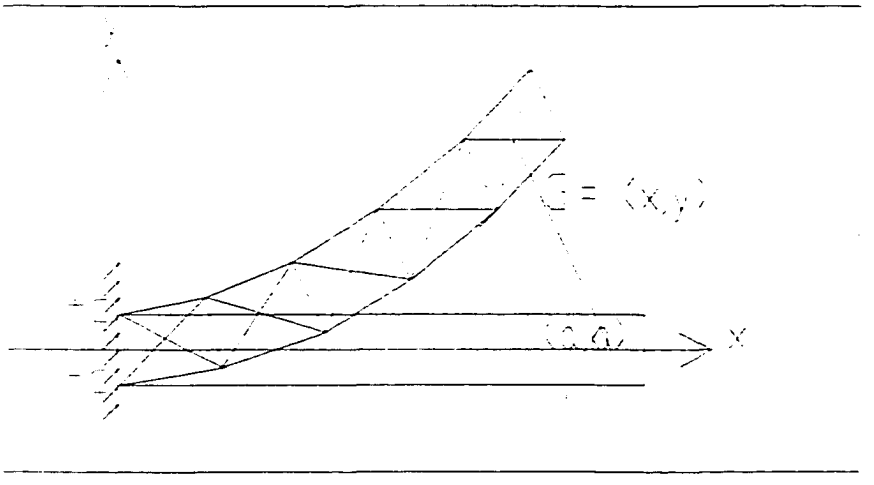

FIGURE 4
Continuous Displacement

order to describe the lattice deformations, a continuous displacement field shown in Fig. 4 (in the plane of the lattice shown in Fig. 1) is introduced below.

For any particle in the plane of the lattice, particle (x,y) $\in \Omega$, where $\Omega =$ $\{\ 0 \le x \le l,\ -c \le y \le c\ \}$, the displacement is given by

$$G(x,y) = u(x,y)\hat{i} + v(x,y)\hat{j} \tag{17}$$

where the x or 'reference' axis extends along lattice at mid-depth.

Kinematic assumptions are introduced which place restrictions on the horizontal and vertical displacement components u, v respectively. The restrictions are premised on the assumptions that global displacements of beam-like lattices (Fig. 4) follow the patterns describing beam behavior obtained by using classical Timoshenko theory [10]. In particular, it will be assumed that cross-sectional planes remain plane and are not required to be perpendicular to the reference axis. In addition, thickness strains, i.e., strains perpendicular to the reference axis, will be neglected ($\in$y=0); this assumes axially stiff battens normal to the chords. [5]

The above assumptions allow the displacements of points off the reference axis to be simply related to the displacements of points on the reference axis of the lattice. The result is a one-dimensional representation of lattice displacements permitting the deformation (strain) of the lattice to be described by overall bending and axial and shear deformation modes as shown in Figure 3.

According to the experiments done by McCallen and Romstad [5], it was found that the cross section stress resultants defined in Fig. 5 could be used to accurately describe the strain energy stored in most lattice configurations. Forces F1 and F2 are the

axial forces in the chords, and force F3 is the axial component of the force resultant from the diagonal elements. A generalized section shear is represented by V, and Mc represents chord moments resulting from the global curvature of the reference axis (present only in rigid-joint lattices). In rigid-joint lattices there will also be element shears and moments due to the shear deformation mode (Fig. 3c) which will not be defined explicitly as stress resultants; instead, the strain energies of the individual elements due to shear deformation will be accounted for in the generalized shear strain energy term.

Applying the principle of virtual displacements[7] mentioned earlier, the corresponding change in the strain energy of the beam must be equal to the work done by the external forces during the assumed virtual displacement. So the general equation is

$$\textit{Strain energy} = \textit{lateral load} + \textit{moment} + \textit{shear}.$$

The approximate strain energy expression for the lattice $\hat{U}_L$ describes the approximate strain energy stored in the lattice in terms of the five stress

---

[7] For the principle of virtual displacements, we assume that an infinitely small variation δw of the deflections w of the beam is produced. Then the corresponding change in the strain energy of the beam must be equal to the work done by the external forces during the assumed virtual displacement. In calculating this work we must consider not only the lateral load q distributed over the surface of the beam but also the bending moments M_n and transverse shear forces $Q_n - (\partial M_{nt} / \partial s)$ distributed along the boundary of the plate. Hence the general equation, given by the principle of virtual displacements, is

$$\delta V = \iint q\,\delta w\,dx\,dy - \int M_n \frac{\partial \delta w}{\partial n}\,ds + \int \left(Q_n - \frac{\partial M_{nt}}{\partial s} \right) \delta w\,ds$$

The first integral on the right-hand side of this equation represents the work of the lateral load during the displacement δw. The second, extended along the boundary of the beam, represents the work of the bending moments due to the rotation $\partial(\delta w) / \partial n$ of the edge of the plate. The minus sign follows from the directions chosen for M_n and the normal n. The third integral represents the work of the transverse forces applied along the edge of the beam. [12]

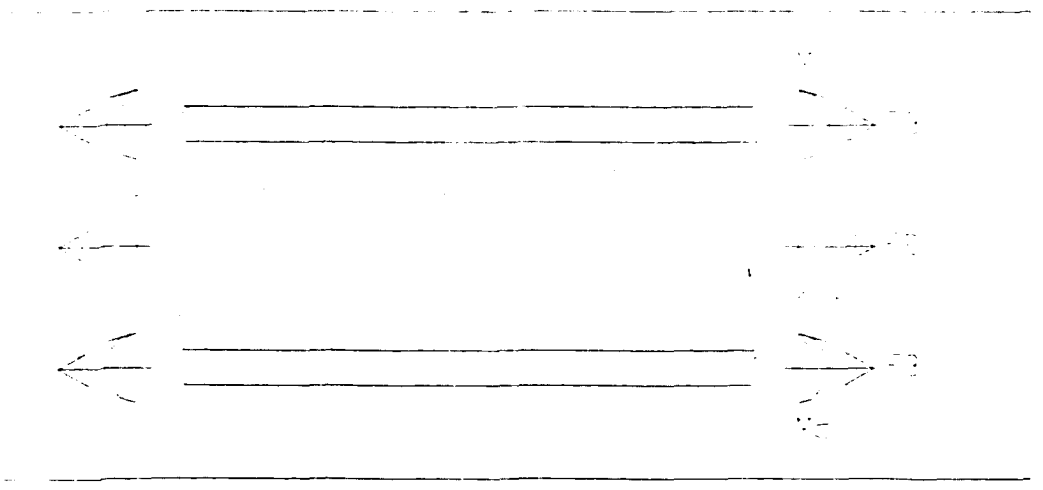

FIGURE 5
Stress Resultants Used in Expressing Strain Energy

resultants defined at a lattice cross section (shown in Fig. 5). Utilizing Eq.(16), the above discussion about virtual displacement and a generalized section shear force V , resulting from the assumed deformations, the approximate lattice strain energy may be written as

$$\hat{U}_L = \int_0^L \left\{ \begin{array}{l} \frac{1}{2}F_1\bar{\varepsilon}(x,c) + \frac{1}{2}F_2\bar{\varepsilon}(x,-c) + \frac{1}{2}F_3\varepsilon(x,0) \\ +2(\frac{1}{2})M_c K(x) + \frac{1}{2}V\phi(x) \end{array} \right\} dx \qquad (18)$$

The bar on the strain term denotes the **strain**[8] at a point located off the reference axis, Mc = the bending moment of the chord, K(x) = curvature of the reference axis and Ø(x) = slope of the reference axis due to shear deformation.

Chord axial forces F1 and F2 may be simply written in terms of the strain field as

[8] The continuous medium, for the case here being the particles at the location of (x,c), is said to be **strained** when the relative position of two particles is altered.

$$F1(x) = EAc\,\bar{\epsilon}(x,c) \tag{19}$$

$$F2(x) = EAc\,\bar{\epsilon}(x,-c), \tag{20}$$

in which E = modulus of elasticity and Ac = chord cross sectional area.

The axial force component F3 is found from the forces in the diagonal elements. The strains in the diagonal elements are obtained from the strain transformation (Appendix A)

$$\varepsilon_{di}(x,0) = \frac{\varepsilon(x,0)}{2} + \frac{\varepsilon(x,0)}{2}\cos 2\alpha_i \tag{21}$$

where α_i is measured counter-clockwise from the reference axis to the position of the diagonal member shown in Fig. 5. Note that this transformation takes $\varepsilon_y = 0$ and neglects the shear strain term (this contribution will also be included in the shear strain energy term). In general, components of symmetrical diagonal axial forces in the direction of the reference axis due to pure shear deformation cancel each other. The resultant, F_3, contributed by all diagonals due to global axial strain, is then given by

$$F_3 = \sum_{i=1}^{ND} EA_{di}\varepsilon_{di}(x,0)\cos\alpha_i \tag{22}$$

where ND is the number of diagonal elements at a given cross section.

The shear force resultant V is related to a generalized shear strain $\phi(x)$ (Appendix C) found from the transverse displacement of the reference axis due to the shear deformation mode

$$V = GA_s\phi(x)\,. \tag{25}$$

The effective shear area A_s may be obtained by analyzing a typical repeating cell of the lattice structure. The repeating cell is defined as the smallest symmetrical repeating pattern which can be identified in the lattice structure.[2]

In the continuum model methodology, an approximate strain energy expression $\hat{U}_L$ for the lattice of a model building is developed in terms of the bending moment Mci and axial force Fci in the vertical elements (columns), and a generalized section shear force V, resulting from the assumed deformations and utilizing Eq.(18). The approximate lattice strain-energy expression[9] is given by

$$\hat{U}_L = \int_0^L \left\{ \begin{array}{l} \frac{1}{2}F_1\bar{\varepsilon}(x,c) + \frac{1}{2}F_2\bar{\varepsilon}(x,-c) + \frac{1}{2}F_3\varepsilon(x,0) \\ +2(\frac{1}{2})M_c K(x) + \frac{1}{2}V\phi(x) \end{array} \right\} dx \qquad (26)$$

where the chord axial forces F_1, F_2, and F_3 in the ith column with $\sigma = E\varepsilon$ -> $\frac{N}{A} = E\varepsilon$ -> N=EAε -> $F = EA\varepsilon$ are

$$F_{1i} = N_{1i}(x) = EA_{Ci}\bar{\varepsilon}(x,y) \qquad (27)$$

$$F_{2i} = N_{2i}(x) = EA_{Ci}\bar{\varepsilon}(x,-y) \qquad (28)$$

$$F_{3i} = N_{3i}(x) = \sum_{i=1}^{NC} EA_{di}\varepsilon_{di}(x,0)\cos\alpha_i \qquad (29)$$

and F_{3i} is the resultant force contributed by the summation of all the diagonal elements in the frame due to global chord axial strain,

---

[9] Another way is to apply the energy, E, formula

$$E = \frac{1}{2}F * D$$

where F and D are the force and displacement respectively, to cover all the three modes of deformation.

$$M_{Ci} = \frac{EI_{Ci}}{\rho} = EI_{Ci}k(x) = EI_{Ci}(\frac{d^2v}{dx^2}) \tag{30}$$

= the bending moments in the *i*th column,

where $\frac{1}{\rho} = \frac{1}{\rho} = k(x) = \frac{d^2v}{dx^2}$ = curvature of the *i*th column.

$V = GA_s\phi(x)$ = the total transverse shear, (31)

(from Appendix C, $\tau_{XY} = G\gamma_{XY} = \frac{V}{A} = G\phi(x)$,

where $\gamma_{xy} = \phi(x)$ = strain defined as an angle,

$\bar{\varepsilon}(x, y)$ = off-axis strain,

$k(x)$ = curvature of the reference axis,

$\phi(x)$ = slope of the reference axis due to shear deformation,

NC = number of columns in the lattice cross section,

A_{Ci} = cross-sectional areas of the columns,

A_s = an effective shear area of the "repeated cell",

I_{Ci} = moment of inertia of column I.

The total transverse displacement V results from the sum of global shear and bending deformations. Thus M_{Ci} can be rewritten as

$$M_{Ci} = EI_{Ci}(\frac{d^2v_s}{dx^2} + \frac{d^2v_b}{dx^2}) \tag{32}$$

The local deformation pattern of a cell in a frame is dependent on the relative stiffness of the columns and beams. When the columns are stiff relative to the beams,

they tend to bend in single curvature (Fig. 5a) and the local curvature of the individual columns matches the global curvature of the lattice. When the columns are flexible relative to the beams, they tend to bend in double curvature (Fig. 6b) and the curvature is not the same at the local and global levels. To be completely versatile, the continuum model must capture the behavior of lattices having all ratios of column-to-beam stiffness. The effective shear stiffness found from Eq.(31), does not accurately approximate the behavior of lattices where the columns are stiff relative to the beams. Because the columns bend in reverse curvature in the shear deforming mode used to find the effective shear area A_s, the Timoshenko model does not accurately represent column moments due to a lack of continuity of the first derivative of shear displacement (i.e. the continuity of $\frac{dv_s}{dx}$). So, the shear curvature term given by $\frac{d^2 v_s}{dx^2}$ in Eq.(32) was included to help represent the column moments in such cases, and it proved essential in enabling accurate models for any combination of column and beam stiffness. [5]

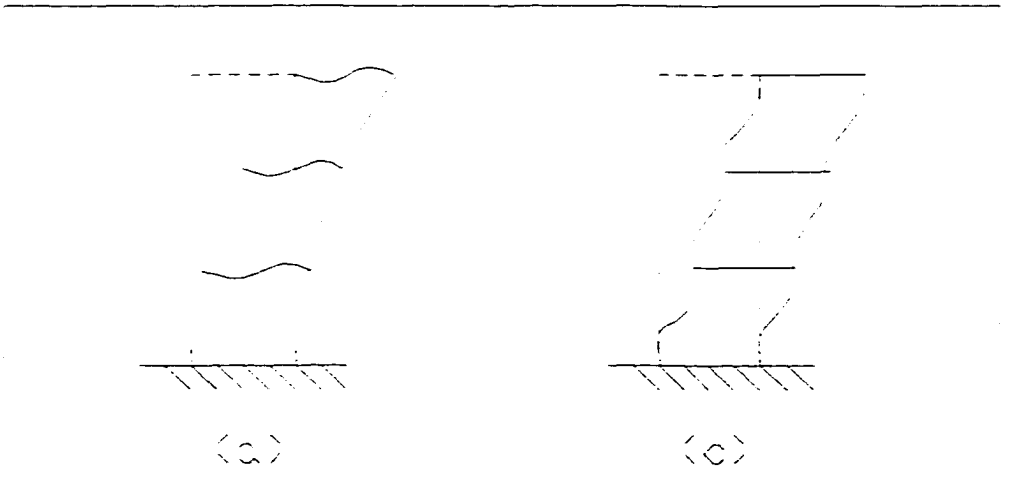

FIGURE 6
Deformation Pattern for (a) Stiff Columns and Flexible Beams (b) Flexible Columns and Stiff Beams.

Setting $U_C = \hat{U}_L$ and substituting the constitutive equations (38,39,40) into Eq. (26) yields

$$U_C = \int_0^L \left\{ \begin{array}{l} \frac{1}{2} EA_C \left[\bar{\varepsilon}(x,c)\right]^2 + \frac{1}{2} EA_C \left[x,-c\right]^2 \\ + \frac{1}{2}\left[\sum_{I=1}^{NC} EA_{di}\varepsilon_{di}(x,0)\cos\alpha_i\right]\varepsilon(x,o) \\ +2\left(\frac{1}{2}\right) EI_C\left[k(x)\right]^2 + \frac{1}{2} GA_S\left[\phi(X)\right]^2 \end{array} \right\} dx \tag{33}$$

Inserting Eq. (42b, 43, 44) which are part of Timoshenko theory kinematic equations as below

$$\bar{\varepsilon}(x,y) = \varepsilon - y\left[k(x) + \frac{d\phi(x)}{dx}\right] \tag{34}$$

where the second and third terms have negative effects on the bending and shear respectively, and with $k(x) = \frac{d^2 v}{dx^2}$

$$\bar{\varepsilon}(x,y) = \varepsilon - y\frac{d}{dx}\left[\frac{dv}{dx} + \phi(x)\right] = \varepsilon - \frac{d\theta}{dx} y \tag{35}$$

where $\theta = \frac{dv}{dx} + \phi$ = the total cross-sectional rotation,

$$\varepsilon = \frac{du}{dx} + \frac{1}{2}\left(\frac{dv}{dx}\right)^2 \tag{36}$$

where the second term is non-linear shear curvature not found in classical Timoshenko theory,

$$\varepsilon_{di}(x,0) = \frac{\varepsilon(x,0)}{2} + \frac{\varepsilon(x,0)}{2}\cos 2\alpha_i \tag{37}$$

into the continuum strain energy expression of Eq.(33) gives

$$U_C = \int_0^L \left\{ \begin{array}{l} \otimes_1 \; \frac{1}{2}EA_C\left(\varepsilon - \frac{d\theta}{dx}y\right)^2 + \frac{1}{2}EA_C\left(\varepsilon - \frac{d\theta}{dx}y\right)^2 \\ + \otimes_2 \; \frac{1}{2}\left\langle \sum_{i=1}^{ND} EA_{di}\left[\frac{\varepsilon(x,0)}{2} + \frac{\varepsilon(x,0)}{2}\cos 2\alpha_i\right]\cos\alpha_i \right\rangle \\ \left[\frac{du}{dx} + \frac{1}{2}\left(\frac{dv}{dx}\right)^2\right] + \otimes_3 \; EI_C\left[k(x)\right]^2 + \otimes_4 \; \frac{1}{2}GA_S\left[\phi(X)\right]^2 \end{array} \right\} dx \tag{38}$$

where

$$\otimes_1 = \frac{1}{2}EA_C\left(\varepsilon - \frac{d\theta}{dx}y\right)^2 + \frac{1}{2}EA_C\left(\varepsilon - \frac{d\theta}{dy}y\right)^2$$

$$= EA_C\left(\varepsilon - \frac{d\theta}{dx}y\right)^2$$

$$= EA_C\left[\varepsilon^2 - 2\varepsilon\frac{d\theta}{dx}y + \left(\frac{d\theta}{dx}\right)^2 y^2\right]$$

$$= \begin{array}{l} EA_C\left[\left(\frac{du}{dx}\right) + 2\left(\frac{1}{2}\right)\frac{du}{dx}\left(\frac{dv}{dx}\right)^2 + \frac{1}{4}\left(\frac{dv}{dx}\right)^4\right] \\ -EA_C\left\{2\left[\frac{du}{dx} + \frac{1}{2}\left(\frac{dv}{dx}\right)^2\right]\frac{d\theta}{dx}y\right\} + EA_C\left(\frac{d\theta}{dx}\right)^2 y^2 \end{array}$$

where again

$$\theta = \phi + \frac{dv}{dx} \quad \Rightarrow \quad \frac{d\theta}{dx} = \frac{d\phi}{dx} + \frac{d^2v}{dx^2}$$

which makes higher order for the product of the related terms and after all the higher order terms being neglected,

$$= EA_C\left(\frac{du}{dx}\right)^2 + EA_C\frac{du}{dx}\left(\frac{dv}{dx}\right)^2 + EA_C\left(\frac{d\theta}{dx}\right)^2 y^2$$

where

$$\otimes_2 = \frac{1}{2}\left\{\sum_{i=1}^{ND} EA_{di}\left\langle \begin{array}{l} \frac{1}{2}\left[\frac{du}{dx}+\frac{1}{2}\left(\frac{dv}{dx}\right)^2\right] \\ +\frac{1}{2}\left[\frac{du}{dx}+\frac{1}{2}\left(\frac{dv}{dx}\right)^2\right] \\ \left(2\cos^2\alpha_i - 1\right) \end{array} \right\rangle \cos\alpha_i \right\}\left[\frac{du}{dx}+\frac{1}{2}\left(\frac{dv}{dx}\right)^2\right]$$

where $\cos 2\alpha_i = 2\cos^2\alpha_i - 1$

$$= \frac{1}{2}\left\{\sum_{I=1}^{ND} EA_{di}\left\langle \begin{array}{l} \frac{1}{2}\cos\alpha_i\left[\frac{du}{dx}+\frac{1}{2}\left(\frac{dv}{dx}\right)^2\right] \\ +\frac{1}{2}\left[\frac{du}{dx}+\frac{1}{2}\left(\frac{dv}{dx}\right)^2\right]\left(2\cos^3\alpha_i - \cos\alpha_i\right) \end{array} \right\rangle \right\}\left[\frac{du}{dx}+\frac{1}{2}\left(\frac{dv}{dx}\right)^2\right]$$

$$= \frac{1}{2}\left\{ \begin{array}{l} \sum_{i=1}^{ND} EA_{di}\left(\frac{1}{2}\right)\cos\alpha_i\left[\frac{du}{dx}+\frac{1}{2}\left(\frac{dv}{dx}\right)^2\right]^2 \\ +\sum_{i=1}^{ND} EA_{di}\cos^3\alpha_i\left[\frac{du}{dx}+\frac{1}{2}\left(\frac{dv}{dx}\right)^2\right]^2 \\ -\sum_{i=1}^{ND} EA_{di}\left(\frac{1}{2}\right)\cos\alpha_i\left[\frac{du}{dx}+\frac{1}{2}\left(\frac{dv}{dx}\right)^2\right]^2 \end{array} \right\}$$

After canceling out the first and third terms

$$= \frac{1}{2}\sum_{i=1}^{ND} EA_{di}\cos^3\alpha_i\left[\left(\frac{du}{dx}\right) + \frac{du}{dx}\left(\frac{dv}{dx}\right)^2 + \left(\frac{dv}{dx}\right)^4\right]$$

Neglecting the higher order terms again

$$= \frac{1}{2}\sum_{i=1}^{ND} EA_{di}\cos^3\alpha_i\left(\frac{du}{dx}\right)^2 + \frac{1}{2}\sum_{i=1}^{ND} EA_{di}\cos^3\alpha_i\left[\frac{du}{dx}\left(\frac{dv}{dx}\right)^2\right]$$

Simplifying $\otimes_1$ and $\otimes_2$ give

$$(EA_C + \frac{1}{2}\sum_{i=1}^{ND} EA_{di}\cos^3\alpha_i)\left(\frac{du}{dx}\right)^2 + \left(EA_C + \frac{1}{2}\sum_{i=1}^{ND} EA_{di}\cos^3\alpha_i\right)\left[\frac{du}{dx}\left(\frac{dv}{dx}\right)^2\right]$$

where

$$\otimes_3 = EI_C\left[k(x)\right]^2 = EI_c\left(\frac{d^2v}{dx^2}\right)^2$$

and where

$$\otimes_4 = \frac{1}{2}GA_S\left[\phi(x)\right]^2$$

where the total cross-sectional rotation θ being

$$\theta = \phi + \frac{dv}{dx} \quad \Rightarrow \quad \phi = \theta - \frac{dv}{dx}$$

$$= \frac{1}{2}GA_S(\theta - \frac{dv}{dx})^2$$

$$= \frac{1}{2}GA_S\theta^2 - GA_S\theta\frac{dv}{dx} + \frac{1}{2}GA_S\left(\frac{dv}{dx}\right)^2$$

Finally,

$$U_C = \int_0^L \left\{ \begin{array}{l} \left(EA_C + \frac{1}{2}\sum_{i=1}^{ND} EA_{di}\cos^3\alpha_i \right)\left(\frac{du}{dx}\right)^2 \\ +\left(EA_C + \frac{1}{2}\sum_{i=1}^{ND} EA_{di}\cos^3\alpha_i \right)\left[\frac{du}{dx}\left(\frac{dv}{dx}\right)^2\right] \\ +EA_C y^2\left(\frac{d\theta}{dx}\right)^2 y^2 + EI_C\left(\frac{d^2v}{dx^2}\right)^2 \\ +\frac{1}{2}GA_S\theta^2 - GA_S\theta\left(\frac{dv}{dx}\right) + \frac{1}{2}GA_S\left(\frac{dv}{dx}\right)^2 \end{array} \right\} \qquad (39)$$

where E and G are the Young's modulus and shear modulus of the structural material, respectively; A_C, I_C are the area and moment of inertia of the columns; A_s is the effective shear area of the member; A_{di} is the cross-sectional area of the diagonal element; du, dv and $d\theta$ are the longitudinal,

transverse and rotational differential displacements respectively.

As mentioned before, the equivalence of the continuum and lattice is established by setting the continuum strain energy equal to the approximate lattice strain energy (i.e. $U_C = \hat{U}_L$). Thus, U_C can be viewed as representing either an approximate strain energy expression for the lattice, or an exact strain energy expression for the continuum. Please note that the continuum strain energy expression characterizes the force-displacement behavior of the continuum media as described before under the theory of virtual work in this chapter.

As discussed above, using the standard energy minimization principles (Appendix F), a beam-like finite element for the continuum model is formed. Additional degrees of freedom in the continuum element, not found in the typical Timoshenko beam elements, are needed as a result of continuum strain energy terms not found in the standard

Timoshenko beam theory. The derived first-order continuum finite element with nine degrees of freedom is shown in Fig. 7 and the associated element stiffness matrix is given in Appendix D.

The above continuum model element provides C_1 continuity[10] of both shear and bending displacement. With regard to the geometrical representation of the displacement, the degrees of freedom shown in Fig. 7 (P.43) that (1) u_1 and u_2 are longitudinal displacements and are used to get axial strains; (2) v_1 and v_2 are transverse displacements; (3) $\frac{dv_1}{dx}$ and $\frac{dv_2}{dx}$ are slopes along the centerline of the continuum element and are used to get values of curvature; and (4) θ_1, θ_2 and θ_3 are associated with rotations of the cross section and are used to get axial strains due to rotations of the cross section.

---

[10] Continuity. A vector function v(t) is said to be continuous at $t = t_0$ if it is defined in some neighborhood of t_0 and

$$\lim_{t \to t_0} v(t) = v(t_0)$$

If we introduce a Cartesian coordinate system, we may write

$$v(t) = [v_1(t), v_2(t), v_3(t)] = v_1(t)i + v_2(t)j + v_3(t)k .$$

Then v(t) is continuous at t_0 if and only if its three components are continuous at t_0. [8]

Functions that are required to be continuous are commonly known as C^0 functions, the 0 superscript referring to the zeroth derivative. In general, C^n - continuity means that the n-derivative is continuous.

For a fourth-order problem, the interpolation functions are required to be at least complete cubic polynomials. An arbitrary cubic polynomial contains four arbitrary constants. For a fourth-order problem, these four constants are used to enforce continuity of the function and its first derivative at the inter-element boundaries (nodes). Physically this corresponds to requiring the displacement *and* slope to be continuous at the nodes. This is referred to as C^1 continuity. [13]

Since the deformations of the lattice are limited to combinations of the assumed modes of deformation, the lattice energy expressions is only approximate and its accuracy depends on how well assumed modes represent actual deformations. [5]

CHAPTER 3

CONTINUUM MODEL METHODOLOGY

3-1. CONTINUUM MODEL ANALYSIS BY GLOBAL STIFFNESS MATRIX

For the point load situation, the change in potential of the loads is a linear combination of the global displacements

$$\Omega_C = -\sum P_i X_i \tag{40}$$

The total potential energy (V_C) of the continuum media

with Eq. (40) is

$$V_C = U_C + \Omega_C = U_C - \sum P_i X_i \tag{41}$$

It will be used to derive the global stiffness matrix with the energy minimization method.

If the change in potential energy can be related to the linear combination of the displaced shape of a structural system, the potential energy can be represented by a function of a generalized global displacements, such as

$$V = V\left(\{d_i\}\right) \tag{42}$$

where $\{d_i\} \in R^n$, and R is a vector space with n number of degrees of freedom.

The potential energy can be considered a function from the vector space $\boldsymbol{R}$. A stable equilibrium configuration of the structure is achieved only if the external applied load at each degree of freedom 'i' (i.e. P_i) is in equilibrium with the internal resisting force of the structure (denoted by Q_i) for all degrees of freedom. If the space vector $\{R(\{d_i\})\} \in R^n$, is defined as the difference between the applied load and the internal resisting force vector,

$$\{R(\{d_i\})\} = \{\{P\} - \{Q(\{d_i\})\}\} \tag{43}$$

then the equilibrium configuration $\{d_i^*\}$ yields a null space vector, i.e.

$$\{R(\{d_i^*\})\} = \{0\} \tag{44}$$

Since the potential energy V is represented as a function of the space vector R^n, therefore, $V\{(\{d_i^*\})\} = \{0\}$ is a situation to achieve equilibrium in the structure under the external load $\{P\}$ and the internal resisting force $\{Q\}$.

Referring to Appendix F, minimization of the variation of potential energy $V(\{d_i^*\})$ can be utilized for locating an equilibrium configuration $\{d_i^*\}$ of the structural system, i.e., to locate $\{\Delta V(\{d_i^*\})\} = \{0\}$, where

$$\{\Delta V\} \equiv \left\{\frac{\partial V}{\partial x_1}(\{x\}), \frac{\partial V}{\partial x_2}(\{x\}), \cdots, \frac{\partial V}{\partial x_n}(\{x\})\right\}^T \tag{45}$$

where $\partial x_1, \partial x_2, \cdots, \partial x_n$ are the directions of the respective displacements.

If the problem is non-linear geometrically, each component in Eq. (45) is also non-linear. To solve the difficulty, the Newton-Raphson[11] can be used to locate the zeros of $\{\Delta V(\{d^*\})\}$.

If $\{d^*\}$ is the initial guess at $\{d^n\}$, taking a two-terms Taylor series expansion[12] of $\{d^n\}$ makes

$$\{\Delta V(\{d^*\})\} = \{\Delta V(\{d^n\})\} + [\Delta^2 V(\{d^n\})]\{\Delta d\} + (\Delta^3 V(\frac{\Delta d^2}{2!})) \quad (46)$$

$$\{\Delta V(\{d^*\})\} = \{\Delta V(\{d^n\})\} + [\Delta^2 V(\{d^n\})]\{\Delta d\} + (0(\{\frac{\Delta d^2}{2!}\})) \quad (47)$$

where by definition

$$\{\Delta V(\{d^*\})\} = \{0\}$$

and neglecting higher order term, the third term, $\left\{\frac{d^2}{dx^2}\right\}$,

Eq. (46) becomes

$$\{\Delta d\} = -[\Delta^2 V(\{d^n\})]^{-1}\{\Delta V(\{d^n\})\} \quad (48)$$

Substituting Eq. (41) into Eq. (48) yields

---

[11] A Newton-Raphson procedure is an incremental -iterative solution algorithm in which the load is
applied incrementally and equilibrium iterations are employed to drive the space vector to zero within each increment.

[12] By Taylor series expansion, for any general function $f(x)$, we have

$$f_{x+dx} = f_x + \frac{df}{dx}dx + \frac{d^2 f}{dx^2}\frac{dx^2}{2!} + \cdots$$

$$\{\Delta d\} = -\left[\Delta^2 U(\{d^n\})\right]^{-1}\left\{\frac{\partial U}{\partial x} - P\right\}$$

since we only consider P as a concentrated point with one direction of movement, P will disappear under double partial differentiation, leaving only $\Delta^2 U$ which has many directions of displacements,

$$= \left[\Delta^2 U(\{d^n\})\right]^{-1}\left\{P - \frac{\partial U}{\partial x}\right\} \tag{49}$$

where $\left[\Delta^2 U(\{d^n\})\right]$

$$= \left[\frac{\partial^2 U}{\partial x_i \partial x_i}\right]$$

$$= \begin{bmatrix} \frac{\partial^2 U}{\partial x_1 \partial x_1} & \frac{\partial^2 U}{\partial x_2 \partial x_1} & \frac{\partial^2 U}{\partial x_3 \partial x_1} & \cdots & \frac{\partial^2 U}{\partial x_n \partial x_1} \\ \frac{\partial^2 U}{\partial x_1 \partial x_2} & \ddots & & & \vdots \\ \frac{\partial^2 U}{\partial x_1 \partial x_3} & & \ddots & & \vdots \\ \vdots & & & \ddots & \vdots \\ \frac{\partial^2 U}{\partial x_1 \partial x_n} & \cdots & \cdots & \cdots & \frac{\partial^2 U}{\partial x_n \partial x_n} \end{bmatrix} \tag{50}$$

where U represents the continuum strain energy expression U_C in Eq. (39) and $\partial x_1 \partial x_2$, $\partial x_1 \partial x_3$ can be $\partial x \partial y$, $\partial x \partial z$, etc. For a nine degrees of freedom, the matrix will have the order of 9x9 as the one shown in Appendix D.

3-2. NONLINEAR SOLUTION FRAMEWORK

The non-linear case is related to the strain energy consisting of quadratic forms in the generalized strains. When the strains are linear in the generalized displacements, the

strain energy is also quadratic in the displacement. So it does not change. Therefore,

$\frac{\partial^2 U}{\partial x_i \partial x_j} = [K]$ is a constant stiffness matrix which is not a function of displacements.

Then, for the non-linear strain displacements, the strain energy will be non-quadratic (constant) with the following forms

$$\frac{\partial^2 U}{\partial x_i \partial x_j} = \left[K^I(\{d\})\right] \tag{51}$$

where $\left[K^I(\{d\})\right]$ is the instantaneous (tangent) stiffness at a given displacement level $\{d\}$. Invoking Castigliano's theorem, $\left\{\frac{\partial U}{\partial x_i}\right\} = \{F_{\text{int}}\}$ the internal resisting force provided by the structure in the direction of displacement x_i and introducing the non-equilibrium residual vector $\{R(\{d\})\}$,

Eq. (49) with Eq. (51) becomes

$$\left[K^I(\{d\})\right]\{\Delta d\} = \{R(\{d\})\} \tag{52}$$

Using the Newton-Raphson iterative solution algorithm mentioned above, the external loads applied in increments and equilibrium iterations are utilized to converge the residual vector $\{R(\{d\})\}$ to zero with the same purpose of minimization of potential energy on $\{V(\{d^*\})\}$ as in Eq. (45f, 45i) for the linear case.[5]

So, the standard energy-minimization technique mentioned above is used to derive the global stiffness matrix of the special nine-degrees-of-freedom element shown in Fig. 7. With regard to the geometrical representation of the displacement degrees of freedom $\{U_1, U_2, ..., U_9\}$, the displacement coordinates U_1 and U_6 define the

longitudinal displacements u and associated values of axial strain; the displacement coordinates U_2 and U_7 represent the transverse displacements; the displacement coordinates U_3 and U_8 are associated with slopes along the centerline of the continuum element, which are used to get curvature values; and the displacement coordinates U_4, U_5 and U_9 are associated with rotations $\theta(\theta = \frac{d_{vb}}{d_x})$ of the cross section.

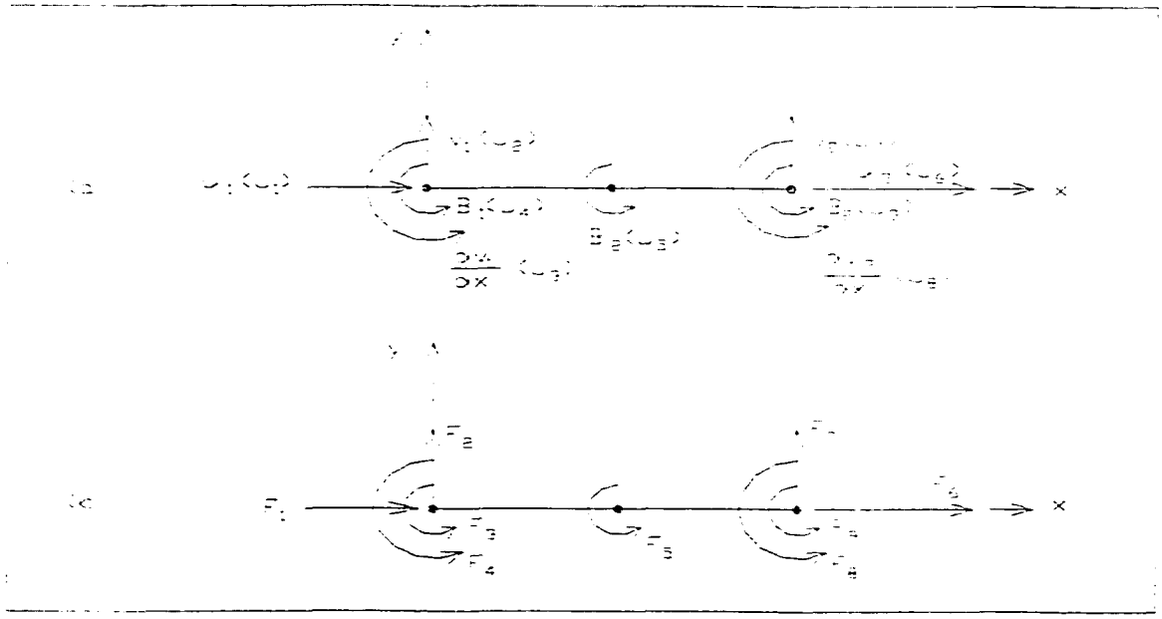

FIGURE 7
Continuum Finite Element (a) Degrees of Freedom and
(b) Generalized Forces

For the associated generalized forces $\{F_1, F_2, ..., F_9\}$, F_1 and F_6 represent element axial forces; F_2 and F_7 represent element shear forces; F_3 and F_8 represent moments due to centerline curvature; and F_4, F_5, and F_9 represent moments due to shear deformation and axial force couples resulting from both bending and shear deformation.

In the development of the continuum finite element, a value for the shear area A_s is needed. The shear area for cells in multi-bay frames is found by analyzing the discrete cell under a state of pure shear. When the analysis is conducted, the boundary conditions must be properly modeled so that no axial force is created in the beams. Furthermore, one must be careful to take the proper section properties for the beams (using only half the section properties if the beam is part of another cell). A symmetric cell (corresponding to a cell located in the interior of the lattice) having appropriate boundary conditions is shown in Fig. 8.

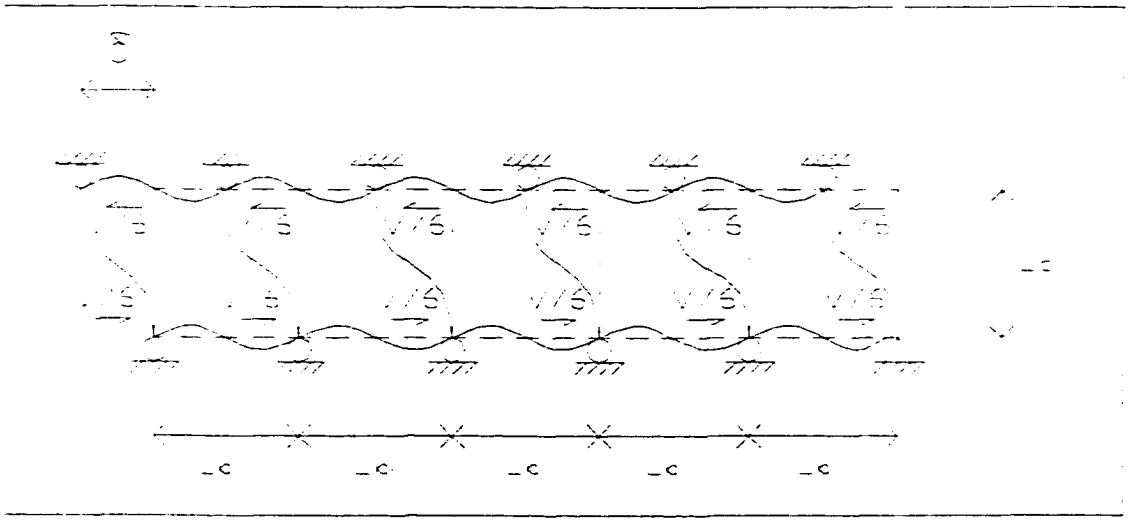

FIGURE 8
Symmetric Shear Cell

Based upon the behavior of a differential element in a state of pure shear (Fig. 9), and the lateral deflection δ given by the analysis of the shear cell subjected to a shear V, the effective shear cell area A_s is given by

$$A_s = \frac{VL}{\delta G} \tag{53}$$

where L = height of the cell; and G = shear modulus of the lattice material.

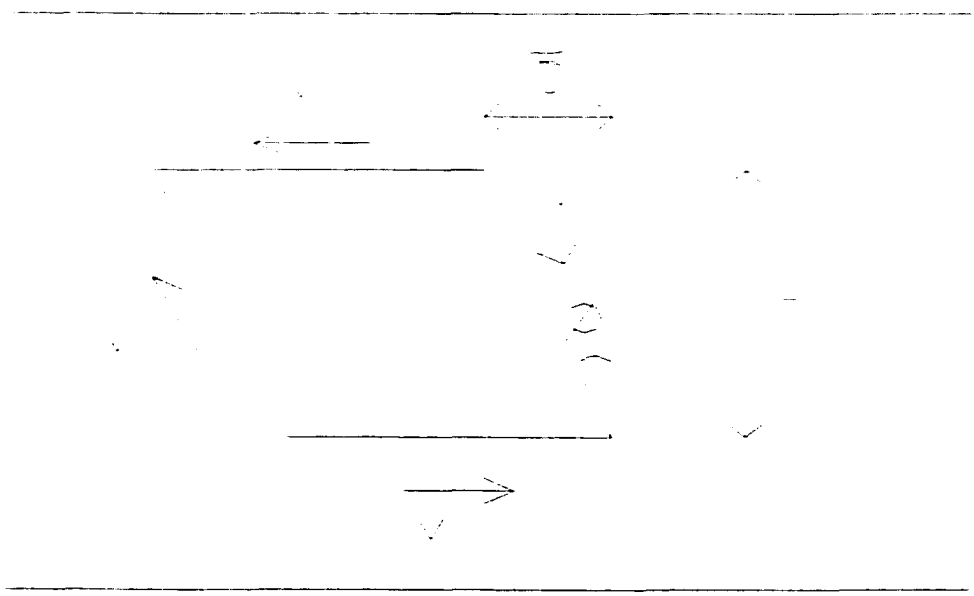

FIGURE 9
Differential Element in Pure Shear

3-3. DISPLACEMENT CALCULATIONS

The method for finding nodal displacements of discrete finite-element models using linear elastic analysis can be simply used in the continuum model. The formulation and solution of the matrix equation is given by

$$\mathbf{Q} = \mathbf{KX} \tag{54}$$

where $\mathbf{Q}$ = set of externally applied forces in a column matrix; $\mathbf{K}$ = system stiffness matrix; and $\mathbf{X}$ = set of nodal displacements in a column matrix. The formulation of the system stiffness matrix and the solution of the simultaneous equations are significant steps in the analysis. The computational effort required to find the nodal displacements is largely a function of the size and bandwidth of the stiffness matrix. We define the

stiffness matrix as follows: For an element, a **stiffness matrix** $\hat{k}$ is a matrix such that $\hat{f} = \hat{k}\hat{d}$, where $\hat{k}$ relates local-coordinate $(\hat{x}, \hat{y}, \hat{z})$nodal displacements $\hat{d}$ to local forces $\hat{f}$ of a single element. (Through this paper, the bold notation denotes a matrix, and the ^ symbol denotes quantities referred to a local-coordinate system set up to be convenient for the element.) For a continuous medium or structure comprising a series of elements, a stiffness matrix **K** relates global-coordinate (x,y,z) nodal displacements **D** to global forces **F** of the whole medium or structure. (Lower-case letters such as x,y, and z without the ^ symbol denote global-coordinate variables.)

In the continuum analysis, the stiffness of each continuum element is found by using Eq. (D1-13) in the nine-by-nine continuum element stiffness matrix in Appendix D. Element stiffness in element coordinates are transformed to system coordinates and summed into a system stiffness matrix by Direct Stiffness Method. A system load matrix is formed and modified for known displacement conditions. Finally, Eq. (54) is solved yielding the nodal displacements.

According to Osterkamp's (1988) study of single-bay, fixed-base frames and Chajes' (1990) work on multiple bay fixed- and pinned-base frames indicate that continuum models are most accurate in predicting lateral displacements when U_4 is restrained and U_3 is not. Both studies showed that models that were too stiff resulted when the centerline slope and the cross-section rotation were restrained.[5]

CHAPTER 4

EXAMPLES OF X-Y STEEL FRAMES FOR A 3,20,40 STORIES BUILDING BY CONTINUUM MODEL ANALYSIS IN COMPARISON WITH DISCRETE FINITE ELEMENT PROGRAMS

4-1. MULTIPLE-BAY PLANE FRAME ANALYSES

During the 1989 Loma Prieta earthquake, an office tower with 47 above-grade stories located in the Lower Marker area of San Francisco was selected for the study of torsion effect on building. 18 accelerometers were installed throughout the building by the California Strong Motion Instrumentation Program (CSMIP) of the California Division of Mines and Geology, of the Division of Conservation. The purpose was to evaluate what role translation and torsion had played. In the study of torsion effect, a comparison of displacements of parallel sensors at the 44th floor indicated little torsion response. That was consistent with the findings of Astaneh (1993) and Celebi (1993), who also found torsional response to be insignificant. As a result, the east-west and north-south moment-resisting frames can be studied individually as two-dimensional systems. Because the continuum methodology has been developed for regular lattice framing systems, it can be used to analyze the framing structure of a building by just

studying the east-west and north-south frames or any one dimensional framework of a symmetrical building individually.

As we have discussed above, torsion is insignificant in studying the framework on a building. To analyze the framing systems of a building, one can just need to look at any one dimensional frame of the building individually.

4-2. 3 STORY X-Y FRAME

Starting with a three story moment-resisting frame drawn by Risa 3-D as shown in Fig. 10, every story is considered as one typical cell element as mentioned in Chapter 2. Applying the stiffness matrix shown in Appendix D, the following global stiffness matrix is formed by substituting the related figures. To simply the process, the properties of one shape member has been applied to all members and the result is still close to the one obtained from a commercial computer program Plannar Frame Structural Analysis as shown in Appendix G where the figure of the 3 story frame is provided.

Matrix 1 Global Stiffness Matrix for the three bays 3 Story Frame

Total Columns	N = 4	
Length	L = 120	in
Shear Area	As = 42.7	in^2
Moment Inertia	Ii = 1710	in^4
Elasticity Modulus	E = 29000	ksi
Rigidity Modulus	G = 12000	ksi
Dist. to Neu.-Axis	Yi = 60	in
Load	P = 400	kips
Shear Force	V = 6.7	kips

$$
\begin{bmatrix}
\frac{NEAi}{L} & 0 & 0 & 0 & 0 & \frac{NEAi}{L} & 0 & 0 & 0 \\
0 & \frac{N12EIi}{L^3}+\frac{6GAs}{5L} & \frac{N6EIi}{L^2}+\frac{GAs}{10} & \frac{GAs}{10} & \frac{4GAs}{5} & 0 & \frac{N12EIi}{L^3}+\frac{6GAs}{5L} & \frac{N6EIi}{L^2}+\frac{GAs}{10} & \frac{GAs}{10} \\
0 & \frac{N6EIi}{L^2}+\frac{GAs}{10} & \frac{N4EIi}{L}+\frac{2GAsL}{15} & \frac{7GAsL}{60} & \frac{GAsL}{15} & 0 & \frac{N6EIi}{L^2}+\frac{GAs}{10} & \frac{N2EIi}{L}+\frac{GAsL}{30} & 0 \\
0 & \frac{GAs}{10} & \frac{7GAsL}{60} & \frac{N7EAiYi^2}{3L}+\frac{2GAsL}{15} & \frac{N8EAiYi^2}{3L}+\frac{GAsL}{15} & 0 & \frac{GAs}{10} & 0 & \frac{NEAiYi^2}{3L}+\frac{GAsL}{30} \\
0 & \frac{4GAs}{5} & \frac{GAsL}{15} & \frac{N8EAiYi^2}{3L}+\frac{GAsL}{15} & \frac{N16EAiYi^2}{3L}+\frac{8GAsL}{15} & 0 & \frac{4GAs}{5} & \frac{GAsL}{15} & \frac{N8EAiYi^2}{3L}+\frac{GAsL}{15} \\
\frac{NEAi}{L} & 0 & 0 & 0 & 0 & \frac{NEAi}{L} & 0 & 0 & 0 \\
0 & \frac{N12EIi}{L^3}+\frac{6GAs}{5L} & \frac{N6EIi}{L^2}+\frac{GAs}{10} & \frac{GAs}{10} & \frac{4GAs}{5} & 0 & \frac{N12EIi}{L^3}+\frac{6GAs}{5L} & \frac{N6EIi}{L^2}+\frac{GAs}{10} & \frac{GAs}{10} \\
0 & \frac{N6EIi}{L^2}+\frac{GAs}{10} & \frac{N2EIi}{L}+\frac{GAsL}{30} & 0 & \frac{GAsL}{15} & 0 & \frac{N6EIi}{L^2}+\frac{GAs}{10} & \frac{N4EIi}{L}+\frac{2GAsL}{15} & \frac{7GAsL}{60} \\
0 & \frac{GAs}{10} & 0 & \frac{NEAiYi^2}{3L}+\frac{GAsL}{30} & \frac{N8EAiYi^2}{3L}+\frac{GAsL}{15} & 0 & \frac{GAs}{10} & \frac{7GAsL}{60} & \frac{N7EAiYi^2}{3L}+\frac{2GAsL}{15}
\end{bmatrix}
$$

Referring to Fig. 7 on page 33, the member in the figure is analyzed as a column standing vertically with displacement u_1 towards the ground. Since one floor is being

analyzed at a time and assuming the column is fixed at the bottom, displacements u_1 and u_2 are zero and deleted from the matrix operation. Besides, according to the experiments done by Chajes and McCallen [5], the results were still close to accurate if the displacements fields of u_4, u_5, and u_9 are neglected and deleted from the matrix operation also. After the stiffness elements relating to these five displacement fields are deleted, i.e., the first, second, forth, fifth and the ninth rows and columns, from the above global stiffness matrix, the only displacement fields and the relating force fields needed to be considered are u_3, u_6, u_7, u_8, F_3, F_6, F_7, and F_8 as shown in the third and the second column vectors respectively in the following matrix operation. **This explanation applies to all the matrices operation for the 20 and 40 story frame examples in this chapter.**

Starting the analysis from the first floor to the third floor, the lateral displacements for the top of the ground floor, second floor and third floor are determined as $d_{1st} = 0.139$ inch, $d_{2nd} = 0.207$ inch and $d_{3rd} = 0.229$ inch respectively as shown in the following matrix analyses.

Matrix 2 Matrix Operation -1st Floor of 3 Story Frame

$$\begin{bmatrix} \frac{N\cdot 4\cdot E\cdot Ii}{L} - \frac{2\cdot G\cdot As\cdot L}{15} & 0 & \frac{-N\cdot 6\cdot E\cdot Ii}{L^2} - \frac{G\cdot As}{10} & \frac{N\cdot 2\cdot E\cdot Ii}{L} - \frac{G\cdot As\cdot L}{30} \\ 0 & \frac{N\cdot E\cdot Ai}{L} & 0 & 0 \\ \frac{-N\cdot 6\cdot E\cdot Ii}{L^2} - \frac{G\cdot As}{10} & 0 & \frac{N\cdot 12\cdot E\cdot Ii}{L^3} - \frac{6\cdot G\cdot As}{5\cdot L} & \frac{-N\cdot 6\cdot E\cdot Ii}{L^2} - \frac{G\cdot As}{10} \\ \frac{N\cdot 2\cdot E\cdot Ii}{L} - \frac{G\cdot As\cdot L}{30} & 0 & \frac{-N\cdot 6\cdot E\cdot Ii}{L^2} - \frac{G\cdot As}{10} & \frac{N\cdot 4\cdot E\cdot Ii}{L} - \frac{2\cdot G\cdot As\cdot L}{15} \end{bmatrix}^{-1} \begin{bmatrix} 3600 \\ -400 \\ 0.5v \\ -1596 \end{bmatrix} = \begin{bmatrix} 0.001043 \\ -0.028736 \\ 0.013924 \\ -2.61997410^{-4} \end{bmatrix}$$

Lateral displacement on the top of the 1st floor

$= 0.013924 - 120 \cdot 0.001043 = 0.139084 \text{in.}$

Matrix 3 Matrix Operation-2nd Floor of 3 Story Frame

$$\begin{bmatrix} \frac{N\cdot 4\cdot E\cdot Ii}{L} - \frac{2\cdot G\cdot As\cdot L}{15} & 0 & \frac{-N\cdot 6\cdot E\cdot Ii}{L^2} - \frac{G\cdot As}{10} & \frac{N\cdot 2\cdot E\cdot Ii}{L} - \frac{G\cdot As\cdot L}{30} \\ 0 & \frac{N\cdot E\cdot Ai}{L} & 0 & 0 \\ \frac{-N\cdot 6\cdot E\cdot Ii}{L^2} - \frac{G\cdot As}{10} & 0 & \frac{N\cdot 12\cdot E\cdot Ii}{L^3} - \frac{6\cdot G\cdot As}{5\cdot L} & \frac{-N\cdot 6\cdot E\cdot Ii}{L^2} - \frac{G\cdot As}{10} \\ \frac{N\cdot 2\cdot E\cdot Ii}{L} - \frac{G\cdot As\cdot L}{30} & 0 & \frac{-N\cdot 6\cdot E\cdot Ii}{L^2} - \frac{G\cdot As}{10} & \frac{N\cdot 4\cdot E\cdot Ii}{L} - \frac{2\cdot G\cdot As\cdot L}{15} \end{bmatrix}^{-1} \begin{bmatrix} 1596 \\ -400 \\ 0.5\cdot v \\ -396 \end{bmatrix} = \begin{bmatrix} 4.917204\cdot 10^{-4} \\ -0.028736 \\ 0.009271 \\ -8.547461\cdot 10^{-6} \end{bmatrix}$$

Lateral displacement on the top of the 2nd floor

$= 0.009271 - 120 \cdot 4.917204 10^{-4} - 0.139084 = 0.207361 \text{ in.}$

Matrix 4 Matrix Operation-3rd Floor of 3 Story Frame

$$\begin{bmatrix} \frac{N\cdot 4\cdot E\cdot Ii}{L} - \frac{2\cdot G\cdot As\cdot L}{15} & 0 & \frac{-N\cdot 6\cdot E\cdot Ii}{L^2} - \frac{G\cdot As}{10} & \frac{N\cdot 2\cdot E\cdot Ii}{L} - \frac{G\cdot As\cdot L}{30} \\ 0 & \frac{N\cdot E\cdot Ai}{L} & 0 & 0 \\ \frac{-N\cdot 6\cdot E\cdot Ii}{L^2} - \frac{G\cdot As}{10} & 0 & \frac{N\cdot 12\cdot E\cdot Ii}{L^3} - \frac{6\cdot G\cdot As}{5\cdot L} & \frac{-N\cdot 6\cdot E\cdot Ii}{L^2} - \frac{G\cdot As}{10} \\ \frac{N\cdot 2\cdot E\cdot Ii}{L} - \frac{G\cdot As\cdot L}{30} & 0 & \frac{-N\cdot 6\cdot E\cdot Ii}{L^2} - \frac{G\cdot As}{10} & \frac{N\cdot 4\cdot E\cdot Ii}{L} - \frac{2\cdot G\cdot As\cdot L}{15} \end{bmatrix}^{-1} \begin{bmatrix} 396 \\ 400 \\ V \\ 0 \end{bmatrix} = \begin{bmatrix} 1.421486\cdot 10^{-4} \\ -0.028736 \\ 0.004583 \\ 4.269777\cdot 10^{-5} \end{bmatrix}$$

Lateral displacement on the top of the 3rd floor

$= 0.004583 - 120 \cdot 1.42148610^{-4} - 0.207361 = 0.229002\,\text{in.}$

ANALYSIS REPORT FOR THE 3 STORY FRAME

Horizontal displacement on the top of the 3rd floor due to net lateral displacement

$= 0.013924 - 0.009271 - 0.004583 = 0.027778$ in

Horizontal displacement on the top of the 3rd floor due to net rotational displacement

Total Rotation $= 0.001043 - 4.917204 \cdot 10^{-4} - 1.421486 \cdot 10^{-4} = 0.001677$ in

Horizontal displacement

$= 120 \cdot 0.001677 = 0.20124$ in

Total horizontal displacement on the top of the 3rd floor

$= 0.027778 - 0.20124 = 0.229$ in

Vertical displacement for the entire frame

$= -0.028736 - 0.028736 - 0.028736 = -0.086$ in

Percentage error comparing to Planar Frame and Truss Analysis, version 1.54, of Structural Analysis, Inc.

$$\text{Horizontal displacement} = \frac{0.231 - 0.229}{0.229} \cdot 100 = 1 \quad \%$$

$$\text{Vertical displacement} = \frac{0.087 - 0.086}{0.086} \cdot 100 = 1.16 \quad \%$$

It matches the result from Planar Frame and Truss Analysis in the horizontal and vertical displacements.

TABLE 1
Comparison of Lateral Displacement between Continuum Model and Plannar Frame Structural Analysis

COMPARISON OF RESULT		
Lateral Displacement	Continuum Model (in)	Plannar Frame (in)
1st Floor	0.139	0.102
2nd Floor	0.207	0.193
3rd Floor	0.229	0.231

As compared to the results obtained from Planar Frame and Truss Analysis, version 1.54, of Structural Analysis Inc., the floor top displacements are almost identical.

4-3. 20 STORY X-Y FRAME

For a 20 story frame as shown in Fig. 11, a global stiffness matrix has been derived in matrix 5 through the same way as the 3 story frame. To simply the process again, the properties of one shape member has been applied to all members.

Matrix 5 Global Stiffness Matrix for the two bays 20 story frame

Total Columns	N = 3	
Length of Columns	L = 144	in
Shear Area of Columns	As = 51.8	in^2
Axial Area of Columns	Ai = 51.8	in^2
Moment Inertia of Col.	Ii = 2140	in^4
Elasticity Modulus	E = 29000	ksi
Rigidity Modulus	G = 12000	ksi
Dist. to Neu.-Axis	Yi = 72	in
Vertical Load	P = 58.8	kips
Shear Force	V = 2.88	kips

$$
\begin{bmatrix}
\frac{NEAi}{L} & 0 & 0 & 0 & 0 & \frac{NEAi}{L} & 0 & 0 & 0 \\
0 & \frac{N12EIi}{L^3}+\frac{6GAs}{5L} & \frac{N6EIi}{L^2}+\frac{GAs}{10} & \frac{GAs}{10} & \frac{4GAs}{5} & 0 & \frac{N12EIi}{L^3}+\frac{6GAs}{5L} & \frac{N6EIi}{L^2}+\frac{GAs}{10} & \frac{GAs}{10} \\
0 & \frac{N6EIi}{L^2}+\frac{GAs}{10} & \frac{N4EIi}{L}+\frac{2GAsL}{15} & \frac{7GAsL}{60} & \frac{GAsL}{15} & 0 & \frac{N6EIi}{L^2}+\frac{GAs}{10} & \frac{N2EIi}{L}+\frac{GAsL}{30} & 0 \\
0 & \frac{GAs}{10} & \frac{7GAsL}{60} & \frac{N7EAiYi^2}{3L}+\frac{2GAsL}{15} & \frac{N8EAiYi^2}{3L}+\frac{GAsL}{15} & 0 & \frac{GAs}{10} & 0 & \frac{NEAiYi^2}{3L}+\frac{GAsL}{30} \\
0 & \frac{4GAs}{5} & \frac{GAsL}{15} & \frac{N8EAiYi^2}{3L}+\frac{GAsL}{15} & \frac{N16EAiYi^2}{3L}+\frac{8GAsL}{15} & 0 & \frac{4GAs}{5} & \frac{GAsL}{15} & \frac{N8EAiYi^2}{3L}+\frac{GAsL}{15} \\
\frac{NEAi}{L} & 0 & 0 & 0 & 0 & \frac{NEAi}{L} & 0 & 0 & 0 \\
0 & \frac{N12EIi}{L^3}+\frac{6GAs}{5L} & \frac{N6EIi}{L^2}+\frac{GAs}{10} & \frac{GAs}{10} & \frac{4GAs}{5} & 0 & \frac{N12EIi}{L^3}+\frac{6GAs}{5L} & \frac{N6EIi}{L^2}+\frac{GAs}{10} & \frac{GAs}{10} \\
0 & \frac{N6EIi}{L^2}+\frac{GAs}{10} & \frac{N2EIi}{L}+\frac{GAsL}{30} & 0 & \frac{GAsL}{15} & 0 & \frac{N6EIi}{L^2}+\frac{GAs}{10} & \frac{N4EIi}{L}+\frac{2GAsL}{15} & \frac{7GAsL}{60} \\
0 & \frac{GAs}{10} & 0 & \frac{NEAiYi^2}{3L}+\frac{GAsL}{30} & \frac{N8EAiYi^2}{3L}+\frac{GAsL}{15} & 0 & \frac{GAs}{10} & \frac{7GAsL}{60} & \frac{N7EAiYi^2}{3L}+\frac{2GAsL}{15}
\end{bmatrix}
$$

The formation of the following 4x4 stiffness matrices and their operation with the four matrix-elements force and displacement vector matrices refers to the explanation in the 3 story frame example on page 50.

Matrix 6 Matrix Operation-1st Floor of 20 Story Frame

$$\begin{bmatrix} \frac{N\cdot 4\cdot E\cdot Ii}{L}-\frac{2\cdot GAs\cdot L}{15} & 0 & \frac{N\cdot 6\cdot E\cdot Ii}{L^2}-\frac{GAs}{10} & \frac{N\cdot 2\cdot E\cdot Ii}{L}-\frac{GAs\cdot L}{30} \\ 0 & \frac{N\cdot E\cdot Ai}{L} & 0 & 0 \\ \frac{-N\cdot 6\cdot E\cdot Ii}{L^2}-\frac{GAs}{10} & 0 & \frac{N\cdot 12\cdot E\cdot Ii}{L^3}-\frac{6\cdot GAs}{5\cdot L} & \frac{-N\cdot 6\cdot E\cdot Ii}{L^2}-\frac{GAs}{10} \\ \frac{N\cdot 2\cdot E\cdot Ii}{L}-\frac{GAs\cdot L}{30} & 0 & \frac{N\cdot 6\cdot E\cdot Ii}{L^2}-\frac{GAs}{10} & \frac{N\cdot 4\cdot E\cdot Ii}{L}-\frac{2\cdot GAs\cdot L}{15} \end{bmatrix}^{-1} = \begin{bmatrix} 82944 & 0.005 \\ -P & -0.002 \\ 0.5V & 0.013 \\ -74856.96 & -0.004 \end{bmatrix}$$

Lateral displacement on the top of the 1st floor

$= 0.013 - 1440.005 = 0.733$ in.

Matrix 7 Matrix Operation-2nd Floor of 20 Story Frame

$$\begin{bmatrix} \frac{N\cdot 4\cdot E\cdot Ii}{L}-\frac{2\cdot GAs\cdot L}{15} & 0 & \frac{-N\cdot 6\cdot E\cdot Ii}{L^2}-\frac{GAs}{10} & \frac{N\cdot 2\cdot E\cdot Ii}{L}-\frac{GAs\cdot L}{30} \\ 0 & \frac{N\cdot E\cdot Ai}{L} & 0 & 0 \\ \frac{-N\cdot 6\cdot E\cdot Ii}{L^2}-\frac{GAs}{10} & 0 & \frac{N\cdot 12\cdot E\cdot Ii}{L^3}-\frac{6\cdot GAs}{5\cdot L} & \frac{-N\cdot 6\cdot E\cdot Ii}{L^2}-\frac{GAs}{10} \\ \frac{N\cdot 2\cdot E\cdot Ii}{L}-\frac{GAs\cdot L}{30} & 0 & \frac{-N\cdot 6\cdot E\cdot Ii}{L^2}-\frac{GAs}{10} & \frac{N\cdot 4\cdot E\cdot Ii}{L}-\frac{2\cdot GAs\cdot L}{15} \end{bmatrix}^{-1} = \begin{bmatrix} 74856.96 & 0.004 \\ -P & -0.002 \\ 0.5V & 0.013 \\ -67184.64 & -0.004 \end{bmatrix}$$

Lateraldisplacement on the top of the 2nd floor

$= 0.013 - 1440.004 - 0.733 = 1.322$ in.

Matrix 8 Matrix Operation-3rd Floor of 20 Story Frame

$$\begin{bmatrix} \frac{N\cdot 4\cdot E\cdot Ii}{L}-\frac{2\cdot GAs\cdot L}{15} & 0 & \frac{N\cdot 6\cdot E\cdot Ii}{L^2}-\frac{GAs}{10} & \frac{N\cdot 2\cdot E\cdot Ii}{L}-\frac{GAs\cdot L}{30} \\ 0 & \frac{N\cdot E\cdot Ai}{L} & 0 & 0 \\ \frac{-N\cdot 6\cdot E\cdot Ii}{L^2}-\frac{GAs}{10} & 0 & \frac{N\cdot 12\cdot E\cdot Ii}{L^3}-\frac{6\cdot GAs}{5\cdot L} & \frac{-N\cdot 6\cdot E\cdot Ii}{L^2}-\frac{GAs}{10} \\ \frac{N\cdot 2\cdot E\cdot Ii}{L}-\frac{GAs\cdot L}{30} & 0 & \frac{-N\cdot 6\cdot E\cdot Ii}{L^2}-\frac{GAs}{10} & \frac{N\cdot 4\cdot E\cdot Ii}{L}-\frac{2\cdot GAs\cdot L}{15} \end{bmatrix}^{-1} = \begin{bmatrix} 67184.64 & 0.004 \\ -P & -0.002 \\ 0.5V & 0.012 \\ 59927.04 & -0.003 \end{bmatrix}$$

Lateral displacement on the top of the 3rd floor

$= 0.012 - 1200.004 - 1.322 = 1.814$ in.

Matrix 9 Matrix Operation-4th Floor of 20 Story Frame

$$\begin{bmatrix} \frac{N\cdot 4\cdot E\cdot Ii}{L}-\frac{2\cdot GAs\cdot L}{15} & 0 & \frac{-N\cdot 6\cdot E\cdot Ii}{L^2}-\frac{GAs}{10} & \frac{N\cdot 2\cdot E\cdot Ii}{L}-\frac{GAs\cdot L}{30} \\ 0 & \frac{N\cdot E\cdot Ai}{L} & 0 & 0 \\ \frac{-N\cdot 6\cdot E\cdot Ii}{L^2}-\frac{GAs}{10} & 0 & \frac{N\cdot 12\cdot E\cdot Ii}{L^3}-\frac{6\cdot GAs}{5\cdot L} & \frac{-N\cdot 6\cdot E\cdot Ii}{L^2}-\frac{GAs}{10} \\ \frac{N\cdot 2\cdot E\cdot Ii}{L}-\frac{GAs\cdot L}{30} & 0 & \frac{-N\cdot 6\cdot E\cdot Ii}{L^2}-\frac{GAs}{10} & \frac{N\cdot 4\cdot E\cdot Ii}{L}-\frac{2\cdot GAs\cdot L}{15} \end{bmatrix}^{-1} = \begin{bmatrix} 59927.04 & 0.004 \\ -P & -0.002 \\ 0.5V & 0.011 \\ 53084.16 & -0.003 \end{bmatrix}$$

Lateral displacement on the top of the 4th floor

$= 0.011 - 1440.004 - 1.814 = 2.401$ in.

Matrix 10 Matrix Operation-5th Floor of 20 Story Frame

$$\begin{bmatrix} \frac{N\cdot 4\cdot E\cdot Ii}{L} - \frac{2\cdot GAs\cdot L}{15} & 0 & -\frac{N\cdot 6\cdot E\cdot Ii}{L^2} - \frac{GAs}{10} & \frac{N\cdot 2\cdot E\cdot Ii}{L} - \frac{GAs\cdot L}{30} \\ 0 & \frac{N\cdot E\cdot Ai}{L} & 0 & 0 \\ -\frac{N\cdot 6\cdot E\cdot Ii}{L^2} - \frac{GAs}{10} & 0 & \frac{N\cdot 12\cdot E\cdot Ii}{L^3} - \frac{6\cdot GAs}{5\cdot L} & \frac{N\cdot 6\cdot E\cdot Ii}{L^2} - \frac{GAs}{10} \\ \frac{N\cdot 2\cdot E\cdot Ii}{L} - \frac{GAs\cdot L}{30} & 0 & -\frac{N\cdot 6\cdot E\cdot Ii}{L^2} - \frac{GAs}{10} & \frac{N\cdot 4\cdot E\cdot Ii}{L} - \frac{2\cdot GAs\cdot L}{15} \end{bmatrix}^{-1} \begin{bmatrix} 53084.16 \\ P \\ 0.5V \\ -46656 \end{bmatrix} = \begin{bmatrix} 0.003 \\ -0.002 \\ 0.011 \\ -0.003 \end{bmatrix}$$

Lateral displacement on the top of the 5th floor

$= 0.011 - 1440.003 - 2.401 = 2.844$ in.

Matrix 11 Matrix Operation-6th Floor of 20 Story Frame

$$\begin{bmatrix} \frac{N\cdot 4\cdot E\cdot Ii}{L} - \frac{2\cdot GAs\cdot L}{15} & 0 & -\frac{N\cdot 6\cdot E\cdot Ii}{L^2} - \frac{GAs}{10} & \frac{N\cdot 2\cdot E\cdot Ii}{L} - \frac{GAs\cdot L}{30} \\ 0 & \frac{N\cdot E\cdot Ai}{L} & 0 & 0 \\ -\frac{N\cdot 6\cdot E\cdot Ii}{L^2} - \frac{GAs}{10} & 0 & \frac{N\cdot 12\cdot E\cdot Ii}{L^3} - \frac{6\cdot GAs}{5\cdot L} & -\frac{N\cdot 6\cdot E\cdot Ii}{L^2} - \frac{GAs}{10} \\ \frac{N\cdot 2\cdot E\cdot Ii}{L} - \frac{GAs\cdot L}{30} & 0 & -\frac{N\cdot 6\cdot E\cdot Ii}{L^2} - \frac{GAs}{10} & \frac{N\cdot 4\cdot E\cdot Ii}{L} - \frac{2\cdot GAs\cdot L}{15} \end{bmatrix}^{-1} \begin{bmatrix} 46656 \\ -P \\ 0.5V \\ -40642.56 \end{bmatrix} = \begin{bmatrix} 0.003 \\ -0.002 \\ 0.01 \\ -0.002 \end{bmatrix}$$

Lateral displacement on the top of the 6th floor

$= 0.01 - 1440.003 - 2.844 = 3.286$ in.

Matrix 12 Matrix Operation-7th Floor of 20 Story Frame

$$\begin{bmatrix} \frac{N\cdot 4\cdot E\cdot Ii}{L} - \frac{2\cdot GAs\cdot L}{15} & 0 & \frac{N\cdot 6\cdot E\cdot Ii}{L^2} - \frac{GAs}{10} & \frac{N\cdot 2\cdot E\cdot Ii}{L} - \frac{GAs\cdot L}{30} \\ 0 & \frac{N\cdot E\cdot Ai}{L} & 0 & 0 \\ \frac{N\cdot 6\cdot E\cdot Ii}{L^2} - \frac{GAs}{10} & 0 & \frac{N\cdot 12\cdot E\cdot Ii}{L^3} - \frac{6\cdot GAs}{5\cdot L} & \frac{N\cdot 6\cdot E\cdot Ii}{L^2} - \frac{GAs}{10} \\ \frac{N\cdot 2\cdot E\cdot Ii}{L} - \frac{GAs\cdot L}{30} & 0 & \frac{N\cdot 6\cdot E\cdot Ii}{L^2} - \frac{GAs}{10} & \frac{N\cdot 4\cdot E\cdot Ii}{L} - \frac{2\cdot GAs\cdot L}{15} \end{bmatrix} = \begin{bmatrix} 40642.56 & 0.002 \\ P & 0.002 \\ 0.5\cdot V & 0.009 \\ 35043.84 & 0.002 \end{bmatrix}$$

Lateral displacement on the top of the 7th floor

$= 0.009 - 144 0.002 - 3.286 = 3.583$ in.

Matrix 13 Matrix Operation-8th Floor of 20 Story Frame

$$\begin{bmatrix} \frac{N\cdot 4\cdot E\cdot Ii}{L} - \frac{2\cdot GAs\cdot L}{15} & 0 & \frac{N\cdot 6\cdot E\cdot Ii}{L^2} - \frac{GAs}{10} & \frac{N\cdot 2\cdot E\cdot Ii}{L} - \frac{GAs\cdot L}{30} \\ 0 & \frac{N\cdot E\cdot Ai}{L} & 0 & 0 \\ \frac{N\cdot 6\cdot E\cdot Ii}{L^2} - \frac{GAs}{10} & 0 & \frac{N\cdot 12\cdot E\cdot Ii}{L^3} - \frac{6\cdot GAs}{5\cdot L} & \frac{N\cdot 6\cdot E\cdot Ii}{L^2} - \frac{GAs}{10} \\ \frac{N\cdot 2\cdot E\cdot Ii}{L} - \frac{GAs\cdot L}{30} & 0 & \frac{N\cdot 6\cdot E\cdot Ii}{L^2} - \frac{GAs}{10} & \frac{N\cdot 4\cdot E\cdot Ii}{L} - \frac{2\cdot GAs\cdot L}{15} \end{bmatrix} = \begin{bmatrix} 35043.84 & 0.002 \\ P & 0.002 \\ 0.5\cdot V & 0.009 \\ 29859.84 & 0.002 \end{bmatrix}$$

Lateral displacement on the top of the 8th floor

$= 0.009 - 144 0.002 - 3.583 = 3.88$ in.

Matrix 14 Matrix Operation-9th Floor of 20 Story Frame

$$\begin{bmatrix} \frac{N\cdot 4\cdot E\cdot Ii}{L}-\frac{2\cdot GAs\cdot L}{15} & 0 & \frac{N\cdot 6\cdot E\cdot Ii}{L^2}-\frac{GAs}{10} & \frac{N\cdot 2\cdot E\cdot Ii}{L}-\frac{GAs\cdot L}{30} \\ 0 & \frac{N\cdot E\cdot Ai}{L} & 0 & 0 \\ \frac{N\cdot 6\cdot E\cdot Ii}{L^2}-\frac{GAs}{10} & 0 & \frac{N\cdot 12\cdot E\cdot Ii}{L^3}-\frac{6\cdot GAs}{5\cdot L} & -\frac{N\cdot 6\cdot E\cdot Ii}{L^2}-\frac{GAs}{10} \\ \frac{N\cdot 2\cdot E\cdot Ii}{L}-\frac{GAs\cdot L}{30} & 0 & \frac{N\cdot 6\cdot E\cdot Ii}{L^2}-\frac{GAs}{10} & \frac{N\cdot 4\cdot E\cdot Ii}{L}-\frac{2\cdot GAs\cdot L}{15} \end{bmatrix}^{-1} \begin{bmatrix} 29859.84 \\ -P \\ 0.5\cdot V \\ 25090.56 \end{bmatrix} = \begin{bmatrix} 0.002 \\ -0.002 \\ 0.008 \\ -0.001 \end{bmatrix}$$

Lateral displacement on the top of the 9th floor

$= 0.008 - 144\cdot 0.002 - 3.88 = 4.176$ in.

Matrix 15 Matrix Operation-10th Floor of 20 Story Frame

$$\begin{bmatrix} \frac{N\cdot 4\cdot E\cdot Ii}{L}-\frac{2\cdot GAs\cdot L}{15} & 0 & \frac{N\cdot 6\cdot E\cdot Ii}{L^2}-\frac{GAs}{10} & \frac{N\cdot 2\cdot E\cdot Ii}{L}-\frac{GAs\cdot L}{30} \\ 0 & \frac{N\cdot E\cdot Ai}{L} & 0 & 0 \\ \frac{N\cdot 6\cdot E\cdot Ii}{L^2}-\frac{GAs}{10} & 0 & \frac{N\cdot 12\cdot E\cdot Ii}{L^3}-\frac{6\cdot GAs}{5\cdot L} & -\frac{N\cdot 6\cdot E\cdot Ii}{L^2}-\frac{GAs}{10} \\ \frac{N\cdot 2\cdot E\cdot Ii}{L}-\frac{GAs\cdot L}{30} & 0 & -\frac{N\cdot 6\cdot E\cdot Ii}{L^2}-\frac{GAs}{10} & \frac{N\cdot 4\cdot E\cdot Ii}{L}-\frac{2\cdot GAs\cdot L}{15} \end{bmatrix}^{-1} \begin{bmatrix} 25090.56 \\ -P \\ 0.5\cdot V \\ -20736 \end{bmatrix} = \begin{bmatrix} 0.001 \\ -0.002 \\ 0.007 \\ -0.001 \end{bmatrix}$$

Lateral displacement on the top of the 10th floor

$= 0.007 - 144\cdot 0.001 - 4.176 = 4.327$ in.

Matrix 16 Matrix Operation-11th Floor of 20 Story Frame

$$\begin{bmatrix} \frac{N\cdot 4\cdot E\cdot Ii}{L}+\frac{2\cdot G\cdot As\cdot L}{15} & 0 & \frac{-N\cdot 6\cdot E\cdot Ii}{L^2}-\frac{G\cdot As}{10} & \frac{N\cdot 2\cdot E\cdot Ii}{L}-\frac{G\cdot As\cdot L}{30} \\ 0 & \frac{N\cdot E\cdot Ai}{L} & 0 & 0 \\ \frac{-N\cdot 6\cdot E\cdot Ii}{L^2}-\frac{G\cdot As}{10} & 0 & \frac{N\cdot 12\cdot E\cdot Ii}{L^3}+\frac{6\cdot G\cdot As}{5\cdot L} & \frac{-N\cdot 6\cdot E\cdot Ii}{L^2}-\frac{G\cdot As}{10} \\ \frac{N\cdot 2\cdot E\cdot Ii}{L}-\frac{G\cdot As\cdot L}{30} & 0 & \frac{-N\cdot 6\cdot E\cdot Ii}{L^2}-\frac{G\cdot As}{10} & \frac{N\cdot 4\cdot E\cdot Ii}{L}+\frac{2\cdot G\cdot As\cdot L}{15} \end{bmatrix}^{-1} \cdot \begin{bmatrix} 20736 \\ -P \\ 0.5\cdot V \\ -16796.16 \end{bmatrix} = \begin{bmatrix} 0.001 \\ -0.002 \\ 0.007 \\ -9.079\cdot 10^{-4} \end{bmatrix}$$

Lateral displacement on the top of the 11th floor

$= 0.007 + 144 \cdot 0.001 + 4.327 = 4.478$ in.

Matrix 17 Matrix Operation-12th Floor of 20 Story Frame

$$\begin{bmatrix} \frac{N\cdot 4\cdot E\cdot Ii}{L}+\frac{2\cdot G\cdot As\cdot L}{15} & 0 & \frac{-N\cdot 6\cdot E\cdot Ii}{L^2}-\frac{G\cdot As}{10} & \frac{N\cdot 2\cdot E\cdot Ii}{L}-\frac{G\cdot As\cdot L}{30} \\ 0 & \frac{N\cdot E\cdot Ai}{L} & 0 & 0 \\ \frac{-N\cdot 6\cdot E\cdot Ii}{L^2}-\frac{G\cdot As}{10} & 0 & \frac{N\cdot 12\cdot E\cdot Ii}{L^3}+\frac{6\cdot G\cdot As}{5\cdot L} & \frac{-N\cdot 6\cdot E\cdot Ii}{L^2}-\frac{G\cdot As}{10} \\ \frac{N\cdot 2\cdot E\cdot Ii}{L}-\frac{G\cdot As\cdot L}{30} & 0 & \frac{-N\cdot 6\cdot E\cdot Ii}{L^2}-\frac{G\cdot As}{10} & \frac{N\cdot 4\cdot E\cdot Ii}{L}+\frac{2\cdot G\cdot As\cdot L}{15} \end{bmatrix}^{-1} \cdot \begin{bmatrix} 16796.16 \\ -P \\ 0.5\cdot V \\ -13271.04 \end{bmatrix} = \begin{bmatrix} 0.001 \\ -0.002 \\ 0.006 \\ -7.117\cdot 10^{-4} \end{bmatrix}$$

Lateral displacement on the top of the 12th floor

$= 0.006 + 144 \cdot 0.001 + 4.478 = 4.628$ in.

Matrix 18 Matrix Operation-13th Floor of 20 Story Frame

$$\begin{bmatrix} \frac{N\cdot 4\cdot E\cdot Ii}{L}+\frac{2\cdot G\cdot As\cdot L}{15} & 0 & \frac{-N\cdot 6\cdot E\cdot Ii}{L^2}-\frac{G\cdot As}{10} & \frac{N\cdot 2\cdot E\cdot Ii}{L}-\frac{G\cdot As\cdot L}{30} \\ 0 & \frac{N\cdot E\cdot Ai}{L} & 0 & 0 \\ \frac{-N\cdot 6\cdot E\cdot Ii}{L^2}-\frac{G\cdot As}{10} & 0 & \frac{N\cdot 12\cdot E\cdot Ii}{L^3}+\frac{6\cdot G\cdot As}{5\cdot L} & \frac{-N\cdot 6\cdot E\cdot Ii}{L^2}-\frac{G\cdot As}{10} \\ \frac{N\cdot 2\cdot E\cdot Ii}{L}-\frac{G\cdot As\cdot L}{30} & 0 & \frac{-N\cdot 6\cdot E\cdot Ii}{L^2}-\frac{G\cdot As}{10} & \frac{N\cdot 4\cdot E\cdot Ii}{L}+\frac{2\cdot G\cdot As\cdot L}{15} \end{bmatrix}^{-1} \cdot \begin{bmatrix} 13271.04 \\ -P \\ 0.5\cdot V \\ -10160.64 \end{bmatrix} = \begin{bmatrix} 7.995\cdot 10^{-4} \\ -0.002 \\ 0.005 \\ -5.392\cdot 10^{-4} \end{bmatrix}$$

Lateral displacement on the top of the 13th floor

$= 0.005 + 144\cdot 7.995\cdot 10^{-4} + 4.628 = 4.748$ in.

Matrix 19 Matrix Operation-14th Floor of 20 Story Frame

$$\begin{bmatrix} \frac{N\cdot 4\cdot E\cdot Ii}{L}+\frac{2\cdot GAs\cdot L}{15} & 0 & \frac{-N\cdot 6\cdot E\cdot Ii}{L^2}-\frac{GAs}{10} & \frac{N\cdot 2\cdot E\cdot Ii}{L}-\frac{GAs\cdot L}{30} \\ 0 & \frac{N\cdot E\cdot Ai}{L} & 0 & 0 \\ \frac{-N\cdot 6\cdot E\cdot Ii}{L^2}-\frac{GAs}{10} & 0 & \frac{N\cdot 12\cdot E\cdot Ii}{L^3}+\frac{6\cdot GAs}{5\cdot L} & \frac{-N\cdot 6\cdot E\cdot Ii}{L^2}-\frac{GAs}{10} \\ \frac{N\cdot 2\cdot E\cdot Ii}{L}-\frac{GAs\cdot L}{30} & 0 & \frac{-N\cdot 6\cdot E\cdot Ii}{L^2}-\frac{GAs}{10} & \frac{N\cdot 4\cdot E\cdot Ii}{L}+\frac{2\cdot GAs\cdot L}{15} \end{bmatrix}^{-1} \cdot \begin{bmatrix} 10160.64 \\ -P \\ 0.5\cdot V \\ -7464.96 \end{bmatrix} = \begin{bmatrix} 6.166\,10^{-4} \\ -0.002 \\ 0.005 \\ -3.904\,10^{-4} \end{bmatrix}$$

Lateral displacement on the top of the 14th floor

$= 0.005 + 1446.166\,10^{-4} + 4.748 = 4.842$ in.

Matrix 20 Matrix Operation-15th Floor of 20 Story Frame

$$\begin{bmatrix} \frac{N\cdot 4\cdot E\cdot Ii}{L}+\frac{2\cdot G\cdot As\cdot L}{15} & 0 & \frac{-N\cdot 6\cdot E\cdot Ii}{L^2}-\frac{G\cdot As}{10} & \frac{N\cdot 2\cdot E\cdot Ii}{L}-\frac{G\cdot As\cdot L}{30} \\ 0 & \frac{N\cdot E\cdot Ai}{L} & 0 & 0 \\ \frac{-N\cdot 6\cdot E\cdot Ii}{L^2}-\frac{G\cdot As}{10} & 0 & \frac{N\cdot 12\cdot E\cdot Ii}{L^3}+\frac{6\cdot G\cdot As}{5\cdot L} & \frac{-N\cdot 6\cdot E\cdot Ii}{L^2}-\frac{G\cdot As}{10} \\ \frac{N\cdot 2\cdot E\cdot Ii}{L}-\frac{G\cdot As\cdot L}{30} & 0 & \frac{-N\cdot 6\cdot E\cdot Ii}{L^2}-\frac{G\cdot As}{10} & \frac{N\cdot 4\cdot E\cdot Ii}{L}+\frac{2\cdot G\cdot As\cdot L}{15} \end{bmatrix}^{-1} \cdot \begin{bmatrix} 7464.96 \\ -P \\ 0.5\cdot V \\ -5184 \end{bmatrix} = \begin{bmatrix} 4.574\cdot 10^{-4} \\ -0.002 \\ 0.004 \\ -2.653\cdot 10^{-4} \end{bmatrix}$$

Lateral displacement on the top of the 15 floor

$= 0.004 + 1444.574\,10^{-4} + 4.842 = 4.912$ in.

Matrix 21 Matrix Operation-16th Floor of 20 Story Frame

$$\begin{bmatrix} \frac{N\cdot 4\cdot E\cdot Ii}{L}+\frac{2\cdot G\cdot As\cdot L}{15} & 0 & \frac{-N\cdot 6\cdot E\cdot Ii}{L^2}-\frac{G\cdot As}{10} & \frac{N\cdot 2\cdot E\cdot Ii}{L}-\frac{G\cdot As\cdot L}{30} \\ 0 & \frac{N\cdot E\cdot Ai}{L} & 0 & 0 \\ \frac{-N\cdot 6\cdot E\cdot Ii}{L^2}-\frac{G\cdot As}{10} & 0 & \frac{N\cdot 12\cdot E\cdot Ii}{L^3}+\frac{6\cdot G\cdot As}{5\cdot L} & \frac{-N\cdot 6\cdot E\cdot Ii}{L^2}-\frac{G\cdot As}{10} \\ \frac{N\cdot 2\cdot E\cdot Ii}{L}-\frac{G\cdot As\cdot L}{30} & 0 & \frac{-N\cdot 6\cdot E\cdot Ii}{L^2}-\frac{G\cdot As}{10} & \frac{N\cdot 4\cdot E\cdot Ii}{L}+\frac{2\cdot G\cdot As\cdot L}{15} \end{bmatrix}^{-1} \cdot \begin{bmatrix} 5184 \\ -P \\ 0.5\cdot V \\ -3317.76 \end{bmatrix} = \begin{bmatrix} 3.219\cdot 10^{-4} \\ -0.002 \\ 0.003 \\ -1.638\cdot 10^{-4} \end{bmatrix}$$

Lateral displacement on the top of the 16th floor

$= 0.003 + 144\cdot 3.219\cdot 10^{-4} + 4.912 = 4.961$ in.

Matrix 22 Matrix Operation-17th Floor of 20 Story Frame

$$\begin{bmatrix} \frac{N\cdot 4\cdot E\cdot Ii}{L}+\frac{2\cdot G\cdot As\cdot L}{15} & 0 & \frac{-N\cdot 6\cdot E\cdot Ii}{L^2}-\frac{G\cdot As}{10} & \frac{N\cdot 2\cdot E\cdot Ii}{L}-\frac{G\cdot As\cdot L}{30} \\ 0 & \frac{N\cdot E\cdot Ai}{L} & 0 & 0 \\ \frac{-N\cdot 6\cdot E\cdot Ii}{L^2}-\frac{G\cdot As}{10} & 0 & \frac{N\cdot 12\cdot E\cdot Ii}{L^3}+\frac{6\cdot G\cdot As}{5\cdot L} & \frac{-N\cdot 6\cdot E\cdot Ii}{L^2}-\frac{G\cdot As}{10} \\ \frac{N\cdot 2\cdot E\cdot Ii}{L}-\frac{G\cdot As\cdot L}{30} & 0 & \frac{-N\cdot 6\cdot E\cdot Ii}{L^2}-\frac{G\cdot As}{10} & \frac{N\cdot 4\cdot E\cdot Ii}{L}+\frac{2\cdot G\cdot As\cdot L}{15} \end{bmatrix}^{-1} \cdot \begin{bmatrix} 3317.76 \\ -P \\ 0.5\cdot V \\ -1866.24 \end{bmatrix} = \begin{bmatrix} 2.1\cdot 10^{-4} \\ -0.002 \\ 0.003 \\ -8.611\cdot 10^{-5} \end{bmatrix}$$

Lateral displacement on the top of the 17th floor

$= 0.003 + 1442.1\cdot 10^{-4} + 4.961 = 4.994$ in.

Matrix 23 Matrix Operation-18th Floor of 20 Story Frame

$$\begin{bmatrix} \frac{N\cdot 4\cdot E\cdot Ii}{L}+\frac{2\cdot GAs\cdot L}{15} & 0 & \frac{-N\cdot 6\cdot E\cdot Ii}{L^2}-\frac{GAs}{10} & \frac{N\cdot 2\cdot E\cdot Ii}{L}-\frac{GAs\cdot L}{30} \\ 0 & \frac{N\cdot E\cdot Ai}{L} & 0 & 0 \\ \frac{-N\cdot 6\cdot E\cdot Ii}{L^2}-\frac{GAs}{10} & 0 & \frac{N\cdot 12\cdot E\cdot Ii}{L^3}+\frac{6\cdot GAs}{5\cdot L} & \frac{-N\cdot 6\cdot E\cdot Ii}{L^2}-\frac{GAs}{10} \\ \frac{N\cdot 2\cdot E\cdot Ii}{L}-\frac{GAs\cdot L}{30} & 0 & \frac{-N\cdot 6\cdot E\cdot Ii}{L^2}-\frac{GAs}{10} & \frac{N\cdot 4\cdot E\cdot Ii}{L}+\frac{2\cdot GAs\cdot L}{15} \end{bmatrix}^{-1} \cdot \begin{bmatrix} 1866.24 \\ -P \\ 0.5V \\ -829.44 \end{bmatrix} = \begin{bmatrix} 1.219\,10^{-4} \\ -0.002 \\ 0.002 \\ -3.208\,10^{-5} \end{bmatrix}$$

Lateral displacement on the top of the 18th floor

$= 0.002 + 1441.219\,10^{-4} + 4.994 = 5.014$ in.

Matrix 24 Matrix Operation-19th Floor of 20 Story Frame

$$\begin{bmatrix} \frac{N\cdot 4\cdot E\cdot Ii}{L}+\frac{2\cdot G\cdot As\cdot L}{15} & 0 & \frac{-N\cdot 6\cdot E\cdot Ii}{L^2}-\frac{G\cdot As}{10} & \frac{N\cdot 2\cdot E\cdot Ii}{L}-\frac{G\cdot As\cdot L}{30} \\ 0 & \frac{N\cdot E\cdot Ai}{L} & 0 & 0 \\ \frac{-N\cdot 6\cdot E\cdot Ii}{L^2}-\frac{G\cdot As}{10} & 0 & \frac{N\cdot 12\cdot E\cdot Ii}{L^3}+\frac{6\cdot G\cdot As}{5\cdot L} & \frac{-N\cdot 6\cdot E\cdot Ii}{L^2}-\frac{G\cdot As}{10} \\ \frac{N\cdot 2\cdot E\cdot Ii}{L}-\frac{G\cdot As\cdot L}{30} & 0 & \frac{-N\cdot 6\cdot E\cdot Ii}{L^2}-\frac{G\cdot As}{10} & \frac{N\cdot 4\cdot E\cdot Ii}{L}+\frac{2\cdot G\cdot As\cdot L}{15} \end{bmatrix}^{-1} \cdot \begin{bmatrix} 829.44 \\ -P \\ 0.5\cdot V \\ -207.36 \end{bmatrix} = \begin{bmatrix} 5.75\cdot 10^{-5} \\ -0.002 \\ 0.001 \\ -1.734\cdot 10^{-6} \end{bmatrix}$$

Lateral displacement on the top of the 19th floor

$= 0.001 + 144\cdot 5.75\cdot 10^{-5} + 5.014 = 5.023$ in.

Matrix 25 Matrix Operation-20th Floor of 20 Story Frame

$$\begin{bmatrix} \frac{N\cdot 4\cdot E\cdot Ii}{L}+\frac{2\cdot G\cdot As\cdot L}{15} & 0 & \frac{-N\cdot 6\cdot E\cdot Ii}{L^2}-\frac{G\cdot As}{10} & \frac{N\cdot 2\cdot E\cdot Ii}{L}-\frac{G\cdot As\cdot L}{30} \\ 0 & \frac{N\cdot E\cdot Ai}{L} & 0 & 0 \\ \frac{-N\cdot 6\cdot E\cdot Ii}{L^2}-\frac{G\cdot As}{10} & 0 & \frac{N\cdot 12\cdot E\cdot Ii}{L^3}+\frac{6\cdot G\cdot As}{5\cdot L} & \frac{-N\cdot 6\cdot E\cdot Ii}{L^2}-\frac{G\cdot As}{10} \\ \frac{N\cdot 2\cdot E\cdot Ii}{L}-\frac{G\cdot As\cdot L}{30} & 0 & \frac{-N\cdot 6\cdot E\cdot Ii}{L^2}-\frac{G\cdot As}{10} & \frac{N\cdot 4\cdot E\cdot Ii}{L}+\frac{2\cdot G\cdot As\cdot L}{15} \end{bmatrix}^{-1} \cdot \begin{bmatrix} 207.36 \\ -P \\ 0.5\cdot V \\ 0 \end{bmatrix} = \begin{bmatrix} 1.676\cdot 10^{-5} \\ -0.002 \\ 6.672\cdot 10^{-4} \\ 4.915\cdot 10^{-6} \end{bmatrix}$$

Lateral displacement on the top of the 20th floor

$= 6.672\,10^{-4} + 144\cdot 1.676\,10^{-5} + 5.023 = 5.026$ in.

ANALYSIS REPORT FOR THE 20 STORY FRAME

Total horizontal displacement on the top of the 20th floor

$= 5.026$ in

Vertical displacement for the entire frame

$= -0.002 - 0.002 - 0.002 - 0.002 - 0.002 - 0.002 - 0.002 - 0.002 - 0.002 - 0.002 = -0.02$

$-0.02 - 0.002 - 0.002 - 0.002 - 0.002 - 0.002 - 0.002 - 0.002 - 0.002 - 0.002 = -0.038$

$-.038 - 0.002 = -0.04$

Percentage error comparing to Risa-3D

Horizontal displacement $\frac{5.026 - 4.7}{4.7} \cdot 100 = 6.936\ \%$

Vertical displacement $\frac{-0.04 - (-0.038)}{-0.038} \cdot 100 = 5.26\ \%$

It matches the result from a Risa-3D analysis, shown in Appendix H, in the horiz and vertical displacement.

TABLE 2 Comparison of Preparation and Computer Time

COMPARISON OF PREPARATION & COMPUTER TIME		
Data Preparation	Continuum Model	Discrete Model / Risa 3-D
Data Drafting / Input	20 minutes	23 minutes
Computer Time	2 minutes	3 seconds

4-4. 40 STORY X-Y FRAME

Theoretically, the 40 story frame is 20 more stories extension of the 20 story example , the global stiffness matrix has been using the same one as in the 20 story frame.

Matrix 26 Global Stiffness Matrix for the two bays 40 story frame

Total Columns	N =3
Length of Columns	L =144 in
Shear Areaof Columns	As =51.8 in^2
Axial Area of Columns	Ai =51.8 in^2
Moment Inertiaof Col.	Ii =2140 in^4
Elasticity Modulus	E =29000 ksi
Rigidity Modulus	G =12000 ksi
Dist. to Neu.-Axis	Yi =72 in
Vertical Load	P =58.8 kips
Shear Force	V =2.88 kips

$$\begin{bmatrix}
\frac{NEAi}{L} & 0 & 0 & 0 & 0 & \frac{-NEAi}{L} & 0 & 0 & 0 \\
0 & \frac{N12EIi}{L^3}+\frac{6GAs}{5L} & \frac{N6EIi}{L^2}+\frac{GAs}{10} & \frac{GAs}{10} & \frac{4GAs}{5} & 0 & \frac{-N12EIi}{L^3}-\frac{6GAs}{5L} & \frac{N6EIi}{L^2}-\frac{GAs}{10} & \frac{GAs}{10} \\
0 & \frac{N6EIi}{L^2}-\frac{GAs}{10} & \frac{N4EIi}{L}+\frac{2GAsL}{15} & \frac{-7GAsL}{60} & \frac{GAsL}{15} & 0 & \frac{-N6EIi}{L^2}-\frac{GAs}{10} & \frac{N2EIi}{L}-\frac{GAsL}{30} & 0 \\
0 & \frac{GAs}{10} & \frac{-7GAsL}{60} & \frac{N7EAiYI^2}{3L}-\frac{2GAsL}{15} & \frac{-N8EAiYI^2}{3L}-\frac{GAsL}{15} & 0 & \frac{GAs}{10} & 0 & \frac{NEAiYI^2}{3L}-\frac{GAsL}{30} \\
0 & \frac{4GAs}{5} & \frac{GAsL}{15} & \frac{-N8EAiYI^2}{3L}-\frac{GAsL}{15} & \frac{N16EAiYI^2}{3L}-\frac{8GAsL}{15} & 0 & \frac{-4GAs}{5} & \frac{GAsL}{15} & \frac{N8EAiYI^2}{3L}-\frac{GAsL}{15} \\
\frac{NEAi}{L} & 0 & 0 & 0 & 0 & \frac{NEAi}{L} & 0 & 0 & 0 \\
0 & \frac{-N12EIi}{L^3}-\frac{6GAs}{5L} & \frac{-N6EIi}{L^2}-\frac{GAs}{10} & \frac{-GAs}{10} & \frac{-4GAs}{5} & 0 & \frac{N12EIi}{L^3}+\frac{6GAs}{5L} & \frac{-N6EIi}{L^2}-\frac{GAs}{10} & \frac{-GAs}{10} \\
0 & \frac{N6EIi}{L^2}-\frac{GAs}{10} & \frac{N2EIi}{L}-\frac{GAsL}{30} & 0 & \frac{GAsL}{15} & 0 & \frac{-N6EIi}{L^2}-\frac{GAs}{10} & \frac{N4EIi}{L}+\frac{2GAsL}{15} & \frac{-7GAsL}{60} \\
0 & \frac{GAs}{10} & 0 & \frac{NEAiYI^2}{3L}-\frac{GAsL}{30} & \frac{-N8EAiYI^2}{3L}-\frac{GAsL}{15} & 0 & \frac{-GAs}{10} & \frac{7GAsL}{60} & \frac{N7EAiYI^2}{3L}-\frac{2GAsL}{15}
\end{bmatrix}$$

Again, the formation of the following 4x4 stiffness matrices and their operation with the four matrix-elements force and displacement vector matrices refers to the same explanation in the 3 story frame on page 40. Since the procedures are same as the 20 story frame example, only every fifth level matrices operation are shown below.

Matrix 27 Matrix Operation -5th Floor of 40 Story Frame

$$\begin{bmatrix} \frac{N\cdot 4\cdot E\cdot Ii}{L}-\frac{2\cdot G\cdot As\cdot L}{15} & 0 & \frac{-N\cdot 6\cdot E\cdot Ii}{L^2}-\frac{G\cdot As}{10} & \frac{N\cdot 2\cdot E\cdot Ii}{L}-\frac{G\cdot As\cdot L}{30} \\ 0 & \frac{N\cdot E\cdot Ai}{L} & 0 & 0 \\ \frac{-N\cdot 6\cdot E\cdot Ii}{L^2}-\frac{G\cdot As}{10} & 0 & \frac{N\cdot 12\cdot E\cdot Ii}{L^3}-\frac{6\cdot G\cdot As}{5\cdot L} & \frac{-N\cdot 6\cdot E\cdot Ii}{L^2}-\frac{G\cdot As}{10} \\ \frac{N\cdot 2\cdot E\cdot Ii}{L}-\frac{G\cdot As\cdot L}{30} & 0 & \frac{-N\cdot 6\cdot E\cdot Ii}{L^2}-\frac{G\cdot As}{10} & \frac{N\cdot 4\cdot E\cdot Ii}{L}-\frac{2\cdot G\cdot As\cdot L}{15} \end{bmatrix}^{-1} \begin{bmatrix} 268738.56 \\ -P \\ 0.5\cdot V \\ 254016 \end{bmatrix} = \begin{bmatrix} 0.016 \\ -0.002 \\ 0.024 \\ -0.014 \end{bmatrix}$$

Lateral displacement on the top of the 5th floor

$= 0.024 - 144\cdot 0.016 - 10.183 = 12.511$ in.

Matrix 28 Matrix Operation -10th Floor of 40 Story Frame

$$\begin{bmatrix} \frac{N\cdot 4\cdot E\cdot Ii}{L}-\frac{2\cdot G\cdot As\cdot L}{15} & 0 & \frac{-N\cdot 6\cdot E\cdot Ii}{L^2}-\frac{G\cdot As}{10} & \frac{N\cdot 2\cdot E\cdot Ii}{L}-\frac{G\cdot As\cdot L}{30} \\ 0 & \frac{N\cdot E\cdot Ai}{L} & 0 & 0 \\ \frac{-N\cdot 6\cdot E\cdot Ii}{L^2}-\frac{G\cdot As}{10} & 0 & \frac{N\cdot 12\cdot E\cdot Ii}{L^3}-\frac{6\cdot G\cdot As}{5\cdot L} & \frac{-N\cdot 6\cdot E\cdot Ii}{L^2}-\frac{G\cdot As}{10} \\ \frac{N\cdot 2\cdot E\cdot Ii}{L}-\frac{G\cdot As\cdot L}{30} & 0 & \frac{-N\cdot 6\cdot E\cdot Ii}{L^2}-\frac{G\cdot As}{10} & \frac{N\cdot 4\cdot E\cdot Ii}{L}-\frac{2\cdot G\cdot As\cdot L}{15} \end{bmatrix}^{-1} \begin{bmatrix} 199272.76 \\ -P \\ 0.5\cdot V \\ -186624 \end{bmatrix} = \begin{bmatrix} 0.012 \\ -0.002 \\ 0.021 \\ -0.011 \end{bmatrix}$$

Lateral displacement on the top of the 10th floor

$= 0.021 - 144\cdot 0.012 - 20.376 = 22.125$ in.

Matrix 29 Matrix Operation 15th Floor of 40 Story Frame

$$\begin{bmatrix} \frac{N\cdot 4\cdot E\cdot Ii}{L} - \frac{2\cdot GAs\cdot L}{15} & 0 & \frac{-N\cdot 6\cdot E\cdot Ii}{L^2} - \frac{GAs}{10} & \frac{N\cdot 2\cdot E\cdot Ii}{L} - \frac{GAs\cdot L}{30} \\ 0 & \frac{N\cdot E\cdot Ai}{L} & 0 & 0 \\ \frac{-N\cdot 6\cdot E\cdot Ii}{L^2} - \frac{GAs}{10} & 0 & \frac{N\cdot 12\cdot E\cdot Ii}{L^3} - \frac{6\cdot GAs}{5\cdot L} & \frac{-N\cdot 6\cdot E\cdot Ii}{L^2} - \frac{GAs}{10} \\ \frac{N\cdot 2\cdot E\cdot Ii}{L} - \frac{GAs\cdot L}{30} & 0 & \frac{-N\cdot 6\cdot E\cdot Ii}{L^2} - \frac{GAs}{10} & \frac{N\cdot 4\cdot E\cdot Ii}{L} - \frac{2\cdot GAs\cdot L}{15} \end{bmatrix}^{-1} \begin{bmatrix} 140175.36 \\ P \\ 0.5\cdot V \\ 129600 \end{bmatrix} = \begin{bmatrix} 0.008 \\ -0.002 \\ 0.017 \\ -0.007 \end{bmatrix}$$

Lateral displacement on the top of the 15th floor

$= 0.017 - 144 \cdot 0.008 - 27.817 = 28.986$ in.

Matrix 30 Matrix Operation -20th Floor of 40 Story Frame

$$\begin{bmatrix} \frac{N\cdot 4\cdot E\cdot Ii}{L} - \frac{2\cdot GAs\cdot L}{15} & 0 & \frac{-N\cdot 6\cdot E\cdot Ii}{L^2} - \frac{GAs}{10} & \frac{N\cdot 2\cdot E\cdot Ii}{L} - \frac{GAs\cdot L}{30} \\ 0 & \frac{N\cdot E\cdot Ai}{L} & 0 & 0 \\ \frac{N\cdot 6\cdot E\cdot Ii}{L^2} - \frac{GAs}{10} & 0 & \frac{N\cdot 12\cdot E\cdot Ii}{L^3} - \frac{6\cdot GAs}{5\cdot L} & \frac{-N\cdot 6\cdot E\cdot Ii}{L^2} - \frac{GAs}{10} \\ \frac{N\cdot 2\cdot E\cdot Ii}{L} - \frac{GAs\cdot L}{30} & 0 & \frac{-N\cdot 6\cdot E\cdot Ii}{L^2} - \frac{GAs}{10} & \frac{N\cdot 4\cdot E\cdot Ii}{L} - \frac{2\cdot GAs\cdot L}{15} \end{bmatrix}^{-1} \begin{bmatrix} 91445.76 \\ -P \\ 0.5\cdot V \\ -82944 \end{bmatrix} = \begin{bmatrix} 0.005 \\ -0.002 \\ 0.014 \\ -0.005 \end{bmatrix}$$

Lateral displacement on the top of the 20th floor

$= 0.014 - 144 \cdot 0.005 - 32.937 = 33.671$ in.

Matrix 31 Matrix Operation -25th Floor of 40 Story Frame

$$\begin{bmatrix} \frac{N\cdot 4\cdot E\cdot Ii}{L} - \frac{2\cdot GAs\cdot L}{15} & 0 & \frac{-N\cdot 6\cdot E\cdot Ii}{L^2} - \frac{GAs}{10} & \frac{N\cdot 2\cdot E\cdot Ii}{L} - \frac{GAs\cdot L}{30} \\ 0 & \frac{N\cdot E\cdot Ai}{L} & 0 & 0 \\ \frac{-N\cdot 6\cdot E\cdot Ii}{L^2} - \frac{GAs}{10} & 0 & \frac{N\cdot 12\cdot E\cdot Ii}{L^3} - \frac{6\cdot GAs}{5\cdot L} & \frac{-N\cdot 6\cdot E\cdot Ii}{L^2} - \frac{GAs}{10} \\ \frac{N\cdot 2\cdot E\cdot Ii}{L} - \frac{GAs\cdot L}{30} & 0 & \frac{-N\cdot 6\cdot E\cdot Ii}{L^2} - \frac{GAs}{10} & \frac{N\cdot 4\cdot E\cdot Ii}{L} - \frac{2\cdot GAs\cdot L}{15} \end{bmatrix}^{-1} = \begin{bmatrix} 53084.16 & 0.003 \\ P & -0.002 \\ 0.5\cdot V & 0.011 \\ 46656 & -0.003 \end{bmatrix}$$

Lateral displacement on the top of the 25th floor

$= 0.011 - 144\cdot 0.003 - 36.072 = 36.515$ in.

Matrix 32 Matrix Operation -30th Floor of 40 Story Frame

$$\begin{bmatrix} \frac{N\cdot 4\cdot E\cdot Ii}{L} - \frac{2\cdot GAs\cdot L}{15} & 0 & \frac{-N\cdot 6\cdot E\cdot Ii}{L^2} - \frac{GAs}{10} & \frac{N\cdot 2\cdot E\cdot Ii}{L} - \frac{GAs\cdot L}{30} \\ 0 & \frac{N\cdot E\cdot Ai}{L} & 0 & 0 \\ \frac{N\cdot 6\cdot E\cdot Ii}{L^2} - \frac{GAs}{10} & 0 & \frac{N\cdot 12\cdot E\cdot Ii}{L^3} - \frac{6\cdot GAs}{5\cdot L} & \frac{-N\cdot 6\cdot E\cdot Ii}{L^2} - \frac{GAs}{10} \\ \frac{N\cdot 2\cdot E\cdot Ii}{L} - \frac{GAs\cdot L}{30} & 0 & \frac{-N\cdot 6\cdot E\cdot Ii}{L^2} - \frac{GAs}{10} & \frac{N\cdot 4\cdot E\cdot Ii}{L} - \frac{2\cdot GAs\cdot L}{15} \end{bmatrix}^{-1} = \begin{bmatrix} 25090.56 & 0.001 \\ P & -0.002 \\ 0.5\cdot V & 0.007 \\ 20736 & -0.001 \end{bmatrix}$$

Lateral displacement on the top of the 30th floor

$= 0.007 - 144\cdot 0.001 - 37.847 = 37.998$ in.

Matrix 33 Matrix Operation -35th Floor of 40 Story Frame

$$\begin{pmatrix} \frac{N\cdot 4\cdot E\cdot Ii}{L} - \frac{2\cdot GAs\cdot L}{15} & 0 & \frac{N\cdot 6\cdot E\cdot Ii}{L^2} - \frac{GAs}{10} & \frac{N\cdot 2\cdot E\cdot Ii}{L} - \frac{GAs\cdot L}{30} \\ 0 & \frac{N\cdot E\cdot Ai}{L} & 0 & 0 \\ \frac{N\cdot 6\cdot E\cdot Ii}{L^2} - \frac{GAs}{10} & 0 & \frac{N\cdot 12\cdot E\cdot Ii}{L^3} - \frac{6\cdot GAs}{5\cdot L} & \frac{N\cdot 6\cdot E\cdot Ii}{L^2} - \frac{GAs}{10} \\ \frac{N\cdot 2\cdot E\cdot Ii}{L} - \frac{GAs\cdot L}{30} & 0 & \frac{N\cdot 6\cdot E\cdot Ii}{L^2} - \frac{GAs}{10} & \frac{N\cdot 4\cdot E\cdot Ii}{L} - \frac{2\cdot GAs\cdot L}{15} \end{pmatrix}^{-1} \begin{pmatrix} 7464.96 \\ P \\ 0.5\cdot V \\ 5184 \end{pmatrix} = \begin{pmatrix} 4.574\cdot 10^{-4} \\ 0.002 \\ 0.004 \\ -2.653\cdot 10^{-4} \end{pmatrix}$$

Lateral displacement on the top of the 35 floor

$= 0.004 - 144\cdot 4.574\cdot 10^{-4} - 38.513 = 38.583$ in.

Matrix 34 Matrix Operation -40th Floor of 40 Story Frame

$$\begin{pmatrix} \frac{N\cdot 4\cdot E\cdot Ii}{L} - \frac{2\cdot GAs\cdot L}{15} & 0 & \frac{N\cdot 6\cdot E\cdot Ii}{L^2} - \frac{GAs}{10} & \frac{N\cdot 2\cdot E\cdot Ii}{L} - \frac{GAs\cdot L}{30} \\ 0 & \frac{N\cdot E\cdot Ai}{L} & 0 & 0 \\ \frac{N\cdot 6\cdot E\cdot Ii}{L^2} - \frac{GAs}{10} & 0 & \frac{N\cdot 12\cdot E\cdot Ii}{L^3} - \frac{6\cdot GAs}{5\cdot L} & \frac{N\cdot 6\cdot E\cdot Ii}{L^2} - \frac{GAs}{10} \\ \frac{N\cdot 2\cdot E\cdot Ii}{L} - \frac{GAs\cdot L}{30} & 0 & \frac{N\cdot 6\cdot E\cdot Ii}{L^2} - \frac{GAs}{10} & \frac{N\cdot 4\cdot E\cdot Ii}{L} - \frac{2\cdot GAs\cdot L}{15} \end{pmatrix}^{-1} \begin{pmatrix} 207.36 \\ P \\ 0.5V \\ 0 \end{pmatrix} = \begin{pmatrix} 1.67610^{-5} \\ -0.002 \\ 6.67210^{-4} \\ 4.91510^{-6} \end{pmatrix}$$

Lateral displacement on the top of the 40th floor

$=6.67210^{-4} - 1441.67610^{-5} - 38.694=38.697$ in.

ANALYSIS REPORT FOR THE 40 STORY FRAME

Total horizontal displacement on the top of the 40th floor

$= \quad 38.697 \quad \text{in}$

Vertical displacement for the entire frame

$= \ 40 \cdot (-0.002) = -0.08 \quad \text{in}$

Percentage error comparing to Risa-3D

$$\text{Horizontal displacement} = \frac{38.697 - 26.3}{26.3} \cdot 100 = 47 \ \%$$

$$\text{Vertical displacement} = \frac{0.08 - (-0.075)}{-0.075} \cdot 100 = 6.67 \ \%$$

It matches the result from an analysis with Risa-3D, as shown in Appendix I, in the vertical displacement and the difference in the horizontal displacement is due to the approximate strain energy expression of the lattice and is relative to the height of the building frame.

TABLE 3 Comparison of Preparation and Computer Time

COMPARISON OF PREPARATION & COMPUTER TIME		
Data Preparation	Continuum Model	Discrete Model / Risa 3-D
Data Drafting / Input	37 minutes	33 minutes
Computer Time	3 minutes	3 seconds

An approximate solution found by using the stiffness method will always provide an approximate value of potential energy greater than or equal to the correct one. This

method also results in a structure behavior that is predicted to be physically stiffer than, or at best to have the same stiffness as, the actual one. This is explained by the fact that the structural model is allowed to displace only into shapes defined by the terms of the assumed displacement field within each element of the structure. The correct shape is usually only approximated by the assumed field, although the correct shape can be the same as the assumed field. The assumed field effectively constrains the structure from deforming in its natural manner. This constraint effect stiffens the predicted behavior of the structure.

For the tall building frames as above, it takes about 30 minutes to get the data from draft in the continuum model. It also takes about 30 minutes to input the members in the discrete model Risa 3-D computer program. Using a 300 MHz processor, there is not much difference in computational time between continuum and discrete methodology . Results from both methods come out in couple blinks of eye through Risa 3-D and Mathcad respectively. The advantage of the continuum methodology is, as an engineer, to have a actual feeling on the displacement behavior of a tall building, not just taking whatever a computer program spitting out.

CHAPTER 5

SEISMIC ANALYSIS USING CONTINUUM STIFFNESS MATRIX

5-1. DYNAMIC ANALYSIS

The most general representation of the equations of motion for a multiple-degree-of freedom (MDOF) system subjected to a forcing function is given by

$$F_I + F_D + F_S = F \tag{55}$$

where F_I = the inertial force vector; F_D = the damping force vector; F_S = the spring force vector; and F = the applied load vector.

Methods for solving equations of motion for MDOF dynamic systems fall into two categories: modal analysis and direct integration. Modal analysis is the more computationally efficient of the two methods and is best suited for linear systems subjected to long duration loading. Direct integration is the most practical way of solving nonlinear dynamic problems. Assume the building experiences relatively low base accelerations, and have a peak average drift ratio of less than the allowable design drift ratio of 0.005 (UBC 1976), the behavior is assumed to be linear elastic.

For a time dependent problem having a base excitation, the inertial, damping, and spring force terms of Eq. (55) can be rewritten in terms of absolute accelerations, relatively, to give

$$M\ddot{v}(t) + C\dot{v}(t) + Kv(t) = -M\ddot{v}_g(t) \tag{56}$$

where M = the system's mass matrix; C = the system's damping matrix; K = the system's stiffness matrix; $\ddot{v}$ = the system's absolute acceleration vector; $\dot{v}$ = the system's relative displacement vector; and $\ddot{v}_g$ = the ground acceleration vector.

For any modal component v_n, the displacements are given by the product of the mode-shape vector ϕ_n and the modal amplitude Y_n; thus

$$v_n = \phi_n Y_n \tag{57}$$

The total displacement vector V is then obtained by summing the modal vectors as expressed by

$$V = \varphi_1 Y_1 + \varphi_2 Y_2 + \cdots + \phi_N Y_N = \sum_{n=1}^{N} \phi_n Y_n \tag{58}$$

or, in matrix form

$$V = \Phi Y \tag{59}$$

In this equation, it is apparent that the NxN mode-shape matrix Φ serves to transform the generalized coordinate vector Y to the geometric coordinate vector V. The generalized components in vector Y are called the normal coordinates of the structure.

By making use of the modal orthogonality, to evaluate any arbitrary normal coordinate, Y_n for example, pre-multiply Eq. (58) by $\phi_n^T m$ to obtain

$$\phi_n^T m V = \phi_n^T m \phi_1 Y_1 + \phi_n^T m \phi_2 Y_2 + \cdots + \phi_n^T m \phi_N Y_N \tag{60}$$

Because of the orthogonality property with respect to mass, i.e., $\phi_n^T m \phi_m = 0$ for $m \neq n$, all terms on the right hand side of this equation vanish, except for the term containing $\phi_n^T m \phi_n$, leaving

$$\phi_n^T m V = \phi_n^T m \phi_n Y_n \tag{61}$$

from which

$$Y_n = \frac{\phi_n^T m V}{\phi_n^T m \phi_n} \qquad n = 1,2,\cdots,N \tag{62}$$

For a time dependent vector V, the Y_n coordinates will also be time dependent; so, taking the time derivative of Eq. (62) yields

$$\dot{Y}_n(t) = \frac{\phi_n^T m \dot{V}(t)}{\phi_n^T m \phi_n} \tag{63}$$

The above procedure is equivalent to that used to evaluate the coefficients in the Fourier series (APPENDIX G).

For the undamped system, Eq. (56) becomes

$$m\ddot{v}(t) + kv(t) = p(t) = -M1\ddot{v}_g(t) \tag{64}$$

where $-\ddot{v}_g(t)$ is the time dependent horizontal earthquake ground-motion excitation and $M1$ is the mass system matrix. Introducing Eq. (59) and its second time derivative $\ddot{v} = \Phi\ddot{Y}$ (noting that the mode shapes do not change with time) leads to

$$m\Phi\ddot{Y}(t) + k\Phi Y(t) = -M1\ddot{v}_g(t) \tag{65}$$

If Eq. (65) is pre-multiplied by the transpose of the nth mode-shape vector ϕ_n^T, it becomes

$$\phi_n^T m\Phi\ddot{Y}(t) + \phi_n^T k\Phi Y(t) = -\phi_n^T M1\ddot{v}_g(t) \tag{66}$$

but if the two terms on the left hand side are expanded as shown in Eq. (60), all terms except the nth will vanish because of the mode-shape orthogonality properties; hence the result is

$$\phi_n^T m \phi_n \ddot{Y}_n(t) + \phi_n^T k \phi_n Y_n(t) = -\varphi_n^T M 1 \ddot{v}_g(t) \tag{67}$$

Here, new symbols are defined as follows:

$$M_n \equiv \phi_n^T m \phi_n \tag{68}$$

$$K_n \equiv \phi_n^T k \phi_n \tag{69}$$

$$P_n(t) \equiv -\phi_n^T M 1 \ddot{v}_g(t) \tag{70}$$

which are called the normal-coordinate generalized mass, generalized stiffness, and generalized load for mode n, respectively. With them Eq. (67) can be written as

$$M_n \ddot{Y}_n(t) + K_n Y_n(t) = P_n(t) = -\phi_n^T M 1 \ddot{v}_g(t) \tag{71}$$

Back to the damped system in Eq. (56), again introducing the normal-coordinate expression of Eq. (59) and its time derivatives and pre-multiplying by the transpose of the nth mode-shape vector ϕ_n^T lead to

$$\phi_n^T m \Phi \ddot{Y}(t) + \phi_n^T c \Phi \dot{Y}(t) + \phi_n^T k \Phi Y(t) = -\phi_n^T M 1 \ddot{v}_g(t) \tag{72}$$

It was noted above that the orthogonality conditions

$$\phi_m^T m \phi_n = 0 \qquad m \neq n$$

$$\phi_m^T k \phi_n = 0 \qquad m \neq n$$

because all components except the nth-mode term in the mass and stiffness expressions of Eq. (72) to vanish. A similar reduction will apply to the damping expression if it is

assumed that the corresponding orthogonality condition applies to the damping matrix; that is assume that

$$\phi_m^T c \phi_n = 0 \qquad m \neq n \tag{73}$$

Then, Eq. (72) becomes

$$M_n \ddot{Y}_n(t) + C_n \dot{Y}_n(t) + K_n Y_n(t) = -\phi_n^T M 1 \ddot{v}_g(t) \tag{74}$$

where the definitions of modal coordinate mass, stiffness, and load have been introduced from Eqs. (80-82) and where the modal coordinate viscous damping coefficient is defined similarly

$$C_n = \phi_n^T c \phi_n \tag{75}$$

If Eq. (74) is divided by the generalized mass and specifically for the *i*th mode, by making use of orthogonality, this modal matrix expression can be alternatively uncoupled into a series of modal equations of motion given by

$$\ddot{Y}_i(t) + 2\xi_i \omega_i \dot{Y}_i(t) + \omega_i^2 Y_i(t) = -\frac{\phi_i^T M 1 \ddot{v}_g(t)}{\phi_i^T M \phi_i} = -\Gamma_i \ddot{v}_g(t) \tag{76}$$

$$\Gamma_i = \frac{\phi_i^T M 1}{\phi_i^T M \phi_i} = \frac{\phi_i^T M 1}{M_i} \tag{77}$$

where Γ_i is the modal participation factor; and for *i*th mode shape ϕ_i, Y_i is the generalized coordinate, ξ_i is the modal damping, ω_i is the circular frequency of the mode; and $K_n = \omega_n^2 M_n$ has been used to rewrite the stiffness term and where the second term on the left hand side represents a definition of the modal viscous damping ratio

$$\xi_n = \frac{C_n}{2\omega_n M_n} \tag{78}$$

It is generally more convenient and physically reasonable to define the damping of a MDOF system using the damping ratio for each mode in this way rather than to evaluate the coefficients of the damping matrix C because the modal damping ratios ξ_n can be determined experimentally or estimated with adequate precision in many cases. With regard to damping, the use of a more sophisticated wavelet transform [described in detail in Chajes and Finch (1993) and Kirby et al. (1992)] has indicated that damping of the fundamental mode ξ_1 during free vibration (end of the response record) is roughly 2.2 % of critical damping. This value is in line with the 2.0-2.6 % of critical damping suggested by Astaneh et al. (1991)[6]. From Eq. (58) and its first and second time derivatives, the system displacement, velocity, and acceleration vectors are given as

$$V = \sum_{i=1}^{N} \phi_i Y_i \tag{79}$$

$$\dot{V} = \sum_{i=1}^{N} \phi_i \dot{Y}_i \tag{80}$$

$$\ddot{V} = \sum_{i=1}^{N} \phi_i \ddot{Y}_i \tag{81}$$

To solve the modal equations of motion Eq. (76), the mode shapes and frequencies must first be found. In the continuum dynamic analysis, the mode shapes ϕ_n ($n = 1,2,\cdots$) and frequencies ω_n are found from the eigenvalue equation

$$\left[K - \omega_n^2 M\right]\phi_n = 0 \tag{82}$$

where the system matrix **K** is found by appropriately combining continuum element stiffness matrices coefficient S_{77} as defined in Appendix D by the Direct Stiffness

Method. The mode shapes can be found from Eq. (82) with $\tilde{E}^{(n)} = k - \omega_n^2 m$ and the displacement amplitude vector by

assuming the first element of the displacement vector has a unit amplitude as below,

$$\hat{V}_{0n} = \phi_n = \begin{Bmatrix} \phi_{1n} \\ \phi_{2n} \\ \vdots \\ \phi_{Nn} \end{Bmatrix} = -(\tilde{E}_{00}^{(n)})^{-1} \tilde{E}_{01}^{(n)} \tag{83}$$

Once the individual mode shapes and frequencies are found, a variety of well-known numerical integration methods can be used to solve Eq. (76).

Using the frequency domain solution as follows, the total response of the MDOF system can be obtained by solving the N uncoupled modal equations and superposing their effects, as indicated by Eq. (84)

$$Y_n(t) = \frac{1}{2\pi} \int_{-\infty}^{\infty} H_n(i\varpi) P_n(i\varpi) \exp i\varpi t d\varpi \tag{84}$$

where

$$H_n(i\varpi) = \frac{1}{\omega_n^2 M_n} \left[\frac{\left(1-\beta_n^2\right) - i\left(2\xi_n \beta_n\right)}{\left(1-\beta_n^2\right)^2 + \left(2\xi_n \beta_n\right)^2} \right] \qquad \xi_n \geq 0 \tag{85}$$

where $\beta_n \equiv \dfrac{\varpi}{\omega_n}$

and the complex load function $P_n(i\varpi)$ is the Fourier transform of the modal loading $P_n(t)$, given by

$$P_n(i\varpi) = \int_{-\infty}^{\infty} P_n(t) \exp(-i\varpi t) dt \tag{86}$$

Solving Eq. (84) for any general modal loading yields the modal response $Y_n(t)$ for $t \geq 0$, assuming zero initial conditions, i.e., $Y_n(0) = \dot{Y}_n(0) = 0$. Should the initial conditions not equal zero, the damped free-vibration response Eq. (87), as shown below, must be added to the forced-vibration response given by Eq. (84).

$$Y_n(t) = \left[Y_n(0)\cos\omega_{D_n} t + \left(\frac{\dot{Y}_n(0) + Y_n(0)\xi_n\omega_n}{\omega_{D_n}} \right) \sin\omega_{D_n} t \right] esp(-\xi_n\omega_n t) \qquad (87)$$

where the initial conditions, using Eq. (74,75), are

$$Y_n(0) = \frac{\phi_n^T m v(0)}{\phi_n^T m \phi_n} \qquad (88)$$

and

$$\dot{Y}_n(0) = \frac{\phi_n^T m \dot{v}(0)}{\phi_n^T m \phi_n} \qquad (89)$$

Having generated the total response for each mode $Y_n(t)$ using Eq. (84) and Eq. (87), the displacements expressed in the geometric coordinates can be obtained using Eq. (58), i.e.,

$$v(t) = \phi_1 Y_1(t) + \phi_2 Y_2(t) + \cdots + \phi_N Y_N(t) \qquad (90)$$

which superposes the separate modal displacement contributions, commonly known as mode superposition method, is used to derive the time-histories in vector $v(t)$.

Again, when a system vibrates with a given natural frequency ω_i, that unique shape with arbitrary amplitude corresponding to ω_i is called the *mode*. In general, for an n-degree-of-freedom discrete system, there are n natural modes and frequencies. For most types of loading, the displacements contributions generally are greatest for the lowest

mode and tends to decrease for the higher modes. Consequently, the lowest modes and frequencies are approximated most often. It is not necessary to include all the higher modes of vibration in the superposition process since the higher frequencies are damped out more rapidly and are usually of less importance, especially for the critical damping case, there is no oscillation. So, the series can be truncated when the response has been obtained to a certain degree of accuracy.

5-2. CONTINUUM MODEL

In the continuum model, the effects of rotary inertia and vertical vibration were neglected. This allowed the number of degrees of freedom associated with the continuum model to be condensed to just the same as the number of frame stories of the building. The model used can represent a single dimension moment-resisting frame of a building.

To conduct a dynamic analysis using a continuum model, system stiffness **K** and mass **M** matrices are needed. Determination of the system stiffness matrix for the lattice structure first involves the formation of individual continuum element stiffness matrices **S**, defined in Appendix D. To form these element stiffness matrices, member section properties for the beams and columns were used. Both story heights and beam spans were based on centerline-to-centerline dimensions. At the ground, fixed-base boundary conditions were assumed. The final formulation of the element stiffness matrix **K** involves the appropriate summation of the element stiffness matrices **S**. In forming the mass matrix **M**, a lumped mass model was used. The masses were computed based on dead-load contributions (including framing elements and floor slabs), as well as designed live loads.

5-3. 3 STORY FRAME

This frame used has the following properties.

Total Columns	N = 4	
Length	L = 120	in
Shear Area	As = 18.8	in^2
Moment Inertia	Ii = 272	in^4
Elasticity Modulus	E = 29000	ksi
Rigidity Modulus	G = 12000	ksi

The nine-by-nine continuum element stiffness matrix with the stiffness coefficient

$$S_{77} = \frac{N \cdot 12 \cdot E \cdot Ii}{L^3} - \frac{6 \cdot G \cdot As}{5 \cdot L} = 2.475 \cdot 10^3$$

3 story stiffness matrix

$$\begin{bmatrix} k_1 - k_2 & -k_2 & 0 \\ -k_2 & k_2 - k_3 & -k_3 \\ 0 & -k_3 & k_3 \end{bmatrix}$$

where $k_1 = k_2 = S_{77} = 2475$

With Eq. (94)

$$K - \omega^2 \cdot M \Rightarrow V 0$$

$$\begin{bmatrix} 4950 & -2475 & 0 \\ -2475 & 4950 & -2475 \\ 0 & -2475 & 2475 \end{bmatrix} - \omega^2 \cdot \begin{bmatrix} 1 & 0 & 0 \\ 0 & 1.5 & 0 \\ 0 & 0 & 2 \end{bmatrix} = 0$$

$$\omega = \begin{matrix} 16.2 \\ 52.6 \\ 80.2 \end{matrix} \frac{rad}{sec}$$

$$\text{Frequency, } f = \frac{\omega}{2 \cdot \pi} = \begin{matrix} 2.58 \\ 8.38 \\ 12.8 \end{matrix}$$

It is close to the results obtained from Risa 3-D shown in Appendix J.

For the period of vibration ,

$$T_1 = \frac{2\cdot\pi}{16.2} = 3.879 \cdot 10^{-1} \quad \text{sec}$$

$$T_2 = \frac{2\cdot\pi}{52.6} = 0.119 \quad \text{sec}$$

$$T_3 = \frac{2\cdot\pi}{80.2} = 0.078 \quad \text{sec}$$

Analysis of Vibrational Mode Shape :

Using Eq. (95)

For the first mode

$\omega_1 = 16.8$

$$\begin{bmatrix}\phi_{2n}\\ \phi_{3n}\end{bmatrix} = \begin{bmatrix}4950 - 1.5\cdot 16.8^2 & -2475\\ -2475 & 2475 - 2\cdot 16.8^2\end{bmatrix}^{-1} \cdot \begin{bmatrix}-2475\\ 0\end{bmatrix} = \begin{bmatrix}1.874\\ 2.428\end{bmatrix}$$

$$\begin{bmatrix}\phi_{11}\\ \phi_{21}\\ \phi_{31}\end{bmatrix} = \begin{bmatrix}1\\ 1.874\\ 2.428\end{bmatrix}$$

For the second mode

$\omega_2 = 52.6$

$$\begin{bmatrix}\phi_{22}\\ \phi_{32}\end{bmatrix} = \begin{bmatrix}4950 - 1.5\cdot 52.6^2 & -2475\\ -2475 & 2475 - 2\cdot 52.6^2\end{bmatrix}^{-1} \cdot \begin{bmatrix}-2475\\ 0\end{bmatrix} = \begin{bmatrix}0.883\\ -0.715\end{bmatrix}$$

$$\begin{bmatrix}\phi_{12}\\ \phi_{22}\\ \phi_{32}\end{bmatrix} = \begin{bmatrix}1\\ 0.883\\ -0.715\end{bmatrix}$$

For the third mode

$\omega_3 = 80.2$

$$\begin{bmatrix}\phi_{21}\\ \phi_{31}\end{bmatrix} = \begin{bmatrix}4950 - 1.5\cdot 80.2^2 & -2475\\ -2475 & 2475 - 2\cdot 80.2^2\end{bmatrix}^{-1} \cdot \begin{bmatrix}-2475\\ 0\end{bmatrix} = \begin{bmatrix}-0.602\\ 0.144\end{bmatrix}$$

$$\begin{bmatrix}\phi_{13}\\ \phi_{23}\\ \phi_{33}\end{bmatrix} = \begin{bmatrix}1\\ -0.602\\ 0.144\end{bmatrix}$$

Using Eq. (62), (76) or (77),

$$Y_n = [M]^{-1} * [\phi^T] * [m] * [v_n]$$

where $[M]_n^{-1} = \{\phi_n^T\} * [m] * \{\phi_n\}$

For the first mode

$$\begin{matrix}\phi_{11}\\ \phi_{21}\\ \phi_{31}\end{matrix} = \begin{matrix}1\\ 1.874\\ 2.428\end{matrix}$$

$$M_1 = \begin{pmatrix}1 & 1.874 & 2.428\end{pmatrix} \cdot \begin{matrix}1 & 0 & 0\\ 0 & 1.5 & 0\\ 0 & 0 & 2\end{matrix} \cdot \begin{matrix}1\\ 1.874\\ 2.428\end{matrix} = 18.058 \quad \frac{kip \cdot sec^2}{in}$$

For the second mode

$$\begin{matrix}\phi_{12}\\ \phi_{22}\\ \phi_{32}\end{matrix} = \begin{matrix}1\\ 0.883\\ -0.715\end{matrix}$$

$$M_2 = \begin{pmatrix}1 & .883 & -.715\end{pmatrix} \cdot \begin{matrix}1 & 0 & 0\\ 0 & 1.5 & 0\\ 0 & 0 & 2\end{matrix} \cdot \begin{matrix}1\\ 0.883\\ -0.715\end{matrix} = 3.192 \quad \frac{kip \cdot sec^2}{in}$$

For the third mode

$$\begin{matrix}\phi_{13}\\ \phi_{23}\\ \phi_{33}\end{matrix} = \begin{matrix}1\\ -0.602\\ 0.144\end{matrix}$$

$$M_3 = \begin{pmatrix}1 & -0.602 & 0.144\end{pmatrix} \cdot \begin{matrix}1 & 0 & 0\\ 0 & 1.5 & 0\\ 0 & 0 & 2\end{matrix} \cdot \begin{matrix}1\\ -0.602\\ 0.144\end{matrix} = 1.585 \quad \frac{kip \cdot sec^2}{in}$$

Now,

$$[M] = \begin{bmatrix} M_1 & 0 & 0 \\ 0 & M_2 & 0 \\ 0 & 0 & M_3 \end{bmatrix}$$

Our equation was

$$[Y_n] = [M]^{-1} * [\phi^T] * [m] * [v_n]$$

Assuming the velocity and acceleration vector matrices are measured as $[v_0]$ and $[\dot{v}_0]$ given by the followings,

$$[v_0] = \begin{Bmatrix} 0.5 \\ 0.4 \\ 0.3 \end{Bmatrix}, \qquad [\dot{v}_0] = \begin{Bmatrix} 0 \\ 9 \\ 0 \end{Bmatrix}, \text{ then}$$

$$[Y_0] = [M]^{-1} * [\phi^T] * [m] * [v_0]$$

$$= \begin{bmatrix} 18.058 & 0 & 0 \\ 0 & 3.192 & 0 \\ 0 & 0 & 1.585 \end{bmatrix}^{-1} \begin{bmatrix} 1 & 1.874 & 2.428 \\ 1 & .883 & -.715 \\ 1 & -.602 & .144 \end{bmatrix} \cdot \begin{bmatrix} 1 & 0 & 0 \\ 0 & 1.5 & 0 \\ 0 & 0 & 2 \end{bmatrix} \cdot \begin{bmatrix} 0.5 \\ 0.4 \\ 0.3 \end{bmatrix} = \begin{bmatrix} 0.171 \\ 0.188 \\ 0.142 \end{bmatrix}$$

$$[\dot{Y}_0] = [M]^{-1} * [\phi^T] * [m] * [\dot{v}_0]$$

$$= \begin{bmatrix} 18.058 & 0 & 0 \\ 0 & 3.192 & 0 \\ 0 & 0 & 1.585 \end{bmatrix}^{-1} \begin{bmatrix} 1 & 1.874 & 2.428 \\ 1 & .883 & -.715 \\ 1 & -.602 & .144 \end{bmatrix} \cdot \begin{bmatrix} 1 & 0 & 0 \\ 0 & 1.5 & 0 \\ 0 & 0 & 2 \end{bmatrix} \cdot \begin{bmatrix} 0 \\ 9 \\ 0 \end{bmatrix} = \begin{bmatrix} 1.401 \\ 3.734 \\ -5.127 \end{bmatrix}$$

For a free vibration situation

$$[Y_n] = \frac{\dot{Y}_{0n}}{\omega_n} \sin \omega_n t + Y_{0n} \cos \omega_n t \tag{91}$$

$$= \begin{bmatrix} \frac{1.401}{16.2} \cdot \sin(16.2 \cdot t) - 0.171 \cdot \cos(16.2 \cdot t) \\ \frac{3.734}{52.6} \cdot \sin(52.6 \cdot t) - 0.188 \cdot \cos(52.6 \cdot t) \\ \frac{5.127}{80.2} \cdot \sin(80.2 \cdot t) - 0.142 \cdot \cos(80.2 \cdot t) \end{bmatrix}$$

Finally, from Eq. (79)

$$[V_n] = [\phi] * [Y_n]$$

$$\begin{bmatrix} v_1 \\ v_2 \\ v_3 \end{bmatrix} = \begin{matrix} 1 & 1 & 1 \\ 1.874 & 0.883 & -0.602 \\ 2.428 & -0.715 & 0.144 \end{matrix} \cdot \begin{bmatrix} \frac{1.401}{16.2}\cdot\sin(16.2t) - 0.171\cos(16.2t) \\ \frac{3.734}{52.6}\cdot\sin(52.6t) - 0.188\cos(52.6t) \\ \frac{5.127}{80.2}\cdot\sin(80.2t) - 0.142\cos(80.2t) \end{bmatrix}$$

The displacements for the first ten seconds are calculated and plotted in a graph as follows:

For $t = 0$,

$$\begin{bmatrix} v_1 \\ v_2 \\ v_3 \end{bmatrix} = \begin{matrix} 1 & 1 & 1 \\ 1.874 & 0.883 & -0.602 \\ 2.428 & -0.715 & 0.144 \end{matrix} \cdot \begin{bmatrix} \frac{1.401}{16.2}\cdot\sin(16.2\cdot t) - 0.171\cdot\cos(16.2\cdot t) \\ \frac{3.734}{52.6}\cdot\sin(52.6t) - 0.188\cos(52.6t) \\ \frac{-5.127}{80.2}\cdot\sin(80.2\cdot t) - 0.142\cos(80.2\cdot t) \end{bmatrix} = \begin{matrix} 0.501 \\ 0.401 \\ 0.301 \end{matrix}$$

For $t = 1$,

$$\begin{bmatrix} v_1 \\ v_2 \\ v_3 \end{bmatrix} = \begin{matrix} 1 & 1 & 1 \\ 1.874 & 0.883 & -0.602 \\ 2.428 & -0.715 & 0.144 \end{matrix} \cdot \begin{bmatrix} \frac{1.401}{16.2}\cdot\sin(16.2\cdot t) - 0.171\cdot\cos(16.2\cdot t) \\ \frac{3.734}{52.6}\cdot\sin(52.6\cdot t) - 0.188\cdot\cos(52.6\cdot t) \\ \frac{-5.127}{80.2}\cdot\sin(80.2\cdot t) - 0.142\cdot\cos(80.2\cdot t) \end{bmatrix} = \begin{matrix} -0.194 \\ -0.475 \\ -0.398 \end{matrix}$$

For t = 2,

$$\begin{bmatrix} v_1 \\ v_2 \\ v_3 \end{bmatrix} = \begin{bmatrix} 1 & 1 & 1 \\ 1.874 & 0.883 & -0.602 \\ 2.428 & -0.715 & 0.144 \end{bmatrix} \cdot \begin{bmatrix} \frac{1.401}{16.2}\cdot\sin(16.2t) - 0.171\cos(16.2t) \\ \frac{3.734}{52.6}\cdot\sin(52.6t) - 0.188\cos(52.6t) \\ \frac{5.127}{80.2}\cdot\sin(80.2t) - 0.142\cos(80.2t) \end{bmatrix} = \begin{bmatrix} -0.013 \\ 0.034 \\ -0.397 \end{bmatrix}$$

For t = 3,

$$\begin{bmatrix} v_1 \\ v_2 \\ v_3 \end{bmatrix} = \begin{bmatrix} 1 & 1 & 1 \\ 1.874 & 0.883 & -0.602 \\ 2.428 & -0.715 & 0.144 \end{bmatrix} \cdot \begin{bmatrix} \frac{1.401}{16.2}\cdot\sin(16.2t) - 0.171\cos(16.2t) \\ \frac{3.734}{52.6}\cdot\sin(52.6t) - 0.188\cos(52.6t) \\ \frac{5.127}{80.2}\cdot\sin(80.2t) - 0.142\cos(80.2t) \end{bmatrix} = \begin{bmatrix} -0.013 \\ 0.034 \\ -0.397 \end{bmatrix}$$

For t = 4,

$$\begin{bmatrix} v_1 \\ v_2 \\ v_3 \end{bmatrix} = \begin{bmatrix} 1 & 1 & 1 \\ 1.874 & 0.883 & -0.602 \\ 2.428 & -0.715 & 0.144 \end{bmatrix} \cdot \begin{bmatrix} \frac{1.401}{16.2}\cdot\sin(16.2t) - 0.171\cdot\cos(16.2t) \\ \frac{3.734}{52.6}\cdot\sin(52.6t) - 0.188\cdot\cos(52.6t) \\ \frac{5.127}{80.2}\cdot\sin(80.2t) - 0.142\cdot\cos(80.2t) \end{bmatrix} = \begin{bmatrix} -0.057 \\ -0.201 \\ 0.178 \end{bmatrix}$$

For t = 5,

$$\begin{pmatrix} v_1 \\ v_2 \\ v_3 \end{pmatrix} = \begin{pmatrix} 1 & 1 & 1 \\ 1.874 & 0.883 & -0.602 \\ 2.428 & 0.715 & 0.144 \end{pmatrix} \cdot \begin{pmatrix} \frac{1.401}{16.2}\cdot\sin(16.2t) - 0.171\cos(16.2t) \\ \frac{3.734}{52.6}\cdot\sin(52.6t) - 0.188\cos(52.6t) \\ \frac{5.127}{80.2}\cdot\sin(80.2t) - 0.142\cos(80.2t) \end{pmatrix} = \begin{pmatrix} 0.260 \\ 0.130 \\ 0.163 \end{pmatrix}$$

For t = 6,

$$\begin{pmatrix} v_1 \\ v_2 \\ v_3 \end{pmatrix} = \begin{pmatrix} 1 & 1 & 1 \\ 1.874 & 0.883 & -0.602 \\ 2.428 & -0.715 & 0.144 \end{pmatrix} \cdot \begin{pmatrix} \frac{1.401}{16.2}\cdot\sin(16.2t) - 0.171\cos(16.2t) \\ \frac{3.734}{52.6}\cdot\sin(52.6t) - 0.188\cos(52.6t) \\ \frac{-5.127}{80.2}\cdot\sin(80.2t) - 0.142\cos(80.2t) \end{pmatrix} = \begin{pmatrix} -0.146 \\ -0.147 \\ -0.449 \end{pmatrix}$$

For t = 7,

$$\begin{pmatrix} v_1 \\ v_2 \\ v_3 \end{pmatrix} = \begin{pmatrix} 1 & 1 & 1 \\ 1.874 & 0.883 & -0.602 \\ 2.428 & -0.715 & 0.144 \end{pmatrix} \cdot \begin{pmatrix} \frac{1.401}{16.2}\cdot\sin(16.2t) - 0.171\cos(16.2t) \\ \frac{3.734}{52.6}\cdot\sin(52.6t) - 0.188\cos(52.6t) \\ \frac{-5.127}{80.2}\cdot\sin(80.2t) - 0.142\cos(80.2t) \end{pmatrix} = \begin{pmatrix} -0.140 \\ 0.265 \\ 0.578 \end{pmatrix}$$

For t = 8,

$$\begin{pmatrix} v_1 \\ v_2 \\ v_3 \end{pmatrix} \begin{matrix} 1 & 1 & 1 \\ 1.874 & 0.883 & 0.602 \\ 2.428 & 0.715 & 0.144 \end{matrix} \cdot \begin{pmatrix} \frac{1.401}{16.2}\cdot\sin(16.2\cdot t) - 0.171\cdot\cos(16.2\cdot t) \\ \frac{3.734}{52.6}\cdot\sin(52.6\cdot t) - 0.188\cdot\cos(52.6\cdot t) \\ \frac{5.127}{80.2}\cdot\sin(80.2\cdot t) - 0.142\cdot\cos(80.2\cdot t) \end{pmatrix} = \begin{matrix} 0.057 \\ -0.227 \\ -0.555 \end{matrix}$$

For t = 9,

$$\begin{pmatrix} v_1 \\ v_2 \\ v_3 \end{pmatrix} = \begin{matrix} 1 & 1 & 1 \\ 1.874 & 0.883 & -0.602 \\ 2.428 & -0.715 & 0.144 \end{matrix} \cdot \begin{pmatrix} \frac{1.401}{16.2}\cdot\sin(16.2t) - 0.171\cos(16.2t) \\ \frac{3.734}{52.6}\cdot\sin(52.6t) - 0.188\cos(52.6t) \\ \frac{-5.127}{80.2}\cdot\sin(80.2t) - 0.142\cos(80.2t) \end{pmatrix} = \begin{matrix} 0.232 \\ 0.117 \\ 0.372 \end{matrix}$$

For t = 10,

$$\begin{pmatrix} v_1 \\ v_2 \\ v_3 \end{pmatrix} = \begin{matrix} 1 & 1 & 1 \\ 1.874 & 0.883 & -0.602 \\ 2.428 & -0.715 & 0.144 \end{matrix} \cdot \begin{pmatrix} \frac{1.401}{16.2}\cdot\sin(16.2t) - 0.171\cos(16.2t) \\ \frac{3.734}{52.6}\cdot\sin(52.6t) - 0.188\cos(52.6t) \\ \frac{-5.127}{80.2}\cdot\sin(80.2t) - 0.142\cos(80.2t) \end{pmatrix} = \begin{matrix} -0.198 \\ -0.166 \\ -0.047 \end{matrix}$$

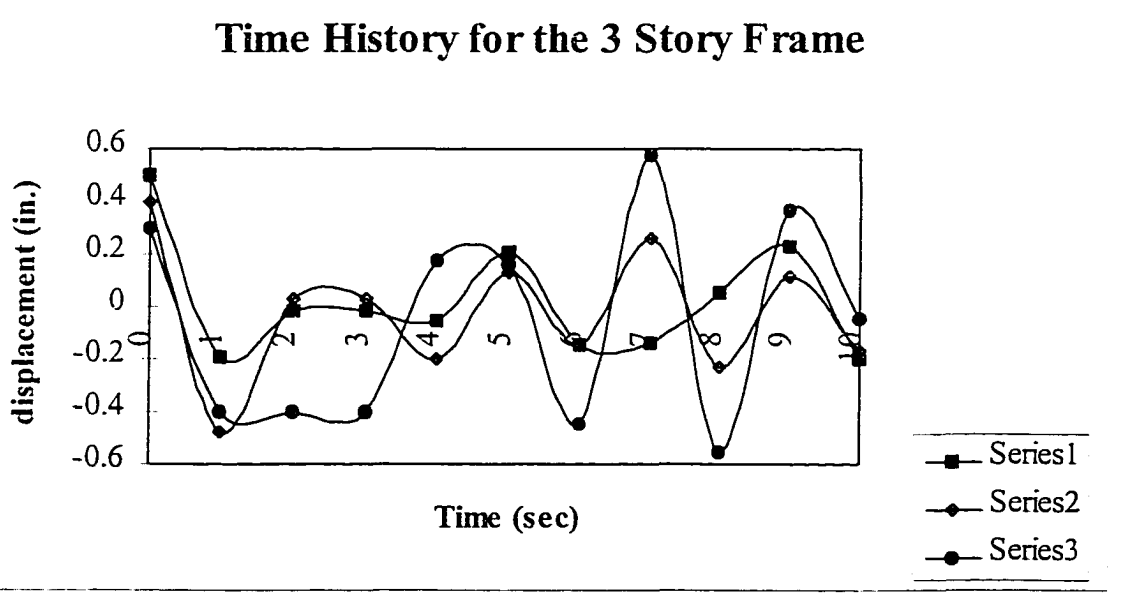

Chart 1
Time History for the 3 Story Frame for the first ten seconds

With an alternative method, the time history of the 3 stories frame has be plotted for the three modes in the first ten seconds with the functionsof displacement $v(t)$ and the time t running from zero to ten seconds. Assuming the excitation damps out after 60 seconds, a graph between displacement v and time t can be plotted the same way. With these graph, the maximum displacement will be found and the maximum moment can be calculated as follows:

$$Shear\ \ Force = (Stiffness,\ \ K) * (Displacement,\ \ v)$$

$$Moment = \left(Shear\ \ Force \right) * Distance$$

Using these data, one can determine the sizes and shapes of members to be used in the structure.

Most of the above are general seismic analysis method. The trick is to utilize the stiffness data obtained from the continuum model stiffness matrix element S_{77}. This

stiffness element applies to the stiffness of all the elements in a repeated cell for the overall structure. Through this way, it save much effort in calculating the stiffness of a lot of structural members.

TABLE 4 Comparison of Approximate Preparation and Computer Time

COMPARISON OF PREPARATION & COMPUTER TIME		
Data Preparation	Continuum Model	Discrete Model / Rias 3-D
Data Drafting / Input	20 minutes	15 minutes
Computer Time	2 minutes	1 seconds

CHAPTER 6

CONCLUSION

As shown in chapters 4 & 5, the continuum model can provide an idea on the behavior of the building. Examples were solved by continuum methodology and compared with results obtained from commercially available computer programs. Some designers who are using discrete finite element models may only know the application of those programs without any idea how the buildings suppose to behave. It could induce horrible results if those programs go wrong somehow. By using the continuum finite element model, a designer will be able to easily understand the approximate behavior of a building under different load conditions.

Users of discrete finite element programs may be so impressed by the power of the method that its limitations are ignored. Whether computer-based or not, analytical methods rely on assumptions and on theory that is not universally applicable. The analyst may overlook or misjudge important aspects of physical behavior. There may be an error in the computer program. A large program has many options and many computational paths. Perhaps some paths have never before been exercised, were not anticipated by the program designers, and have never been checked. Far more likely causes of incorrect results are user errors, such as using an inappropriate program or supplying an

appropriate program with the wrong data. A poor mesh may be used, an inappropriate element type may be chosen, yielding or buckling may be overlooked, support conditions may be misrepresented, and so on, Users must remember that a structure is not obliged to behave as a computer says it should, regardless of how expensive the program, how many digits are printed in the results, or how elegant the graphic display. Computer graphics has achieved such a level of polish and versatility as to inspire great trust in the underlying analysis, a trust that may be unwarranted.

Powerful computer programs cannot be used without training. Their results cannot be trusted if users have no knowledge of their internal workings and little understanding of the physical theories on which they are based. An error caused by misunderstanding or oversight is not correctable by mesh refinement or by use of a more powerful computer. Some authorities have suggested that users be engaged in a profession in which the potential for damage to the public is substantial. Although the finite element method can make a good engineer better, it can make a poor engineer more dangerous.

It must be remembered, however, that computer programs found in the public domain (including PLTRUSS and PLFRAME) are not, in general, certified; therefore, the responsibility for their proper use and for the validity of the results produced lies with the user and not with the authors or producers of the programs. [11]

In years past, when analysis was done by hand, the analyst was required to invent a mathematical model before undertaking its analysis. Invention of a good model required sound physical understanding of the problem. Understanding can now be replaced by activation of a computer program. Having had little need to sharpen intuition by devising

simple models, the computer user may lack the physical understanding needed to prepare a good model and to check computed results.

Computed results must in some way be judged or compared with expectations. Alternative results, useful for comparison, might be obtained from experiment which may be expensive and has its own pitfalls; from the behavior of similar structures already built or from a different computer program that relies on a different analytical basis. There are also results from a simplified model amenable to hand calculation such as continuum model as described in this paper.

With a Pentium 300 MHz processor computer, a 40 story building, with 7 by 8 bays, and 2296 nodes, it takes about 15 minutes to go through about 13000 equations simultaneously to determine the displacements and member forces of the multi-bay frame by using Risa 3D which is based on discrete finite element analysis. Since the speed of computer is so fast now, comparison of computer time between the continuum model and the discrete model is not much of a big deal. However, a competent analyst still needs to have a sound engineering judgment which is based on experience and the understanding of structural behavior; and that doubts raised in the course of an analysis should be taken seriously. With the continuum finite element model, designer will have a easier control on locating doubts during the design stage.

Continuum methodology is still a good design method especially for tall buildings in the preliminary stages of structural design. Besides, it is also useful to check the results obtained from a commercially available computer structural program. Finally, in the seismic analysis, the trick to utilize the stiffness data obtained from the continuum model

stiffness matrix element saves much effort in calculating the stiffness of a lot of structural members.

APPENDIX A

STRAIN TRANSFORMATION

For strain transformation discussed here is under a rotation of the coordinate axes limited to states of plane strain, i.e., to situations where the deformations of the material take place within parallel planes, and are the same in each of these planes. If the z axis is chosen perpendicular to the planes in which the deformations take

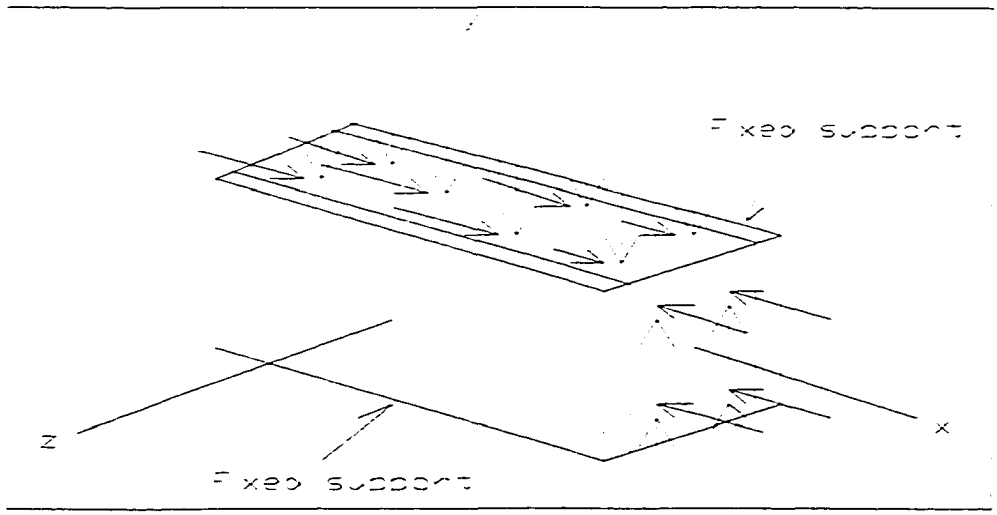

FIGURE A1
Plate Restrained from Expanding or Contracting under Uniform Distributed Loads

place, we have $\epsilon z = \gamma zx = \gamma zy = 0$, and the only remaining strain components are ϵx, ϵy, and γxy. Such a situation occurs in a plate subjected along its edges to uniformly distributed loads and restrained from expanding or contracting laterally by smooth, rigid, and fixed supports (Fig. A1).It would also be found in a bar of infinite length subjected on its sides to uniformly distributed loads since, by reason of symmetry, the elements located in a given transverse plane may not move out of that plane. This idealized model shows that ,in the actual case of a long bar subjected to uniformly distributed transverse loads (Fig. A2), a state of plane strain exists in any given transverse section which is not located too close to either end of the bar.

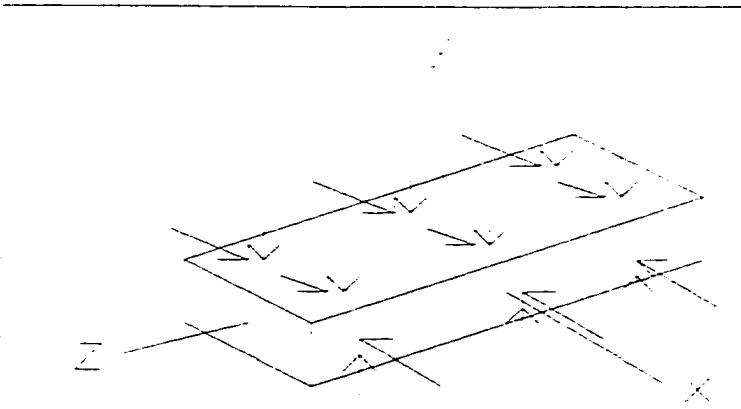

FIGURE A2
Uniform Transverse Load

Assuming that a state of plane strain exists at point Q (with $\epsilon z = \gamma zx = \gamma zy = 0$), and that it is defined by the strain components ϵz, ϵy, and γxy associated with the x and y axes. From Appendix B and D, this means that a square element of center Q, with sides of length Δs respectively parallel to the x and y axes, is deformed into a parallelogram

with sides of length respectively equal to $\Delta s\ (1+\epsilon x)$ and $\Delta s(1+\epsilon y)$, forming angles of $\pi/2-\gamma xy$ and $\pi/2+\gamma xy$ with each other (Fig. Ic). As a result of the deformations of the other elements located in the xy plane, the element considered may also undergo a rigid body motion, but such a motion is irrelevant to the determination of the strains at point Q and will be ignored in this analysis.

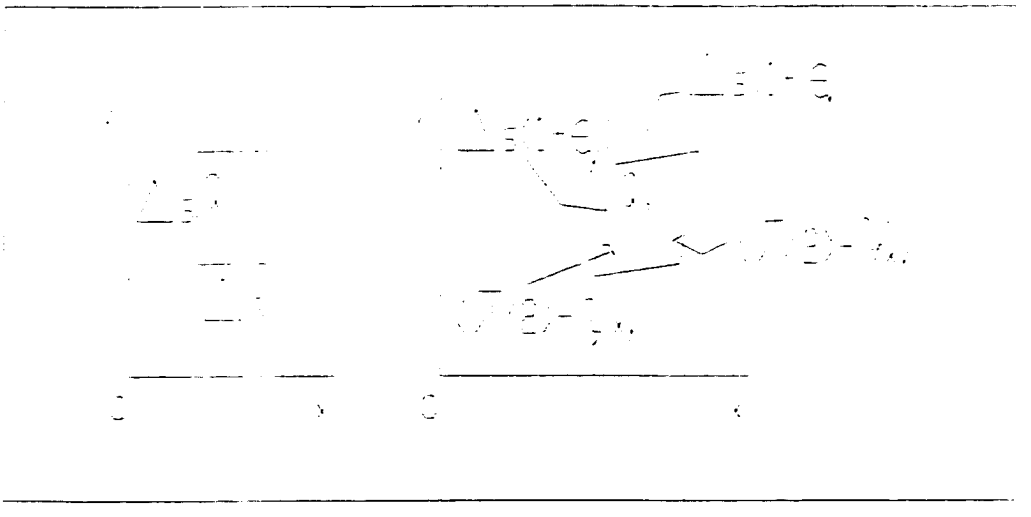

FIGURE A3
Determination of Strains

Our purpose is to determine in terms of ϵx, ϵy, γxy, and θ the stress components $\epsilon x'$, $\epsilon y'$, and $\gamma x'y'$ associated with the frame of reference x'y' obtained by rotating the x and y axes through the angle θ. As shown in Fig. Id, these new strain components define the parallelogram into which a square with sides respectively parallel to the x' and y' axes is deformed.

We shall first derive an expression for the normal

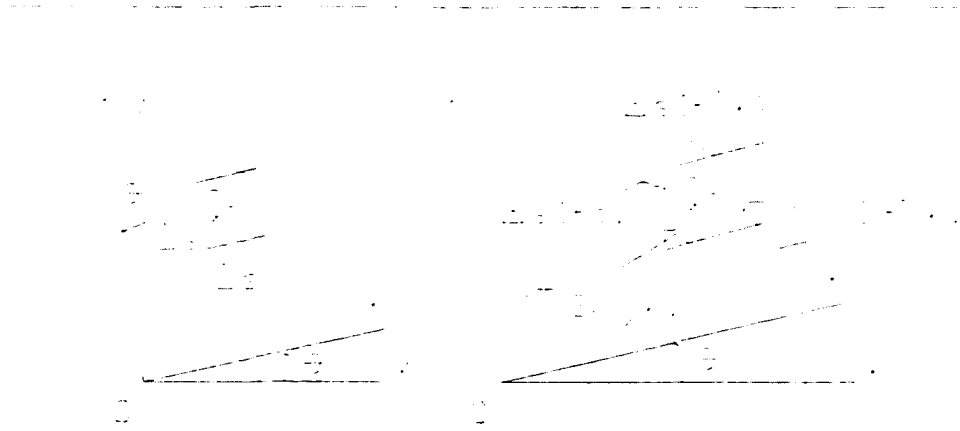

FIGURE A4
Stress Components

strain $\in(\theta)$ along a line AB forming an arbitrary angle with the x axis. To do so, we shall consider the right triangle ABC which has AB for hypotenuse (Fig. A5-1), and the oblique triangle A'B'C' into which triangle ABC is deformed (Fig. A5-2). Denoting by Δs the length of AB, we express the length of A'B' as $\Delta s[1+\in(\theta)]$. Similarly, denoting by Δx and Δy the lengandths of sides AC and CB, we express the lengths of A'B' and C'B' as $\Delta x(1+\in x)$ and $\Delta y(1+\in y)$, respectively. Recalling from Fig. c that the right angle at C in Fig. A5-1 deforms into an angle equal to $\pi/2+\gamma xy$ in Fig. e2, and applying the law of cosines to triangle A'B'C', we write

$$(A'B')^2=(A'C')^2+(C'B')^2-2(A'C')(C'B')\cos(\frac{\pi}{2}+\gamma_{xy})$$

$$(\Delta s)^2[1+\in(\theta)^2]=(\Delta x)^2(1+\in_x)^2+(\Delta y)^2(1+\in_y)^2$$

$$-2(\Delta x)(1+\in_x)(\Delta y)(1+\in_y)\cos(\frac{\pi}{2}+\gamma_{xy}) \qquad \text{(A1)}$$

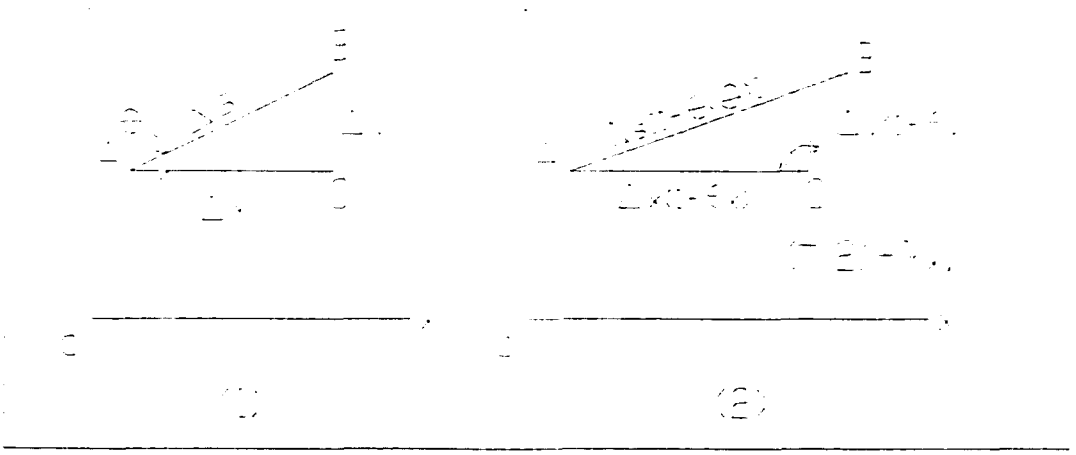

FIGURE A5
Deformed Triangle

But from Fig. A5-1 we have

$$\Delta x = (\Delta s)\cos\theta \qquad \Delta y = (\Delta s)\sin\theta \qquad \text{(A2)}$$

and we note that, since γxy is very small,

$$\cos(\frac{\pi}{2} + \gamma_{xy}) = -\sin\gamma_{xy} \approx -\gamma_{xy} \qquad \text{(A3)}$$

Substituting from Eq. (A2) and (A3)into Eq. (A1), recalling that $\cos^2\theta + \sin^2\theta =$, and neglecting second-order terms in $\epsilon(\theta)$, ϵx, ϵy, and γxy, we write

$$\epsilon(\theta) = \epsilon_x \cos^2\theta + \epsilon_y \sin^2\theta + \gamma_{xy}\sin\theta\cos\theta \qquad \text{(A4)}$$

Equation (A4) enables us to determine the normal strain $\epsilon(\theta)$ in any direction AB in terms of the strain components ϵx, ϵy, γxy, and the angle θ that AB forms with the x axis. We check that, for $\theta = 0$, Eq.(11) yields $\epsilon(0) = \epsilon x$ and that, for $\theta = 90^0$, it yields $\epsilon(90^0) = \epsilon y$. On the other hand, making $\theta = 45^0$ in Eq. (11), we obtain the normal strain

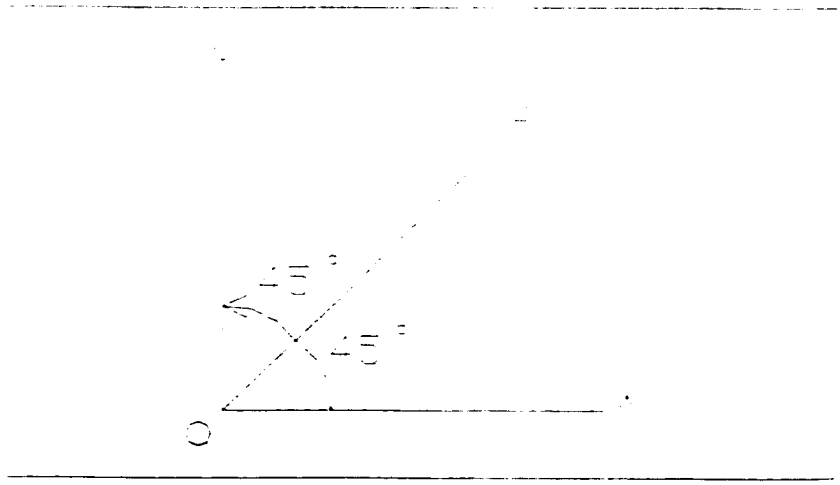

FIGURE A6
Normal Strain in the Direction of the Bisector OB of the Angle Formed by the X and Y Axes.

in the direction of the bisector OB of the angle formed by the x and y axes (Fig. A6). Denoting this strain by $\in ob$, we write

$$\in_{OB} = \in(45^0) = \frac{1}{2}(\in_x + \in_y + \gamma_{xy}) \qquad \text{(A5)}$$

Since the purpose is to express the strain components associated with the frame of reference x'y' of Fig. d in terms of the angle θ and the strain components $\in x$, $\in y$, and γxy associated with the x and y axes, we note that the normal strain $\in x'$ along the x' axis is given by Eq. (A4). Using the following trigonometric relations

$$\sin 2\theta = 2\sin\theta\cos\theta$$

$$\cos 2\theta = \cos^2\theta - \sin^2\theta$$

$$\cos^2\theta = \frac{1+\cos 2\theta}{2}$$

$$\sin^2\theta = \frac{1-\cos 2\theta}{2}$$

we write this equation in the alternative form

$$\epsilon_{x'} = \frac{\epsilon_x + \epsilon_y}{2} + \frac{\epsilon_x - \epsilon_y}{2}\cos 2\theta + \frac{\gamma_{xy}}{2}\sin 2\theta \qquad \text{(A6)}$$

Since the transformation takes $\epsilon y = 0$ and neglects the shear strain term (this contribution will also be included in the shear strain energy term as mention in the text before.) So Eq. (11) becomes

$$\epsilon_{di}(x,o) = \frac{\epsilon(x,0)}{2} + \frac{\epsilon(x,0)}{2}\cos 2\alpha \qquad \text{(A7)}$$

APPENDIX B

NORMAL STRAIN

Consider an element of material in the shape of a cube (Fig. B1). We may assume

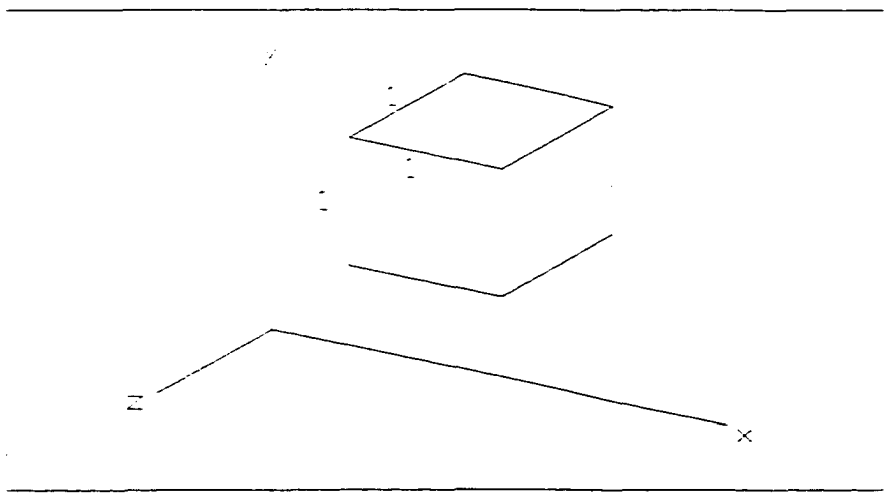

FIGURE B1
Cube with Unit Sides

the side of the cube to be equal to unity, since it is always given multi-axial loading, the element will deform into a rectangular parallelepiped of sides equal, respectively, to $1 + \epsilon x$, $1 + \epsilon y$, and $1 + \epsilon z$, where ϵx, ϵy, and ϵz denote the values of the normal strain

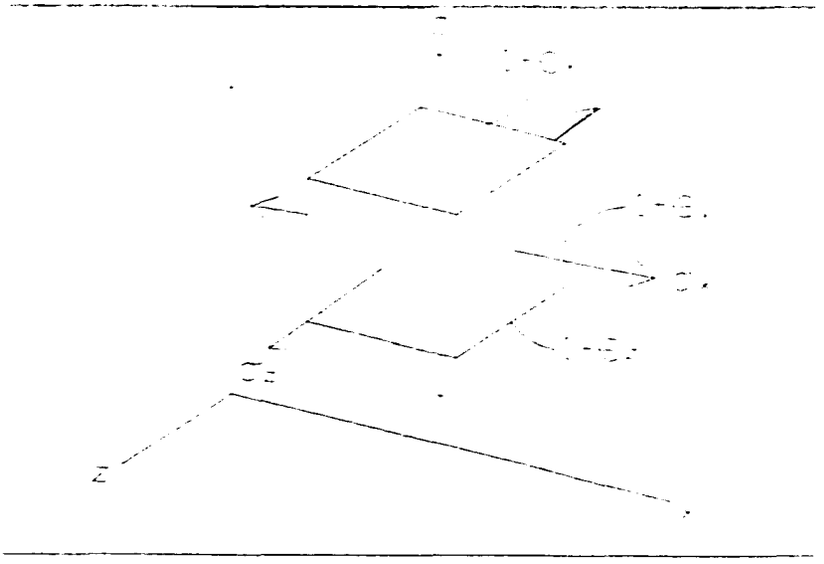

FIGURE B2
Normal Strains

in the directions of the three coordinate axes (Fig. B2).

APPENDIX C

SHEAR STRAIN

The shearing stresses in Fig. C1 will tend to deform a cubic element of material into an oblique parallelepiped (Fig. C2). For a cubic element of side one in Fig. C1

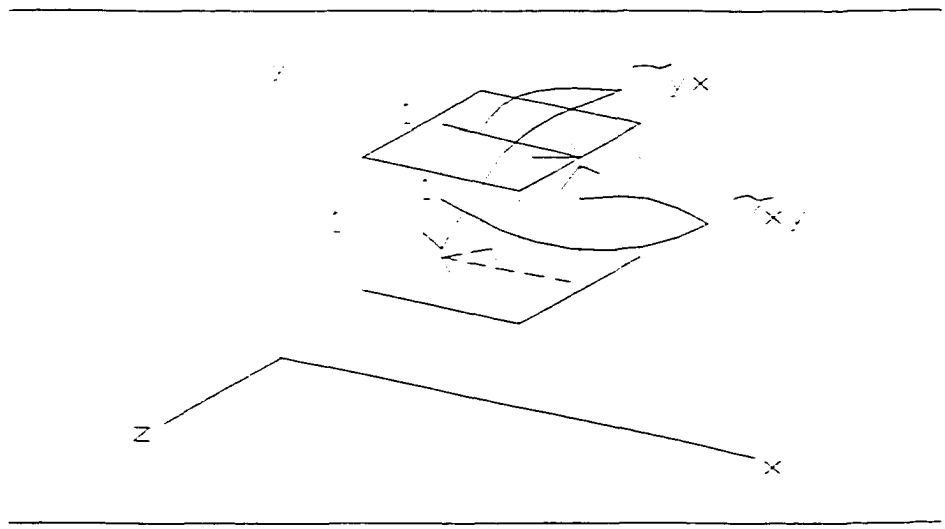

FIGURE C1
Shear Stresses

subjected to no stresses other than the shear stresses τxy and τyx applied to faces of the element respectively perpendicular to the x and y axes. Since $\tau xy = \tau yx$, the element is observed to deform into a rhomboid of sides equal to unity (Fig. C2).

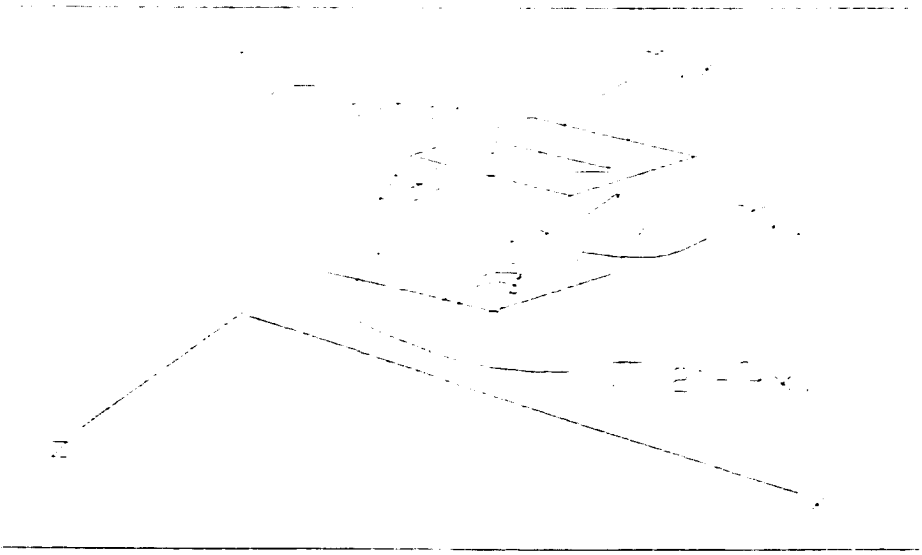

FIGURE C2
Deformed Rhomboid

Two of the angles formed by the four faces under stress are reduced from $\frac{\pi}{2}$ to $\frac{\pi}{2} - \gamma_{xy}$, while the other two are increased from $\frac{\pi}{2}$ to $\frac{\pi}{2} + \gamma_{xy}$. The small angle γxy(expressed in radian) defines the *shear strain* corresponding to the x and y directions.

Plotting successive values of τxy against the corresponding values of γxy, we obtain the shearing stress-strain diagram for the material under consideration. This may be accomplished by carrying out a torsion test. The diagram obtained is similar to the normal stress-strain diagram obtained for the same material from the tensile test. However, the values obtained for the yield strength, ultimate strength, etc., of a given material are only about half as large in shear as they are in tension. As was the case for normal stresses and strains, the initial portion of the shearing stress-strain diagram is a

straight line. For values of the shearing stress which do not exceed the proportional limit in shear, we may therefore write for any homogeneous isotropic material,

$$\tau_{xy} = G\gamma_{xy}$$

This relation is known as *Hooke's law for shearing stress and strain,* and the constant G is called the *modulus of rigidity* or *shear modulus* of the material. Since the strain γxy was defined as an angle in radians, it is dimensionless, and the modulus G is expressed in the same units as τxy, that is, in Pascal or in psi. [3]

APPENDIX D

CONTINUUM ELEMENT STIFFNESS MATRIX

The nine-by-nine continuum element matrix of modulus of elasticity, in other words, the matrix of the ability to resist a deformation within the linear range, or simplily the stiffness matrix, is given by

$$S_{ij} = \begin{vmatrix} S_{11} & \cdot & \cdot & \cdot & S_{19} \\ \cdot & \cdot & & & \cdot \\ \cdot & & \cdot & & \cdot \\ \cdot & & & \cdot & \cdot \\ S_{91} & \cdot & \cdot & \cdot & S_{99} \end{vmatrix}$$

where the stiffness coefficients are given by

$$S_{11} = S_{66} = -S_{16} = \sum_{i=1}^{\#columns} \left(\frac{EA_i}{L} \right) \tag{D1}$$

$$S_{22} = S_{77} = -S_{27} = \left(\sum_{i=1}^{\#columns} \frac{12EI_i}{L^3} \right) + \frac{6GA_s}{5L} \tag{D2}$$

$$S_{23} = S_{28} = -S_{37} = -S_{78} = \left(\sum_{i=1}^{\#column} \frac{6EI_i}{L^2} \right) + \frac{GA_s}{10} \tag{D3}$$

$$S_{33} = S_{88} = \left(\sum_{i=1}^{\#column} \frac{4EI_i}{L} \right) + \frac{2GA_sL}{15} \tag{D4}$$

$$S_{38} = \left(\sum_{i=1}^{\#columns} \frac{2EI_i}{L} \right) - \frac{GA_sL}{30} \tag{D5}$$

$$S_{44} = S_{99} = \left(\sum_{i=1}^{\#columns} \frac{7EA_i y_i^2}{3L} \right) + \frac{2GA_s L}{15} \tag{D6}$$

$$S_{45} = S_{59} = \left(\sum_{i=1}^{\#columns} -\frac{8EA_i y_i^2}{3L} \right) + \frac{GA_s L}{15} \tag{D7}$$

$$S_{49} = \left(\sum_{i=1}^{\#columns} \frac{EA_i y_i^2}{3L} \right) - \frac{GA_s L}{30} \tag{D8}$$

$$S_{55} = \left(\sum_{i=1}^{\#columns} \frac{16EA_i y_i^2}{3L} \right) + \frac{8GA_s L}{15} \tag{D9}$$

$$S_{24} = S_{29} = -S_{47} = -S_{79} = \frac{GA_s}{10} \tag{D10}$$

$$S_{25} = -S_{57} = \frac{4GA_s}{5} \tag{D11}$$

$$S_{34} = S_{89} = -\frac{7GA_s L}{60} \tag{D12}$$

$$S_{35} = S_{58} = \frac{GA_s L}{15} \tag{D13}$$

$$S_{12}=S_{13}=S_{14}=S_{15}=S_{17}=S_{18}=S_{19}=S_{26}=S_{36}=S_{39}=S_{46}=S_{48}=S_{56}=S_{67}=S_{68}=S_{69}=0$$

where L = length of the element; E and G = modulus of elasticity and shear modulus of the lattice material; A_s = shear area of the cell spanned by the element; and I_i, A_i, and y_i = moment of inertia, area, and distance to the neutral axis of bending each column i in the cell.[4]

The matrix above is symmetric. The symmetry can be explained by the following example.

The tensile forces T produce a total elongation (deformation) δ are related through Hooke's law by

$$T = k\delta \tag{D14}$$

where, because δ is the deformation of a spring, we have

$$\delta = \hat{u}(L) - \hat{u}(0) = \hat{d}_{2x} - \hat{d}_{1x} \tag{D15}$$

where L is the length of the spring, $\hat{d}_{2x}$ and $\hat{d}_{1x}$ are the nodal displacements at node 2 and node 1 respectively, i.e., at the end and the beginning of the spring element.

To derive the spring element stiffness matrix by the sign convention for nodal forces, we have

$$\hat{f}_{1x} = -T \qquad \hat{f}_{2x} = T \tag{D16}$$

where $\hat{f}_{1x}$ and $\hat{f}_{2x}$ are the local forces at nodes 1 and 2 respectively.

Using Eqs. (D14), (D15), and (D16), we have

$$T = -\hat{f}_{1x} = k(\hat{d}_{2x} - \hat{d}_{1x})$$

$$T = \hat{f}_{2x} = k(\hat{d}_{2x} - \hat{d}_{1x}) \tag{D17}$$

Rewriting Eqs. (D17), we have

$$\hat{f}_{1x} = k(\hat{d}_{1x} - \hat{d}_{2x})$$

$$\hat{f}_{2x} = k(\hat{d}_{2x} - \hat{d}_{1x}) \tag{D18}$$

Now expressing Eqs. (D18) in a single matrix equation yields

$$\begin{Bmatrix} \hat{f}_{1x} \\ \hat{f}_{2x} \end{Bmatrix} = \begin{bmatrix} k & -k \\ -k & k \end{bmatrix} \begin{Bmatrix} \hat{d}_{1x} \\ \hat{d}_{2x} \end{Bmatrix} \tag{D19}$$

This relationship holds for the spring along the $\hat{x}$ axis. The stiffness matrix we obtained is

$$\hat{K} = \begin{bmatrix} k & -k \\ -k & k \end{bmatrix} \tag{D20}$$

as the stiffness matrix for a linear spring element. Here $\hat{K}$ is called the local stiffness matrix for the element. We observe from Eq. (D20) that $\hat{K}$ is a symmetric (that is, $k_{ij} = k_{ji}$) square matrix.[15]

APPENDIX E

SCALAR PRODUCT OF FORCE AND VELOCITY

If ϕ is the angle between the force **F** acting on a particle traveling along a curve in space and a small displacement ds along that curve, the component of the force parallel to ds is $F_s = F\cos\phi$. The work done by the force over the small displacement is then

$$dW = F_s ds = (F\cos\phi)ds \qquad \text{(E1)}$$

This type of scalar combination of two vectors and the cosine of the angle between them occurs often in physics, and is called the **scalar product** of the vectors. [9]

Since velocity, V = ds/dt, equation V1 gives

$$\frac{dW}{dt} = \frac{F_s ds}{dt} = F_s V \qquad \text{(E2)}$$

which means the rate of working is given by the scalar product of force and velocity.

APPENDIX F

MINIMUM POTENTIAL ENERGY

The principle of minimum potential energy can be used to derive the bar element equations. However, it is applicable only for elastic materials.

The total potential energy π_p of a structure is expressed in terms of displacements. When π_p is minimized with respect to these displacements, equilibrium equations result.

The principle of minimum potential energy can be stated as follows:

Of all the displacements that satisfy the given boundary conditions of a structure, those that satisfy the equations of equilibrium are distinguishable by a stationary value of the potential energy. If the stationary value is a minimum, the equilibrium state is stable.

Total potential energy is defined as the sum of the internal strain energy U and the potential energy of the external forces Ω; that is

$$\pi_p = U + \Omega \tag{F1}$$

Strain energy is the capacity of internal forces(or stresses) to do work through deformations (strains) in the structure; Ω is the capacity of forces such as body forces,

surface traction forces, and applied nodal forces to do work through deformation of the structure.

Recall that a linear spring has force related to deformation by $F=kx$, where k is the spring constant and x is the deformation of the spring.

The differential internal work (or strain energy) dU in the spring is the internal force multiplied by the change in displacement through which the force moves, given by

$$dU = Fdx$$

where $F = kx$

$$dU = kxdx$$

The total strain energy is then given by

$$U = \int_0^x kx\,dx$$

$$U = \frac{1}{2}kx^2 = \frac{1}{2}(kx)x = \frac{1}{2}Fx \qquad \text{(F2)}$$

Eq. (F2) indicates that the strain energy is the area under the force deformation curve.

The potential energy of the external force, being opposite in sign from the external work expression because the potential energy of the external force is lost when the work is done by the external force, is given by

$$\Omega = -Fx$$

Therefore,

$$\pi_p = \frac{1}{2}kx^2 - Fx$$

The concept of a *stationary value* of a function G (used in the definition of the principle of minimum potential energy) is expressed as a function of the variable x. The

stationary value can be a maximum, a minimum, or a neutral point of $G(x)$. To find a value of x yielding a stationary value of $G(x)$, one can use differential calculus to differentiate G with respect to x and set the expression equal to zero, as follows:

$$\frac{dG}{dx} = 0$$

An analogous process is used to replace G with π_p and x with discrete values (nodal displacements) d_i. We used the first variation of π_p (denoted by $\delta\pi_p$) to minimize π_p by differential calculus. To apply the principle of minimum potential energy, that is to minimize π_p, we take the variation of π_p, defined in general as

$$\delta\pi_p = \frac{\partial\pi_p}{\partial d_1}\delta d_1 + \frac{\partial\pi_p}{\partial d_2}\delta d_2 + \cdots + \frac{\partial\pi_p}{\partial d_n}\delta d_n$$

The principle states that equilibrium exists when the d_i define a structure state such that $\delta\pi_p = 0$ for arbitrary admissible variations δd_i from the equilibrium state. An admissible variation is one in which the displacement field still satisfies the boundary conditions and inter-element continuity. Since any of the δd_i might be non-zero, to satisfy $\delta\pi_p = 0$, all coefficients associated with the δd_i must be zero independently. Thus

$$\frac{\partial\pi_p}{\partial d_i} = 0 \qquad (i=1,2,3,\ldots,n) \quad \text{or} \quad \frac{\partial\pi_p}{\partial\{d\}} = 0$$

where n equations must be solved for the n values of d_i or vector displacements {d} that define the static equilibrium state of the structure.[15]

APPENDIX G

COMPARISON OF THREE STORY FRAME ANALYSIS

FIGURE G1 3 Story Frame

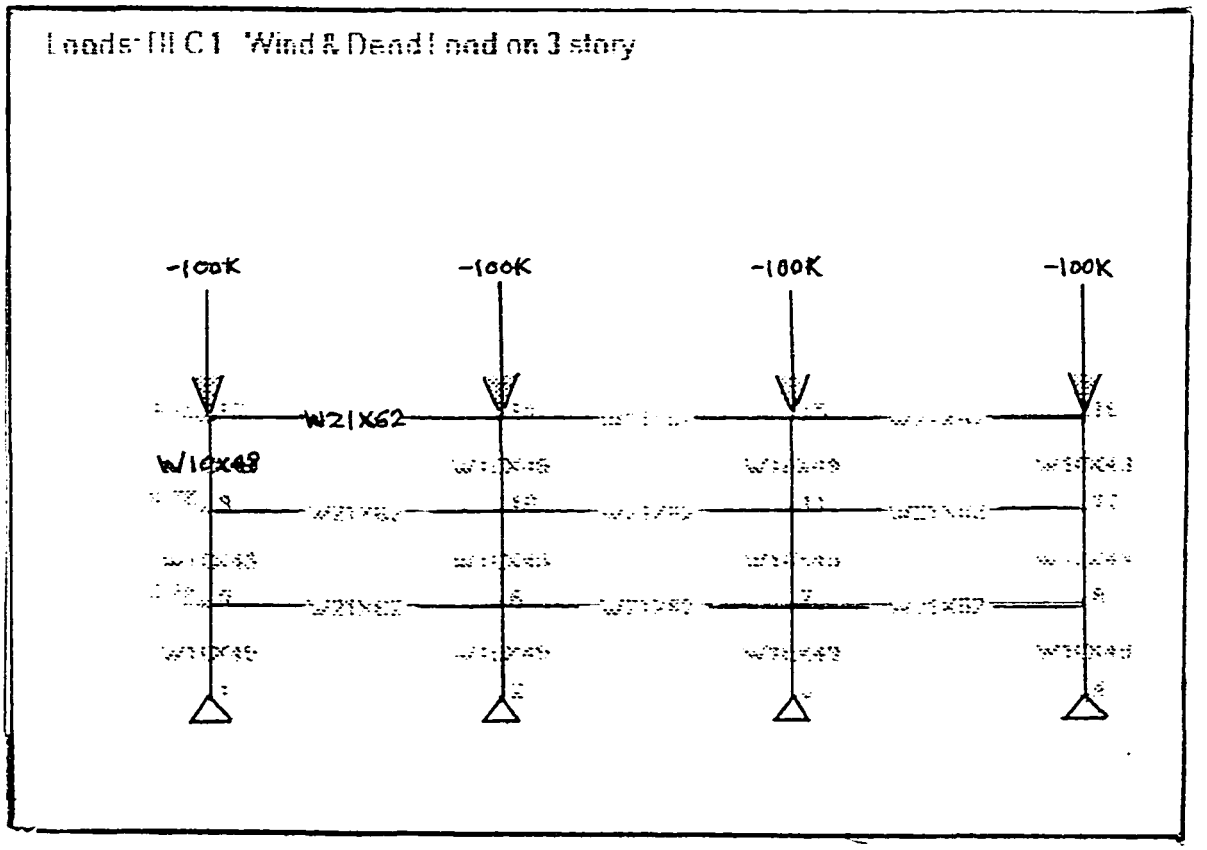

```
SAI: PLANE   - Planar Frame and Truss Analysis
Version 1.54 - 10/09/87 - C4.0
Copyright (C) 1986, Structural Analysis, Inc.
Boca Raton FL  33432     (305) 392-6597

User #*PLANE


Input data filename: gable.dat

DATE: 10-16-1998     TIME: 15:25:41


PROJECT: 3-Story Frame

*** GENERAL DATA ***

        Members:  21
        Joints :  16
Load Conditions:   1
     Elasticity:   29000.0 ksi
      Structure: PLANE FRAME


*** JOINT DATA (feet) ***

 JT          X             Y      R V H
  1          .00           .00    1 1 1
  2        36.00           .00    1 1 1
  3        72.00           .00    1 1 1
  4       108.00           .00    1 1 1
  5          .00         10.00    0 0 0
  6        36.00         10.00    0 0 0
  7        72.00         10.00    0 0 0
  8       108.00         10.00    0 0 0
  9          .00         20.00    0 0 0
 10        36.00         20.00    0 0 0
 11        72.00         20.00    0 0 0
 12       108.00         20.00    0 0 0
 13          .00         30.00    0 0 0
 14        36.00         30.00    0 0 0
 15        72.00         30.00    0 0 0
 16       108.00         30.00    0 0 0
```

*** MEMBER DATA ***

MEM	FM	TO	TYPE	AREA sq in.	INERTIA in**4	E ksi	LENGTH feet
1	1	5	0	14.40	272.0	29000.	10.00
2	2	6	0	14.40	272.0	29000.	10.00
3	3	7	0	14.40	272.0	29000.	10.00
4	4	8	0	14.40	272.0	29000.	10.00
5	5	6	0	18.30	1330.0	29000.	36.00
6	6	7	0	18.30	1330.0	29000.	36.00
7	7	8	0	18.30	1330.0	29000.	36.00
8	5	9	0	14.40	272.0	29000.	10.00
9	6	10	0	14.40	272.0	29000.	10.00
10	7	11	0	14.40	272.0	29000.	10.00
11	8	12	0	14.40	272.0	29000.	10.00
12	9	10	0	18.30	1330.0	29000.	36.00
13	10	11	0	18.30	1330.0	29000.	36.00
14	11	12	0	18.30	1330.0	29000.	36.00
15	9	13	0	14.40	272.0	29000.	10.00
16	10	14	0	14.40	272.0	29000.	10.00
17	11	15	0	14.40	272.0	29000.	10.00
18	12	16	0	14.40	272.0	29000.	10.00
19	13	14	0	18.30	1330.0	29000.	36.00
20	14	15	0	18.30	1330.0	29000.	36.00
21	15	16	0	18.30	1330.0	29000.	36.00

****
*** OUTPUT FOR LOADING CONDITION 1 ***
****

*** JOINT LOADS ***

JT	MOMENT kip-ft	PY kips	PX kips
13	.0	-100.00	3.30
9	.0	.00	6.70
5	.0	.00	6.70
14	.0	-100.00	.00
15	.0	-100.00	.00
16	.0	-100.00	.00

*** JOINT DEFORMATIONS ***

JT	ROTATION radians	VERT inches	HORIZ inches
1	.00000	.000	.000
2	.00000	.000	.000
3	.00000	.000	.000
4	.00000	.000	.000
5	-.00063	-.028	.110
6	-.00036	-.029	.106
7	-.00035	-.029	.103
8	-.00060	-.029	.102
9	-.00032	-.057	.201
10	-.00022	-.058	.197
11	-.00022	-.057	.194
12	-.00033	-.058	.193
13	-.00010	-.085	.235
14	-.00006	-.086	.233
15	-.00006	-.086	.231
16	-.00011	-.087	.231

APPENDIX H

COMPARISON OF TWENTY STORY FRAME ANALYSIS

FIGURE H1 20 Story Frame

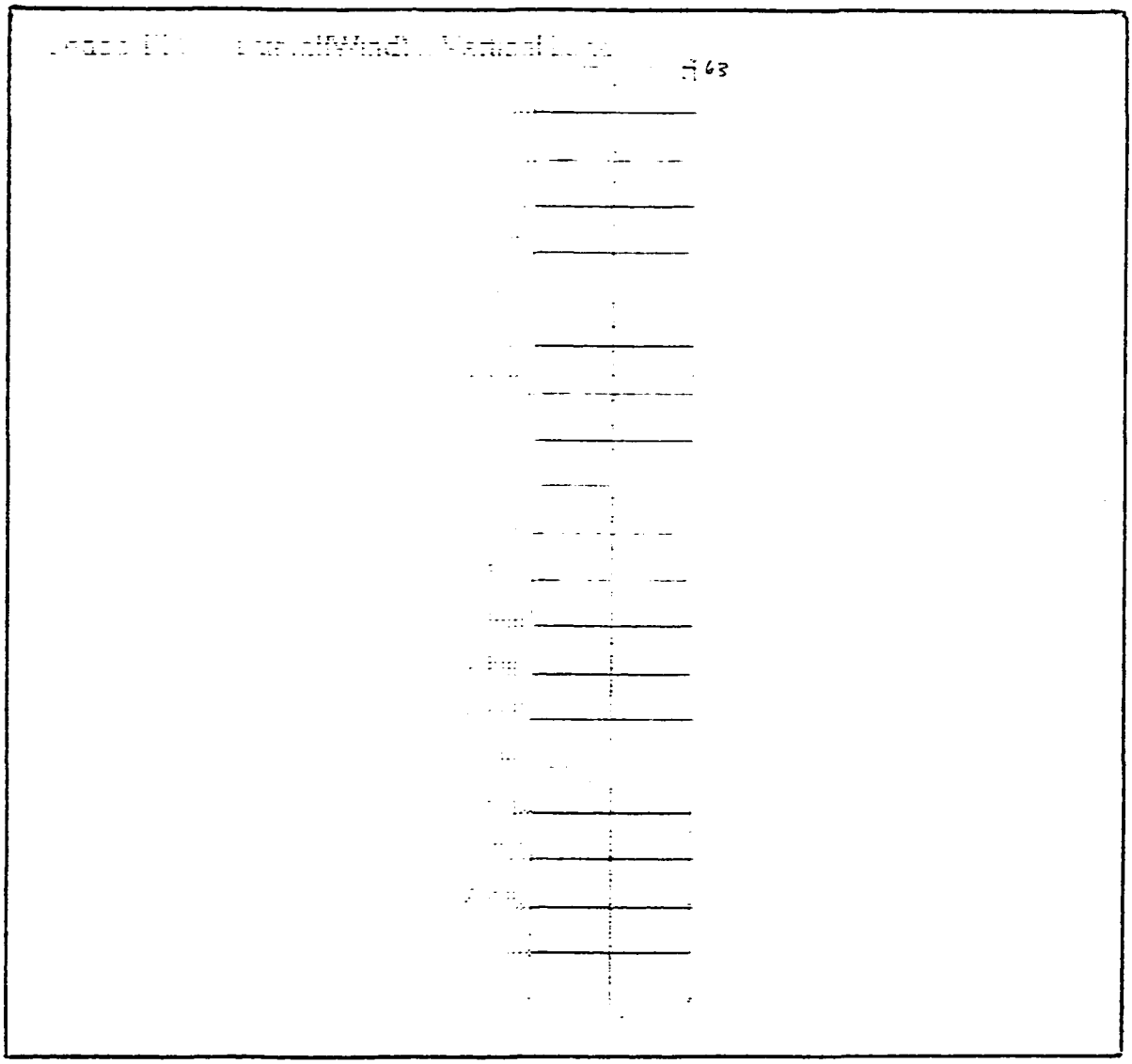

RISA-3D (R) Version 2.1d

American Structural Engineers

Job :
Page:
Date:

A 20 story frame is to compare the results obtained from a continuum model.

Boundary Conditions

Joint No	Translation X	Translation Y	Translation Z	Rotation Mx	Rotation My
	K/in	K/in	K/in	K-ft/rad	K-ft/r
1	Fixed	Fixed	Fixed		
2	Fixed	Fixed	Fixed		
3	Fixed	Fixed	Fixed		

Materials

Material Label	Young's Modulus				Coef.	
					10^-6/F	
STL		11154.00	0.3000			

Section Label	Database Shape	Material Label	Area				
						in^4	
W30X	Wide Flg	STL	51.80	1.2	1.2	000	X

Joint Displacements, LC 1

Joint No	Translation X	Translation Y	Translation Z	Rotation X Polar	Rotation
	in	in	in		
1	0.000	0.000	0.000	0.00000	0.00
2	0.000	0.000	0.000	0.00000	0.00
3	0.000	0.000	0.000	0.00000	0.00
4	0.681	0.013	0.000	0.00000	0.00
5	0.682	0.002	0.000	0.00000	0.00
6	0.681	-0.016	0.000	0.00000	0.00
7	1.086	0.022	0.000	0.00000	0.00
8	1.085	-0.004	0.000	0.00000	0.00
9	1.086	-0.039	0.000	0.00000	
10	1.085	0.031	0.000	0.00000	
11	1.427	-0.006	0.000	0.00000	0.00
12	1.427	0.015	0.000	0.00000	0.00
13	1.787	0.000	0.000	0.00000	0.00
14	1.787	0.000	0.000	0.00000	0.00

Joint No	Joint Displacements			Lateral/vertical Rotati	
	X		Z	X Rotate	Y Rota
	in	in	in	rad	rad
15	1.746	-0.053	0.000	0.00000	0.00
16	2.051	0.045	0.000	0.00000	0.00
17	2.051	-0.009	0.000	0.00000	0.00
18	2.051	-0.064	0.000	0.00000	0.00
19	2.341	0.050	0.000	0.00000	0.00
20	2.340	-0.011	0.000	0.00000	0.00
21	2.340	-0.073	0.000	0.00000	0.00
22	2.616	0.055	0.000	0.00000	0.00
23	2.616	-0.013	0.000	0.00000	0.00
24	2.615	-0.081	0.000	0.00000	0.00
25	2.876	0.058	0.000	0.00000	0.00
26	2.876	-0.015	0.000	0.00000	0.00
27	2.875	-0.088	0.000	0.00000	0.00
28	3.121	0.061	0.000	0.00000	0.00
29	3.120	-0.017	0.000	0.00000	0.00
30	3.120	-0.095	0.000	0.00000	0.00
31	3.349	0.063	0.000	0.00000	0.00
32	3.349	-0.019	0.000	0.00000	0.00
33	3.349	-0.100	0.000	0.00000	0.00
34	3.562	0.064	0.000	0.00000	0.00
35	3.561	-0.021	0.000	0.00000	0.00
36	3.561	-0.105	0.000	0.00000	0.00
37	3.758	0.065	0.000	0.00000	0.00
38	3.757	-0.023	0.000	0.00000	0.00
39	3.757	-0.110	0.000	0.00000	0.00
40	3.937	0.065	0.000	0.00000	0.00
41	3.936	-0.024	0.000	0.00000	0.00
42	3.936	-0.114	0.000	0.00000	0.00
43	4.098	0.064	0.000	0.00000	0.00
44	4.098	-0.026	0.000	0.00000	0.00
45	4.098	-0.117	0.000	0.00000	0.00
46	4.243	0.064	0.000	0.00000	0.00
47	4.243	-0.028	0.000	0.00000	0.00
48	4.242	-0.120	0.000	0.00000	0.00
49	4.370	0.062	0.000	0.00000	0.00
50	4.370	-0.030	0.000	0.00000	0.00
51	4.369	-0.123	0.000	0.00000	0.00
52	4.479	0.061	0.000	0.00000	0.00
53	4.479	-0.032	0.000	0.00000	0.00
54	4.479	-0.125	0.000	0.00000	0.00
55	4.571	-0.059	0.000	0.00000	0.00
56	4.570	-0.034	0.000	0.00000	0.00
57	4.570	-0.127	0.000	0.00000	0.00
58	4.645	0.058	0.000	0.00000	0.00
59	4.645	-0.034	0.000	0.00000	0.00
60	4.644	-0.129	0.000	0.00000	0.00

Joint Displacement ... Lateral/vertical

Joint No.	Translation X	Translation Y	Translation Z	X Rotate	Y Rotate
	in	in	in	rad	rad
61	4.704	0.056	0.000	0.000000	0.000
62	4.704	-0.038	0.000	0.000000	0.000
63	4.704	-0.131	0.000	0.000000	0.000

APPENDIX I

COMPARISON OF FORTY STORY FRAME ANALYSIS

Figure J1 40 Story Frame

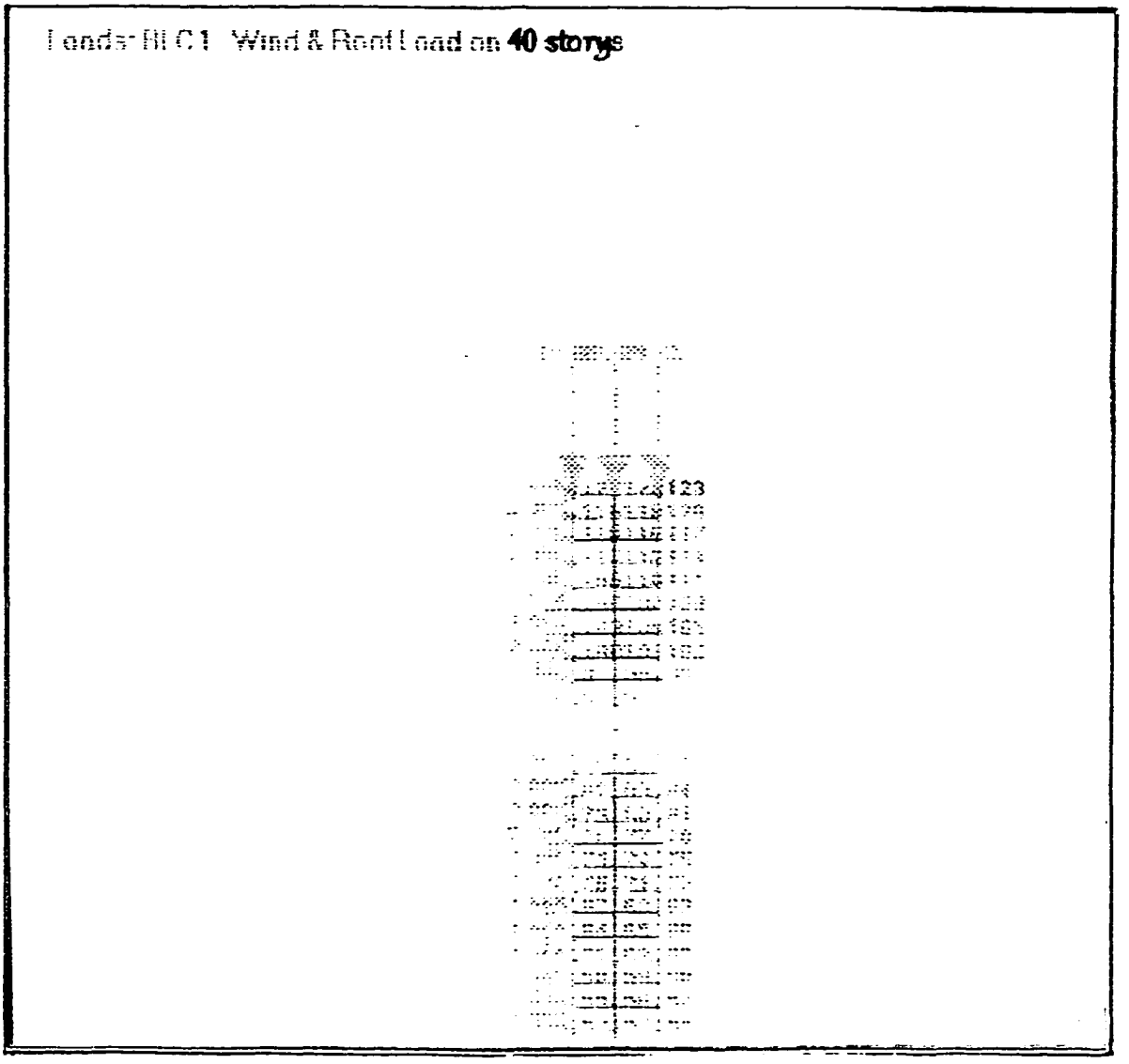

RISA-3D (R) Version 2.1d

American Structural Engineers

Job : 1
Page: 1
Date: 11,

A 40 story frame is to compare the result obtained from a continuum model.

Boundary Conditions

Joint No	Translation X	Translation Y	Translation Z	Rotation Mx	Rotation My
	K/in	K/in	K/in	K-ft/rad	K-ft/rad
1	Fixed	Fixed	Fixed		
2	Fixed	Fixed	Fixed		
3	Fixed	Fixed	Fixed		

Materials (General)

Material Label	Young's Modulus	Shear Modulus	Poisson's Ratio	Thermal Coef.	Weight Density
	Ksi	Ksi		10^5xF	K/ft^3
STL	29000.00	11154.00	0.3000	0.65000	0.49

Sections

Section Label	Database Shape	Material Label	Area	As yy	As zz	I yy	I z
			in^2			in^4	in^4
SEC1	W14X176	STL	51.80	1.2	1.2	838.00	2140

Joint Displacements, LC 1 : WIND & VERTICAL

Joint No.	Translation X	Translation Y	Translation Z	Rotation X Rotate	Rotation Y Rotate
	in	in	in	rad	rad
1	0.000	0.000	0.000	0.00000	0.0000
2	0.000	0.000	0.000	0.00000	0.0000
3	0.000	0.000	0.000	0.00000	0.0000
4	1.406	0.053	0.000	0.00000	0.0000
5	1.407	-0.002	0.000	0.0000	0.0000
6	1.406	-0.057	0.000	0.0000	0.0000
7	2.259	0.103	[illegible]	0.00000	[illegible]
8	2.255	[illegible]	0.000	0.00000	[illegible]
9	[illegible]	-0.110	0.000	[illegible]	[illegible]
[illegible]	3.052	[illegible]	[illegible]	[illegible]	[illegible]
[illegible]	3.031	[illegible]	[illegible]	[illegible]	[illegible]
12	[illegible]	-0.111	[illegible]	[illegible]	[illegible]
13	[illegible]	[illegible]	[illegible]	[illegible]	[illegible]
14	[illegible]	[illegible]	[illegible]	[illegible]	[illegible]

Joint Displacements LC 1 WIND & VERTICAL

	Translation			Rotati	
	Y	Z	X Rotate	Y Rota	
	in	in	rad	rad	
15	3.781	-0.209	0.000	0.00000	0.00
16	4.533	0.235	0.000	0.00000	0.00
17	4.532	-0.009	0.000	0.00000	0.00
18	4.532	-0.254	0.000	0.00000	0.00
19	5.286	0.274	0.000	0.00000	0.00
20	5.286	-0.011	0.000	0.00000	0.00
21	5.285	-0.297	0.000	0.00000	0.00
22	6.041	0.311	0.000	0.00000	0.00
23	6.041	-0.013	0.000	0.00000	0.00
24	6.041	-0.338	0.000	0.00000	0.00
25	6.797	0.346	0.000	0.00000	0.00
26	6.797	-0.015	0.000	0.00000	0.00
27	6.796	-0.376	0.000	0.00000	0.00
28	7.553	0.378	0.000	0.00000	0.00
29	7.552	-0.017	0.000	0.00000	0.00
30	7.552	-0.412	0.000	0.00000	0.00
31	8.307	0.408	0.000	0.00000	0.00
32	8.306	-0.019	0.000	0.00000	0.00
33	8.306	-0.446	0.000	0.00000	0.00
34	9.059	0.437	0.000	0.00000	0.00
35	9.058	-0.021	0.000	0.00000	0.00
36	9.058	-0.478	0.000	0.00000	0.00
37	9.807	0.463	0.000	0.00000	0.00
38	9.807	-0.023	0.000	0.00000	0.00
39	9.806	-0.508	0.000	0.00000	0.00
40	10.551	0.487	0.000	0.00000	0.00
41	10.550	-0.024	0.000	0.00000	0.00
42	10.550	-0.536	0.000	0.00000	0.00
43	11.289	0.509	0.000	0.00000	0.00
44	11.289	-0.026	0.000	0.00000	0.00
45	11.289	-0.562	0.000	0.00000	0.00
46	12.021	0.530	0.000	0.00000	0.00
47	12.021	-0.028	0.000	0.00000	0.00
48	12.021	-0.586	0.000	0.00000	0.00
49	12.746	0.549	0.000	0.00000	0.00
50	12.746	-0.030	0.000	0.00000	0.00
51	12.746	-0.609	0.000	0.00000	0.00
52	13.463	0.566	0.000	0.00000	0.00
53	13.463	-0.032	0.000	0.00000	0.00
54	13.463	-0.630	0.000	0.00000	0.00
55	14.171	0.582	0.000	0.00000	0.00
56	14.171	-0.034	0.000	0.00000	0.00
57	14.171	-0.649	0.000	0.00000	0.00
58	14.870	0.595	0.000	0.00000	0.00
59	14.869	-0.036	0.000	0.00000	0.00
60	14.869	-0.667	0.000	0.00000	0.00

Joint Displacements, LC 1 : WIND & VERTICAL

Joint No.	Translation X in	Translation Y in	Translation Z in	Rotation X rad	Rotation Y rad
61	15.558	0.608	0.000	0.00000	0.00
62	15.557	-0.038	0.000	0.00000	0.00
63	15.557	-0.683	0.000	0.00000	0.00
64	16.235	0.620	0.000	0.00000	0.00
65	16.234	-0.039	0.000	0.00000	0.00
66	16.234	-0.699	0.000	0.00000	0.00
67	16.900	0.630	0.000	0.00000	0.00
68	16.900	-0.041	0.000	0.00000	0.00
69	16.899	-0.712	0.000	0.00000	0.00
70	17.563	0.639	0.000	0.00000	0.00
71	17.552	-0.043	0.000	0.00000	0.00
72	17.552	-0.725	0.000	0.00000	0.00
73	18.193	0.646	0.000	0.00000	0.00
74	18.192	-0.045	0.000	0.00000	0.00
75	18.192	-0.736	0.000	0.00000	0.00
76	18.819	0.652	0.000	0.00000	0.00
77	18.819	-0.047	0.000	0.00000	0.00
78	18.819	-0.746	0.000	0.00000	0.00
79	19.431	0.658	0.000	0.00000	0.00
80	19.431	-0.049	0.000	0.00000	0.00
81	19.431	-0.755	0.000	0.00000	0.00
82	20.029	0.662	0.000	0.00000	0.00
83	20.029	-0.051	0.000	0.00000	0.00
84	20.028	-0.764	0.000	0.00000	0.00
85	20.612	0.666	0.000	0.00000	0.00
86	20.611	-0.053	0.000	0.00000	0.00
87	20.611	-0.771	0.000	0.00000	0.00
88	21.179	0.668	0.000	0.00000	0.00
89	21.178	-0.054	0.000	0.00000	0.00
90	21.178	-0.777	0.000	0.00000	0.00
91	21.730	0.670	0.000	0.00000	0.00
92	21.729	-0.056	0.000	0.00000	0.00
93	21.729	-0.783	0.000	0.00000	0.00
94	22.265	0.672	0.000	0.00000	0.00
95	22.264	-0.058	0.000	0.00000	0.00
96	22.264	-0.788	0.000	0.00000	0.00
97	22.783	0.672	0.000	0.00000	0.00
98	22.783	-0.060	0.000	0.00000	0.00
99	22.783	-0.792	0.000	0.00000	0.00
100	23.285	0.672	0.000	0.00000	0.00
101	23.284	-0.062	0.000	0.00000	0.00
102	23.284	-0.796	0.000	0.00000	0.00
103	23.769	0.672	0.000	0.00000	0.00
104	23.769	-0.064	0.000	0.00000	0.00
105	23.769	-0.800	0.000	0.00000	0.00
106	24.236	0.671	0.000	0.00000	0.00

Joint Displacements, LC 1 : WIND & VERTICAL

Joint No.	Translation X (in)	Translation Y (in)	Translation Z (in)	X Rotate (rad)	Y Rota (rad)
107	24.236	-0.806	0.000	0.00000	0.00
108	24.236	-0.803	0.000	0.00000	0.00
109	24.685	0.670	0.000	0.00000	0.00
110	24.685	-0.068	0.000	0.00000	0.00
111	24.685	-0.805	0.000	0.00000	0.00
112	25.118	0.668	0.000	0.00000	0.00
113	25.117	-0.070	0.000	0.00000	0.00
114	25.117	-0.808	0.000	0.00000	0.00
115	25.532	0.667	0.000	0.00000	0.00
116	25.531	-0.071	0.000	0.00000	0.00
117	25.531	-0.810	0.000	0.00000	0.00
118	25.928	0.665	0.000	0.00000	0.00
119	25.928	-0.073	0.000	0.00000	0.00
120	25.928	-0.812	0.000	0.00000	0.00
121	26.310	0.663	0.000	0.00000	0.00
122	26.310	-0.075	0.000	0.00000	0.00
123	26.310	-0.814	0.000	0.00000	0.00

APPENDIX J

COMPARISON OF FREQUENCY ANALYSIS

RISA-3D (R) Version 2.1d

American Structural Engineers

Job : 1
Page:
Date:

Frequencies Calculation on a 3 Story Frame to Compare with the Results Obtained from Continuum Model.

Boundary Conditions

Joint No	Translation X K/in	Translation Y K/in	Translation Z K/in	Rotation Mx K-ft/rad	Rotation My K-ft/rad
1	Fixed	Fixed	Fixed		
2	Fixed	Fixed	Fixed		
3	Fixed	Fixed	Fixed		
4	Fixed	Fixed	Fixed		

Materials (General)

Material Label	Young's Modulus Ksi	Shear Modulus Ksi	Poisson's Ratio	Thermal Coef. 10^6/F	Weight Density K/ft3
STL	29000.00	11154.00	0.3000	0.65000	0.49

Sections

Section Label	Database Shape	Material Label	Area in^2	As yy	As zz	I yy in^4	I z in^4
COL	W10X49	STL	14.40	1.2	1.2	93.40	272

Frequencies (Periods)

Mode Number	Frequency (Hz)	Period (Sec)	Percent Modal Participation X Spectra	Percent Modal Participation Y Spectra
1	1.036	0.96553		
2	12.827	0.07876		
3	22.496	0.04445		

APPENDIX K

FOURIER SERIES EXPRESSIONS FOR PERIODIC LOADING

Any periodic loading can be expressed as a series of harmonic loading terms. To treat the case of an arbitrary periodic loading of period T_p, it is convenient to express it in a Fourier series form with harmonic loading components at discrete values of frequency. The well-known trigonometry from of the Fourier series is given by

$$p(t) = a_o + \sum_{n=1}^{\infty} a_n \cos \varpi_n t + \sum_{n=1}^{\infty} b_n \sin \varpi_n t \qquad \text{(G1)}$$

in which

$$\varpi_N = n\varpi_1 = n\frac{2\pi}{T_p} \qquad \text{(G2)}$$

and the harmonic amplitude coefficients can be evaluated using the expressions

$$a_o = \frac{1}{T_p}\int_0^{T_p} p(t)dt \qquad \text{(G3)}$$

$$a_n = \frac{2}{T_p}\int_0^{T_p} p(t)\cos \varpi_n t dt \qquad n = 1,2,3,\cdots \qquad \text{(G4)}$$

$$b_n = \frac{2}{T_p}\int_0^{T_p} p(t)\sin \varpi_n t dt \qquad n = 1,2,3,\cdots \qquad \text{(G5)}$$

REFERENCES

1. Chajes, M.J., Romstad, K.M., and McCallen, D.B.(1993). "Analysis of multiple-bay frames using continuum model." Journal of Structural Engineering, vol. 119, issue n2, Feb., 1993, p522(25).

2. Beer, P. F., and Johnson, E. R., Jr., "Mechanics of Materials", McGraw-Hill, New York (1992).

3. Irving, H. S. and Clive, L. D., "Energy and Finite Element Methods in Structural Mechanics", SI unit ed., Taylor & Francis Publisher, Hemisphere Publishing Corp., (1991).

4. Segel, L. A., "Mathematics Applied to Continuum Mechanics", Dover Publications, Inc., New York (1977).

5. McCallen, D. B., and Romstad, K. M. (1988). "A continuum model for the nonlinear analysis of beam-like lattice structures." Computers and Struc., 29(2), 177-197.

6. Chajes, Michael J. (1996). "Dynamic analysis of tall building using reduced-order continuum model." Journal of Structural Engineering, vol. 122, issue n11, Nov., 1996, p1284(8).

7. Haberman, R., "Elementary Applied Partial Differential Equations", 3rd ed., Prentice-Hall, Inc., New Jersey (1998).

8. Kreyszig, E., "Advanced Engineering Mathematics", 7th ed., John Wiley & Sons, Inc., New York (1993).

9. Tipler, P.A., "Physics for Scientists and Engineers", 3rd ed., Worth Publishers, New York (1991).

10. Timoshenko, S.P., and Goodier, J.N., "Theory of Elasticity", McGraw-Hill, Inc., New York (1970).

11. Hibbeler, R.C., "Structural Analysis", 3rd Ed., Prentice Hall, New Jersey (1995).

12. Timoshenko, S., "Theory of Plates and Shells", 2nd Ed., McGraw-Hill, Inc., New York (1959).

13. Logan, D. L., "A First Course in the Finite Element Method Using Algor", PWS Publishing Co., Boston, (1997).

SELECTED REFERENCES

1. Crawley, S.W., Dillon, R.M., "Steel Buildings Analysis and Design", 4th Ed., John Wiley & Sons, Inc., New York (1993).

2. Bickford, W. B., "A First Course in the Finite Element Method", Richard D. Irwin, Inc., Boston, (1990).

3. Manual of Steel Construction, "Load & Resistance Factor Design", 2nd Ed., vol. 1, American Institute of Steel Construction, Inc., (1995).

4. Clough, R. W., and Penzien, J., "Dynamics of Structures", 2nd Ed., McGraw-Hill, New York, (1993).

VITA

Graduate College
University of Nevada, Las Vegas

Simon Graduate Student

Local Address:
3766 Crest Horn Drive,
Las Vegas, Nevada 89147

Degree:
Bachelor of Science, Engineering, 1997
University of Nevada, Las Vegas

Thesis Title: The use of continuum models for conducting both linear and nonlinear analyses for lattice structures

Thesis Examination Committee:
Chairperson, Dr. Gerald R. Frederick, Prof.
Committee Member, Dr. Samaan Ladkany, Prof.
Committee Member, Dr. Barbara A. Luke, Assistant Prof.
Graduate Faculty Representative, Georg F. Mauer, Prof.

IMAGE EVALUATION
TEST TARGET (QA-3)

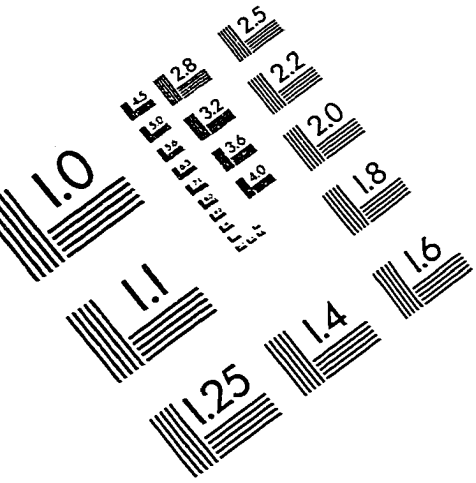

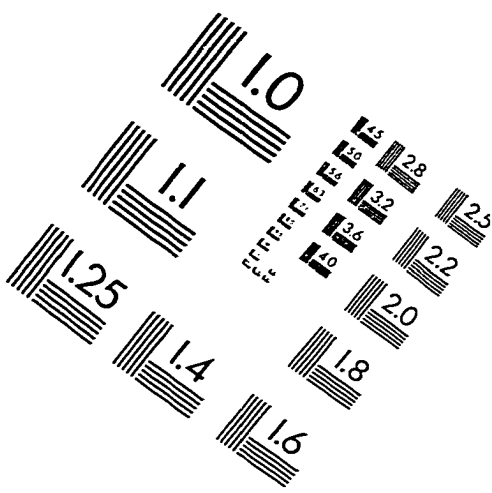

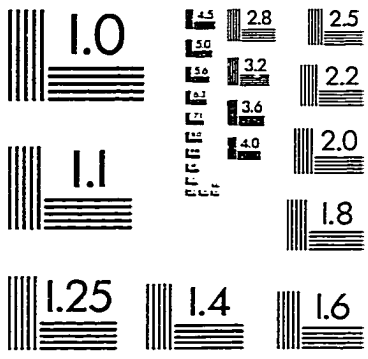

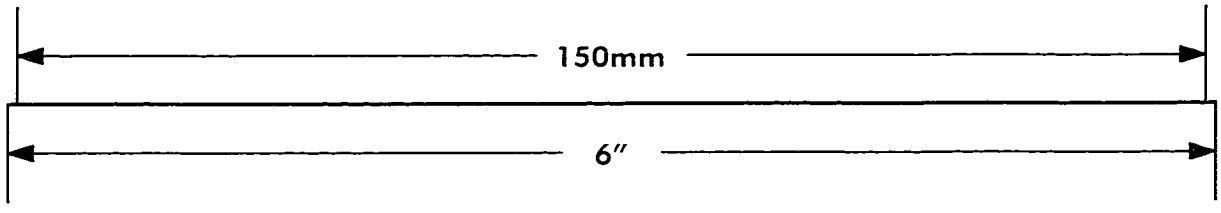

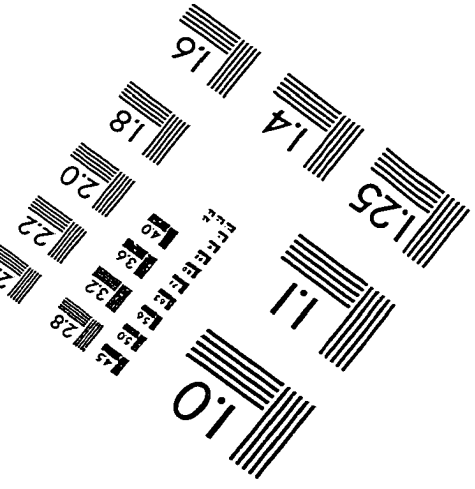

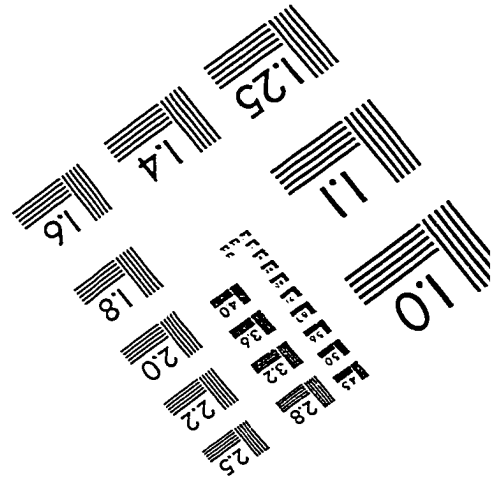

APPLIED IMAGE, Inc
1653 East Main Street
Rochester, NY 14609 USA
Phone: 716/482-0300
Fax: 716/288-5989